AFRL-ML-WP-TR-2001-4162

AUTOMATED CORROSION DETECTION PROGRAM

Wally Hoppe, Jennifer Pierce, and Ollie Scott

University of Dayton Research Institute
300 College Park Avenue
Dayton, OH 45469-0120

OCTOBER 2001

FINAL REPORT FOR 07 APRIL 1997 – 06 OCTOBER 2001

Approved for public release; distribution is unlimited.

MATERIALS AND MANUFACTURING DIRECTORATE
AIR FORCE RESEARCH LABORATORY
AIR FORCE MATERIEL COMMAND
WRIGHT-PATTERSON AIR FORCE BASE, OH 45433-7750

NOTICE

THIS TECHNICAL REPORT HAS BEEN REVIEWED AND IS APPROVED FOR PUBLICATION.

CHARLES F. BUYNAK, Project Engineer
Nondestructive Evaluations Branch
Metals, Ceramics & NDE Division

JAMES C. MALAS, Chief
Nondestructive Evaluations Branch
Metals, Ceramics & NDE Division

GERALD J. PETRAK, Assistant Chief
Metals, Ceramics & NDE Division
Materials & Manufacturing Directorate

REPORT DOCUMENTATION PAGE

Form Approved
OMB No. 0704-0188

1. REPORT DATE *(DD-MM-YY)*	2. REPORT TYPE	3. DATES COVERED *(From - To)*
October 2001	Final	04/07/1997 – 10/06/2001

4. TITLE AND SUBTITLE
AUTOMATED CORROSION DETECTION PROGRAM

5a. CONTRACT NUMBER
F09603-95-D-0175

5b. GRANT NUMBER

5c. PROGRAM ELEMENT NUMBER
63112F

6. AUTHOR(S)
Wally Hoppe, Jennifer Pierce, and Ollie Scott

5d. PROJECT NUMBER
3153

5e. TASK NUMBER
00

5f. WORK UNIT NUMBER
24

7. PERFORMING ORGANIZATION NAME(S) AND ADDRESS(ES)
University of Dayton Research Institute
300 College Park Avenue
Dayton, OH 45469-0120

8. PERFORMING ORGANIZATION REPORT NUMBER
UDR-TR-2002-00083

9. SPONSORING/MONITORING AGENCY NAME(S) AND ADDRESS(ES)
MATERIALS AND MANUFACTURING DIRECTORATE
AIR FORCE RESEARCH LABORATORY
AIR FORCE MATERIEL COMMAND
WRIGHT-PATTERSON AFB, OH 45433-7750

10. SPONSORING/MONITORING AGENCY ACRONYM(S)
AFRL/MLLP

11. SPONSORING/MONITORING AGENCY REPORT NUMBER(S)
AFRL-ML-WP-TR-2001-4162

12. DISTRIBUTION/AVAILABILITY STATEMENT
Approved for public release; distribution is unlimited.

13. SUPPLEMENTARY NOTES
Report contains color.

14. ABSTRACT
An evaluation of several hidden corrosion-detection technologies was performed using a probability of detection (POD) method for percent material loss that is similar to well-established crack detection assessment methods. Several other tasks were performed, with overall goal of contribution to aging aircraft maintainability improvement. Automation concepts were studied and tested for improved speed and accuracy. Nondestructive Evaluation (NDE) requirements were surveyed within the industry for issues and needs pertaining to damage detection and repair. Concepts for new corrosion management maintenance philosophies were studied in terms of data fusion and reproducibility. Advancements were made to a high-temperature sensor design for Air Force application. A facility was established to support Air Force inspection advancements on KC-135 aircraft. A quantitative evaluation method was developed for hidden corrosion detection capability that lends itself to automation and data fusion concepts explored for improved corrosion management maintenance philosophies.

15. SUBJECT TERMS
Corrosion, NDE, probability of detection (POD), KC-135, material loss, data fusion

16. SECURITY CLASSIFICATION OF: a. REPORT	b. ABSTRACT	c. THIS PAGE	17. LIMITATION OF ABSTRACT:	18. NUMBER OF PAGES	19a. NAME OF RESPONSIBLE PERSON (Monitor) / 19b. TELEPHONE NUMBER *(Include Area Code)*
Unclassified	Unclassified	Unclassified	SAR	122	Charles Buynak / (937) 255-9807

HES&S 31-15093-1

Standard Form 298 (Rev. 8-98)
Prescribed by ANSI Std. Z39-18

Table of Contents

Table of Contents

List of Figures

Figure **Page**

List of Tables

Preface

In the spring of 1997, the US Air Force issued a delivery order to the University of Dayton Research Institute (UDRI) titled, *Automated Corrosion Detection Process/System for Cost-Effective Maintainability Improvement*. This program is a delivery order on the Warner Robins Design Engineering Program (USAF Contract F09603-95-D-0175). Technical program management was provided by the Nondestructive Evaluation Branch of the Air Force Research Laboratory (AFRL/MLLP).

The Automated Corrosion Detection Program (ACDP) is an effort to address the potential life-limiting issues surrounding the corrosion inspection and repair costs of maintaining the C/KC-135 aircraft. The goal is to develop and apply new corrosion detection technologies and couple these with automated systems to provide significant maintainability improvement of the C/KC-135 or similar aircraft through the following:

- Accurate corrosion detection at greater than 10 percent material loss,
- Reduced person-hours for corrosion inspection through automation,
- Reduced aircraft downtime due to inspection and repair for corrosion,
- Efficient discrimination of corrosion through data fusion techniques, and
- Accurate reproducibility of inspections from aircraft to aircraft through inspection system reliability.

To meet the objectives of the program, UDRI implemented an evaluation of several hidden corrosion detection technologies using a probability of detection (POD) methodology and performed several other tasks with the overall goal of improving aging aircraft maintainability.

This report satisfies contractual delivery requirements of Scientific and Technical Reports, CDRL 069, in accordance with Data Item Description DID-MISC-80711 and summarizes activities and accomplishments on the program. Program tasks are specifically addressed with special emphasis placed on the formal evaluation of several hidden corrosion detection technologies. Additional details of the formal evaluation appear in the *Automated Corrosion Detection Program Evaluation Report*, dedicated to this major scientific undertaking. The other tasks on the program including the prequalification efforts and the automation developments are highlighted in this report.

Acknowledgements

The UDRI and authors of this report would like to acknowledge and thank the many participants on the ACDP. Technical Program Management was provided by the AFRL/MLLP. Contract monitors were Tobey Cordell, Carol Nove, and Charles Buynak. Other government contributors include the following:

- Donald Nieser (OC-ALC – retired), who provided guidance on the KC-135 corrosion maintenance issues, participated in the probability of detection (POD) survey, and coordinated the cutup of KC-135 aircraft, tail number 2668.
- David Campbell, Steve West, Tommy Smallwood, and Jess Baxter (OC-ALC/LAPEI) advised on depot inspection practices and operated the MAUS – IV eddy current system during the formal evaluation.
- OC-ALC/CLSS preformed the disassembly of the KC-135 aircraft.
- Debra Peeler, John Brausch, and Kenneth LaCivita (AFRL/MLSA) provided advice concerning corrosion management maintenance philosophies, corrosion removal protocols, and performed specimen characterization radiographs.
- Richard Kinzie (AFRL/MLS-OL) participated in the POD survey.
- William Winfree, K. Elliott Cramer, Ray Parker, and Patty Howell of NASA Langley Research Center participated in the formal evaluation of the NASA NDE inspection technologies and provided information concerning NASA aging aircraft NDE activities.
- Floyd Spencer from Sandia National Laboratory and Chris Smith from the Federal Aviation Administration who responded to the questionnaire on corrosion detection methodologies.

The authors and UDRI would also like to thank the following individuals and organizations that took part in this program:

Other POD survey respondents include Grover Hardy (retired), Matt Golis (Advanced Quality Concepts), Ward Rummel (D&W Enterprises, LTD), and Joseph Gallagher (UDRI).

- Joseph Luzar assisted in identifying critical areas on the KC-135 to be cut-up and Nancy Wood provided information on the operation of the MAUS-IV. Both of these individuals are from the Boeing Corporation.
- Robert Thomas, Skip Favro, and Xiaoyan Han (Wayne State University, WSU) were involved in tests of their thermal inspection equipment in the formal evaluation and in the prequalification test.
- Sankaran Sankaran, John Granger, and Richard Churray provided and operated the Analytical Services and Materials (AS&M) ultrasonic system for the evaluation.
- Jerel Smith, Cary Pincus, and June Wang from Advanced Research and Applications Corporation (ARACOR) participated in the formal evaluation of their backscatter radiography technology.

- William Shih and Gerald Fiztpatrick from Physical Research Incorporated (PRI) participated in the formal evaluation of the Magneto-Optical Imaging (MOI) eddy current technology. They also took part in the prequalification test.
- Jim Tucker and Kimberly King from Southern Research Institute (SRI) executed the formal evaluation tests using their swept frequency ultrasonic system.
- Science Applications International Corporation (SAIC) took part in both the formal evaluation and the prequalification tests using the UltraImage eddy current and ultrasonic systems. Individuals involved from this organization include Robert Grills, Glenn Andrew, and Tim MacInnis.
- Advanced Robotic Vehicles Incorporated (ARVI) was involved in the automation portion of the program, optimizing the AutoCrawler, and demonstrating this technology in Oklahoma City. Henry Seemann and Mike Jerome led this effort from ARVI.
- Advanced Power Technology (APT) inspected the round-robin test specimens for the prequalification test using their Remote Acoustic Impact Doppler (RAID) system.
- General Electric Corporation employed their radiography system to inspect the prequalification test specimens.
- The Industrial Material Institute of the National Research Council of Canada (IMI-NRCC) inspected the prequalification specimens with their laser ultrasonic technology.
- George Matzkanin (NTIAC/Texas Research Institute) helped prepare the NDE requirements survey, placed a solicitation for survey respondents on their web page, and assisted in identifying potential survey participants.

Each of the above individuals and organizations made their time, resources, and/or equipment available to this program and their support was greatly appreciated.

Finally, the authors would like to acknowledge several UDRI employees who helped to make this program a success. Important guidance was provided by the Structural Integrity Division Head, Robert Andrews, who maintained program management authority for the program. Susan Reilly, Group Leader, Integrated Methods Material Characterization, for original and ongoing program development and customer liaison, with the assistance of Prasanna Karpur, Brian Frock, and Ira Fiscus.

Primary program contributors to the program were Jennifer Pierce, Norm Schehl, David Petricola, Dennis Buchanan, Richard Martin, Ollie Scott, Ray Ko, Marylea Barlow, and Phillip Gloekler. Other participants that played important roles include James Sebastian, Peter Hovey, Al Berens, Victoria Kramb, David Stubbs, Robert Olding, David Gasper, Gary Andrews, Mike Bohun, George Hartman, Greg Hartman, Marla McClesky, Andrea Snell and David Irwin. Andy Phelps, Jeff Sturgill, Tom Wittberg, Leanne Petry, Dick Tocci, Mark Ruddell, George Stierlin, Mark Laber, and Ross (Eddie) Warrick added to the success of the program in a variety of ways.

Section 1
Summary

The Automated Corrosion Detection Program (ACDP) was established to advance equipment, knowledge, expertise, and tools necessary to implement automatic inspections of aging aircraft for hidden corrosion detection. These technologies address significant economic and safety issues in the aircraft industry. The program applies a comprehensive approach to dealing with the various aspects of this topic. ACDP focused on several aspects of this challenging problem. The activities performed include a formal evaluation of the nondestructive evaluation (NDE) technologies for corrosion detection, a prequalification round-robin inspection, an automation demonstration, a NDE requirements survey, and several other related tasks.

1.1 Evaluation

As a major part of ACDP, the UDRI performed an extensive formal evaluation of different NDE technologies to determine their ability to detect crevice corrosion in lap joints and doublers of KC-135 aircraft. Since no corrosion detection assessment methodology was clearly established as a standard, UDRI needed to define an acceptable, scientifically based evaluation approach. Initially, input from several experts in the field was sought. This input resulted in selecting thickness loss as the metric to characterize corrosion and designing an evaluation experiment built on existing crack detection assessment approaches. The controlled evaluation included specimen design and selection, test procedures, specimen characterization protocols, and data processing plans. A total of ten technologies representing four NDE methods (including ultrasonic, eddy current, thermal, and x-ray) participated in the evaluation. Nine of these technologies inspected a combination of engineered and real aircraft panels in an orchestrated series of tests designed to measure correlation to the metric, spatial resolution, fastener and edge effected zones, and the POD thickness loss in lap joints and doublers.

In general, the eddy current methods (Boeing Mobile Automated Scan, MAUS IV; Science Applications International Corporation, SAIC UltraImage) and the three ultrasonic techniques (SAIC UltraImage; Southern Research Institute, SRI; and Analytical Services and Materials, AS&M) performed well in terms of discrimination capability. All technologies showed the ability to detect corrosion to levels of 6 percent or better, each demonstrating a correlation to thickness loss with varying but respectable spatial resolutions and discrimination capabilities.

The radiography and thermal systems (NASA radiography®[1] and thermal line scan techniques; and the Advanced Research and Applications Corporation, ARACOR radiography technique) showed poor correlation with thickness loss. The MOI eddy current device (Physical Research, Inc.; PRI) had poor sensitivity to thickness loss at levels found in the formal test specimens. WSU withdrew from formal evaluation just prior to the test anticipating difficulties associated with the trapped corrosion products thermally loading the back surface of the front layer of skin (changing the physics of their inspection).

[1] Reverse Geometry X-ray is a registered trademark of Digiray Corporation.

1.2 Prequalification Round-Robin Inspections

A companion study to the formal evaluation performed on the ACDP was also carried out. In this study corrosion detection capabilities of eight technologies were informally investigated with round-robin prequalification inspections of selected aircraft panels. Round-robin prequalification inspections were designed to supplement the formal ACDP evaluation. Due to the magnitude of the formal evaluation effort, it was impractical to include many potential candidates in the evaluation. The prequalification effort was put together to provide a mechanism to screen other technologies and identify those that might be of interest in future evaluations. It was designed to supply information to the government in a timely fashion as well as provide feedback to the participants. Each technology was used to perform inspections of three aircraft pieces, which were subsequently disassembled, cleaned, and characterized. The digitized characterization radiographs were then visually compared to inspection images to qualitatively assess detection capability.

Results from the prequalification effort showed that several of techniques should be considered candidates for further test and possible development. APT RAID technique showed promising results but was not included in the formal ACDP evaluation. The laser ultrasound system shows promise, but required application of a thin latex film to enhance ultrasonic generation. The MOI eddy current system seemed to perform well; however, quantitative formal ACDP tests on 0.063-inch aircraft skins showed poor performance at the level of corrosion present in the test specimen. Prequalification specimens had a variety of skin thicknesses, including some that were less than 0.063-inch, and levels of corrosion in spots were well above levels found in the formal test specimens. As such, the MOI technology may prove to be a viable candidate for other test conditions and applications but it may be limited to manually interpreted applications unless or until a data presentation breakthrough occurs.

1.3 Automation

In addition to the NDE capability studies, automation was investigated. The automation study had three phases: a study of automation concepts, optimization, and demonstration. Automation concepts studied as part of ACDP included a large overhead gantry, a robot that traveled about the circumference of the aircraft on rails, a surface-mounted crawler robot, and several less feasible alternative approaches. Each type was discovered to have strengths, limitations, risks, and associated developmental costs to full implementation. The AutoCrawler surface-crawling robot was selected for optimization and demonstration on ACDP. Overall, the AutoCrawler solution represented the best alternative given the current state of NDE technology, corrosion knowledge, and the realities of the depot maintenance environment. Automation optimization efforts were directed at automated control, adaptation to the KC-135 aircraft, and modification of hardware design expected to interface to NDE hardware.

The AutoCrawler demonstration showed that it could not be moved about on the tail section due to design problems with the suction cups and wheels. The suction cups and wheels require balancing forces to provide adherence to the aircraft and drive force to the wheels. Overcompensation of the corresponding control parameters (suction and wheel drive) along with onsite crawler modifications led to mechanical failure of a drive gear. Controlled motion tests failed due to these mechanical problems. Subsequent tests performed on the repaired robot demonstrated rudimentary control of the robot motion. The limited demonstration revealed several remaining concerns with this technology. Fundamental design of suction cups, wheel drive, and appropriate balance of the corresponding forces has not been established. Laser tracker accuracy and position update rates limit the implementation of control strategies. Motion control schemes and robot movement constraints make path correction difficult, unwieldy, and impractical. Continuous feedback of positions are required to overcome the necessary awkward movements and to maintain acceptable path following capabilities. Complete automation of inspections for hidden corrosion detection in aging aircraft is awaiting a breakthrough in robotics and/or inspection technology that will overcome current automation shortcomings.

1.4 Additional Tasks

An NDE requirements survey collected information from over 60 individuals in the aircraft industry concerning various aspects of inspection capabilities, limitations, and needs. Reproducibility of automated corrosion detection technologies was covered in part by identifying critical variables that should be considered in future depot implementation qualification assessments. Data format and inspection image registration issues were investigated in the area of data fusion. A novel advanced transducer was designed as part of this program. Finally, a detection technology evaluation facility (DTEF) was set up in the Oklahoma City area for testing and evaluating technologies for inspection of aging aircraft.

1.5 Conclusions and Recommendations

In summary, while the entire program addressed corrosion detection on aging aircraft, significant accomplishments of this program are primarily related to the formal evaluation. A baseline capability was measured for each system tested, which also showed general trends for each NDE method represented. The methodology proposed on the program (to assess the capability of hidden corrosion detection technologies) was unequivocally successful. This methodology was based on several critical assumptions that were demonstrated to be valid, confirming the methodology in its general approach and in the bulk of its particulars. The value of this approach is found as an enabling tool for inspection system implementation, automation, data fusion, and corrosion management maintenance philosophies.

Significant recommendations arise from the formal evaluation as shown below:

- Conventional eddy current and ultrasonic technologies should be further advanced and tested.
- Data collected on other ACDP test regions (e.g., doubler sections that have not been processed) should be analyzed.
- Data processing should be extended to extract other information from these data sets, such as the dependence of the results on the cell size.
- Future programs should address alternative POD interpretation schemes and corrosion damage characterization methods. Moreover, the evaluation methodology should be extended to other forms of corrosion and other corrosion metrics.
- The assessment methodology should be developed into a military handbook, incorporating lessons learned from ACDP as a valuable tool available to the industry.

Section 2
Introduction

The KC-135 aircraft is of particular interest to the Air Force due to its large aging fleet and the life-cycle costs due to corrosion repair. The average age of this aircraft is over 35 years with almost 600 aircraft still in service (*Aging of U.S. Air Force Aircraft – Final Report*, National Material Advisory Board, 1997). It is the intent of the Air Force to continue to fly these aircraft perhaps 40 more years. According to a U.S. General Accounting Office Report in 1996 (*U.S. Combat Air Power: Aging Refueling Aircraft Are Costly to Maintain and Operate*, Chapter Report, GAO/NSIAD-96-160), the Air Force had not yet identified a replacement aircraft. At the time this program was implemented, they had modified their plans for a replacement to delay replacement insertion until the year 2013. This same report stated that depot flow days had increased from 158 days in 1991 to 245 days in 1995. This had forced a gradual extension of the depot cycle from four years to five years.

The KC-135 is not flown aggressively; this fact coupled with the age of the fleet makes corrosion prevalent in the aircraft structures. The life-cycle cost of inspection and repair of corrosion makes it the most important life-limiting form of damage in these aircraft. Corrosion occurs in many forms on the KC-135. Crevice corrosion in the lap joints and doublers is of primary interest on this program. Crevice corrosion has associated with it metal thinning, surface roughness, and pillowing. Compounding this problem, each KC-135 aircraft contains over 300 meters of lap joints and 90 square meters of doublers that need to be inspected for crevice corrosion. Current inspection methods for hidden corrosion are manually operated and operator interpreted techniques, which can be subjective as well as time consuming. Under the corrosion maintenance system for military aircraft vehicles, individual areas of fuselage are repaired when suspected to contain corrosion. This can result in corroded areas being repaired even when the level of damage is not detrimental to the structural integrity. Air-readiness continues to suffer beyond the downtime from inspection since replacement parts are unique and are manufactured on an individual basis.

One way to expedite the depot maintenance cycle of military aircraft is to manage corrosion similarly to the damage tolerant philosophy used for managing cracks. This approach will require a thorough understanding of corrosion characteristics and its impact to structural integrity as well as faster and more objective methods for detection and characterization of corrosion within aircraft structures. Automated corrosion inspection technologies should reduce the downtime in the depot compared to manual inspection and reduce the need for operator interpretation of the data.

The National Materials Advisory Board report, referenced above, discussed several NDE needs relative to corrosion inspection on aging aircraft. These needs include improved methods to detect and characterize hidden corrosion and corrosion in multilayered structures. The report stresses the importance of automation of inspection and emphasizes the need for validation of inspection technologies. It states that inspection reliability is one of the most important characteristics of an effective NDE method.

Furthermore,

> The committee believes that the validation of the selected method must include a full demonstration of the method, development of POD relationships, definition of performance limitations, and engineering parameters such as feature and component size, orientation, and accessibility.

The US Air Force issued a delivery order to the UDRI to optimize existing corrosion detection technologies and couple these with an automated system to provide significant maintainability improvements to the C/KC-135 and similar type aircraft. The ACDP is an effort by the Air Force to improve the speed and reliability of inspection methods for hidden corrosion. This program was implemented to demonstrate an improved NDE system for hidden corrosion detection and thickness loss quantification in lap joints and doublers on KC-135 as part of an automated inspection system.

UDRI was responsible for several major tasks. The primary task was to evaluate and select one or more inspection technologies to integrate into an automated system. Included with the evaluation phase of the program are the major tasks of testing the use of a prequalification round-robin inspection as part of future Air Force technology evaluation processes, demonstrating an optimized automated crawler type robot for use with NDE on aircraft, researching the state of NDE technologies for hidden corrosion detection, and developing data fusion and reproducibility techniques for NDE technology capability assessment. Also stemming from the evaluation process were a number of developments that directly contributed to the goals of the program. Work was done to advance the state of UDRI's high-temperature sensor technology for Air Force applications. A detection technology evaluation facility (DTEF) was created for use by the Air Force, which contained real fuselage structures from corroded aircraft for NDE development and evaluation. In addition, UDRI has continued to publish the accomplishments of the ACDP to the aging aircraft, NDE, and materials communities.

This report will first discuss the development, process, and results of the hidden corrosion detection evaluation. The next sections will separately discuss the following activities: prequalification round-robin inspection exercise; the study, optimization, and demonstration of an improved automated system for use with NDE; the NDE Requirements survey performed to research the state of NDE technology; and the NDE data analysis lessons learned. Also discussed by section is the advancement of UDRI's high temperature sensor and the establishment and use of the DTEF.

Section 3.9 lists all of UDRI's publications and presentations given for the ACDP. Section 4 discusses research inferences and conclusions and Section 5 makes recommendations for the future of the ACDP and information gathered here. A list of terms and acronyms follow the appendix, which define the program and technology unique terms and acronyms used within this report.

Section 3
Methods, Assumptions, Procedures, Results, and Discussion

The following sections describe the major projects and accomplishments of the UDRI ACDP. These projects include Evaluation, Prequalification, Automation, NDE Requirements Survey, Data Fusion, Reproducibility, Advanced Transducer Design, and the DTEF projects and Presentations and Publications resulting from these projects. Each of these discussions will cover the methods, assumptions, and procedures of each project as well as the results and any conclusions that made from the research.

3.1 Evaluation

This section describes the evaluation of nondestructive inspection (NDI) systems for hidden corrosion detection as performed by UDRI on the ACDP. First to be discussed is the scope of the evaluation on the program. Next, the evaluation process steps will be described and the observations made during each step of the process. The quantitative and qualitative results for each NDE system are presented with a discussion. Final recommendations for improved depot level inspections are given.

3.1.1 Scope

The evaluation tested current NDE technologies for capability in detecting and quantifying crevice or general type corrosion within lap joints and doublers of C/KC-135 and similar aircraft. This scope was defined through research of depot level inspection issues. Research was conducted through surveys of Air Force and other experts on topics such as NDE requirements, NDI reproducibility, and POD analyses. Detailed descriptions of the research studies are giving in other sections of this report and in the *Automated Corrosion Detection Program Evaluation Report*. Crevice corrosion is associated with metal thinning, surface roughness, and pillowing. The experiments in this evaluation were designed to test the NDE systems on their ability to detect and quantify 10 percent or less thickness loss in the fuselage skin layers of the KC-135 and Boeing 707. Ten-percent material loss represents a potentially significant impact to an aircraft structure and is a challenge for most current inspection technologies to detect.

The NDE techniques tested in the evaluation included thermography, radiography, ultrasonic, and eddy current methods. There were 10 inspection systems included in the program. The system names, NDE methods, and technology developers are listed in Table 1. The inspection systems included in the program evolved from four NDI technologies (originally elected through competitive bid) to 10 inspection systems. The original four technologies included one system each from four different methods. Those included the PULSE ultrasonic (UT), COREX I radiography, Thermal Imaging by WSU, and MOI II eddy current systems. The six additional systems were chosen for participation by the government. WSU was not formally included in the final evaluation due to the immaturity of the system at the time of the evaluation process.

Table 1. Corrosion Detection Systems

Detection System	Technique	Developers/Participants
PULSE	Ultrasonic	Analytical Services and Materials (AS&M)
COREX I	Radiography	Advanced Research and Applications Corporation (ARACOR)
Thermal Imaging	Thermography	Wayne State University (WSU)
MOI II	Eddy Current	Physical Research Incorporated (PRI)
MAUS IV	Eddy Current	Boeing/AFRL
Line Scan Thermography	Thermography	NASA Langley
Reverse Geometry X-Ray ®	Radiography	Digiray/NASA Langley
Ultraspec	Contact Ultrasonic	Southern Research Institute (SRI)
Ultra Image IV	Ultrasonic	Science Applications International Corporation (SAIC)
Ultra Image IV	Eddy Current	SAIC

3.1.2 Methods, Assumptions, and Procedures

There are five major steps to the evaluation process. First, the evaluation methodology was developed. The methodology includes a data analysis procedure to determine POD and an experimental procedure to obtain data for analysis. Next, UDRI worked with the participant NDE developers to optimize their inspection systems to the defined criteria under the ACDP. Subsequently, the NDE data were gathered from each NDE system. Following data acquisition from all of the participant NDE systems, the aircraft or POD test specimens were opened and characterized for actual corrosion content. The data were then analyzed for detection and discrimination capability.

The methods, tests, and analysis are discussed individually. Figure 1 represents the overall outline of this section in chronological order.

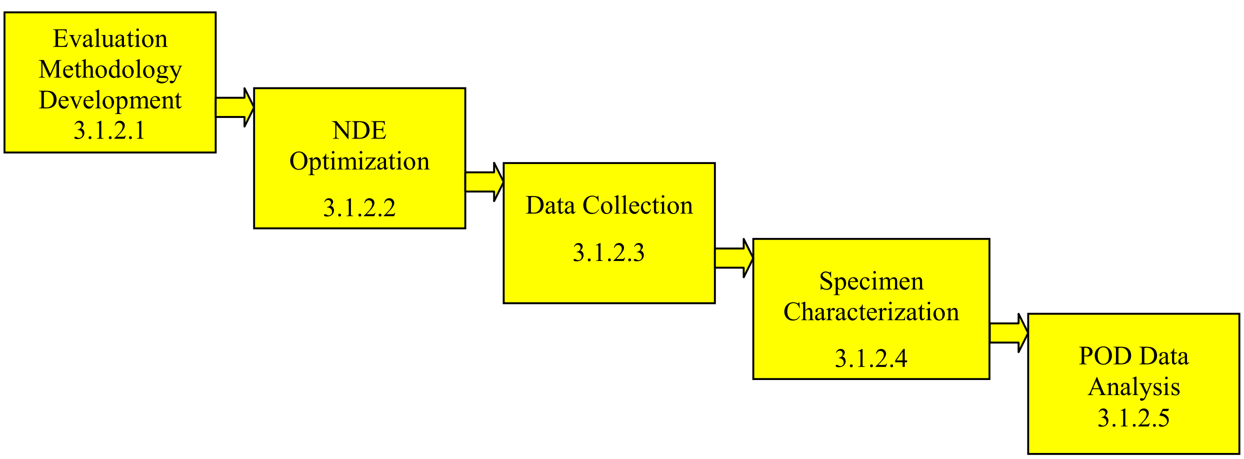

Figure 1. Methods and Procedures Outline

3.1.2.1 Evaluation Methodology Development

The evaluation methodology developed surrounds a quantitative POD analysis aimed at determining the capability of a system to detect ten percent thickness loss in the top layer skin of KC-135 lap joints and doublers. The POD concept is based on the relationship between the output of an NDE system and the actual thickness (or thickness loss) of a corroded surface and directly related to the sensitivity and spatial resolution of the NDE system.

The NDE system output, at a given point in the inspection image, is a function of the corrosion in a small region surrounding this point. This concept is shown by a schematic in Figure 2. The output accuracy is based on the system sensitivity to thickness and to the size of the cell. The cell size is related to the spatial resolution of the system.

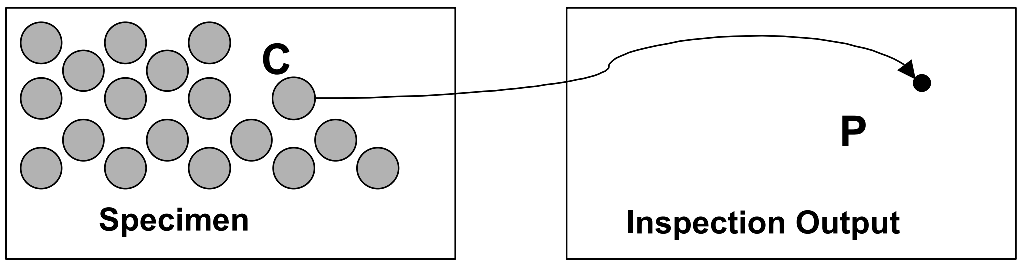

Figure 2. Concept Underlying Corrosion Detection Assessment Methodology

A collection of nonoverlapping cells on the fuselage skin represents independent inspection opportunities and provides data for statistical analysis of the probability of corrosion detection. These data are then analyzed using an "a-hat versus a" or pass/fail analysis. To do so, data pairs are created consisting of the thickness loss detected by the inspection system at the center of the cell (a-hat) and the average actual thickness loss on the fuselage within the cell (a). A model is then established for the trend and for the distribution of the residuals about the trend. Based on the models of the trend and residuals, the POD can be estimated as the probability that the output for a given thickness loss will exceed a given output threshold. Ten-percent thickness loss was chosen for this study. False call rates can be defined by characterizing the output in regions of no thickness loss. Capabilities of the different NDE technologies are then assessed for capability and compared using the attributes of the POD curves at given threshold. More detailed explanations of the methodology development can be found in *Hidden Corrosion Detection Technology Assessment*, a paper presented at the Second Joint DoD/FAA/NASA Conference on Aging Aircraft, 1998.

This evaluation methodology, based on a POD at a given threshold, provides the tools necessary for automation of inspections under a corrosion management maintenance philosophy. In most NDE systems tested on the program, thresholds are not typically applied to the inspection results. Most systems are manually interpreted (the operator looks for changes in the image representing a change in the structure). The ACDP analysis replaces the operator interpretation with a quantitative assessment which could potentially feed into the decision making process of an automated system. The threshold chosen could and should be based on a required defect parameter for repair or for structural integrity modeling under a corrosion management regime. Although 10-percent thickness loss was the parameter applied in this evaluation, this is not the only metric and not necessarily the most significant metric in regard to structural integrity.

However, the premise could extend to other corrosion metrics, other types of corrosion, or in other applications.

3.1.2.2 NDE Optimization

The original four NDE developer/participants (AS&M, ARACOR, WSU, and PRI) were put on subcontract to perform an extensive optimization phase in the program. UDRI sent each developer a representative aircraft section to analyze, inspect, and open. None of the other NDE developers had the same opportunity during their optimization phase in the program. All participants were supplied with a number of trial specimens (which represented both engineered and real aircraft specimens) for a limited time. These trial specimens were not available to be opened and studied. During the optimization phase of the program, UDRI worked with all of the NDE developers to gain a thorough understanding of their technologies. A description of each of the inspection technologies studied on the ACDP is given below. More detailed descriptions can be found in *The Evolution of Hidden Corrosion Technologies on the Automated Corrosion Detection Program*, a paper presented at the Fourth Joint DoD/FAA/NASA Conference on Aging Aircraft, 2000.

AS&M PULSE. The PULSE system, developed by AS&M, uses a pulse-echo ultrasonic method that is sensitive to thickness loss in the top skin layer of aircraft structures. Processing consists of a Fast-Fourier Transform (FFT) of the time domain received pulse followed by a frequency domain search routine. It measures thickness by locating a minimum in the frequency domain associated with thickness resonances of the top skin layer. The algorithm converts the identified resonance frequency to thickness using the known velocity of sound in the material.

The technique uses a conventional 2-inch focused 0.5-inch diameter transducer within a plastic housing that contains a small captured water column above a recirculating water chamber. This assembly is mounted using a gimbal in an encoded X-Y axes arrangement that is designed to be attached to the side of an aircraft with suction cups. The X-Y axes can be used to manually scan up to 8 square inches using an index as fine as 0.05 inch. The gimbal allows the transducer to remain normal to the inspection surface. As it is being scanned, the transducer assembly maintains its standoff by riding on three small plastic feet at the bottom of the plastic housing. The ultrasonic instrument is a conventional pulser-receiver and digitizer, residing in a portable computer. A specialized user interface allows access to the instrument functions, and setup for the frequency domain processing.

ARACOR COREX I. COREX I is a radiography system designed to be sensitive to the oxygen in corrosion byproducts. This is accomplished by separately detecting the Rayleigh and Compton backscattering of x-rays. The Rayleigh backscattering is sensitive to only aluminum since it is significantly dependent on the atomic number of the scattering elements. On the other hand, Compton backscatter is less dependent on atomic number and therefore is sensitive to both aluminum and oxygen in aircraft structures. The ratio of these two backscatter components provides a measure of the oxygen in the inspection volume as a percentage of the aluminum and thus provides an index of the corrosion byproduct content of a test area. An ideal mass determination for the aluminum present in the corrosion byproduct (Al_2O_3) gives an estimate of the aluminum lost due to corrosion.

COREX I is a laboratory breadboard system designed to test the feasibility of this method. The x-ray source is mounted in a brass fixture above the specimen with two proportional gas detectors mounted on either side at fixed angles from the inspection volume. The system incorporates an X-Y scanning table that can index the specimen via computer control under the source and detector assembly.

WSU Thermal Imaging. The thermal imaging system developed by WSU uses high intensity, short duration flash lamps to thermally excite the front surface of a specimen. Infrared (IR) images of the front surface (painted black to enhance emissivity) are then captured at selected time intervals after heat is applied, measuring the rise in temperature of the surface. Sampling times are chosen to be long enough to skip the thermal excitation pulse and allow complete penetration of heat through the first layer, but short enough to allow a 1-dimensional model to apply. Ideally, temperature increase is inversely proportional to thickness of the skin. Areas of the surface that are hotter than surrounding regions indicate areas of relatively thin metal. Relative changes in temperature can be measured by subtracting the output at a given point by the output at a reference point of known thickness. Small relative temperature increases measured in this way are proportional to thickness loss.

With this system, the flash lamps and camera are housed in a shroud which serves to contain the light and shield the operator from the intense flash. The shroud is hand-held and manually indexed across an inspection surface by an operator. Digital images are captured as frames from the infrared camera. In a single layer case, a simple contrast image from a selected time after the heat is applied is sufficient to identify thin regions in the metal. In the multilayered case, more complicated physical processes require more advanced processing. In the laboratory, offline processing can involve temperature-time profile curves for selected regions of interest on a specimen.

PRI MOI Eddy Current. This manual inspection system is a novel eddy current device developed for crack detection that makes use of a magneto-optical sensor to image out-of-plane secondary induced magnetic fields. The interrogating eddy currents are induced by a sheet of current flowing in a conducting foil that lies in a plane just above the specimen. The eddy currents generated in this manner are also planar, running in the specimen. Anomalies in the skin layer such as cracks and changes in thickness result in the generation of out-of-plane secondary magnetic fields. The MOI device is based on the Faraday behavior of the detector film. Linearly polarized light passing through the magneto-optical film will be rotated clockwise or counterclockwise depending on the polarization of the magnetic domains in the film. By passing this light through an analyzer, the magnetic domains can be made to be light or dark depending on their polarization. By applying a bias magnetic field, the domains can be made to grow or shrink under the influence of an applied magnetic field. The PRI device uses this arrangement to cause the secondary induced out-of-plane magnetic fields to be visualized as dark regions in the image. Adjusting the bias and gain can optimize contrast and sharpness of the images.

The magnetic domains that make up the images have a snake-like shape and are readily apparent in the image background. As a result, it is important to constantly move the unit and watch for indications in the form of dark regions that move across the image. These could be associated with anomalies such as corrosion. Due to the nature of the system, there is no direct relationship between the detection of the dark regions and their meaning in terms of thickness loss. It is possible in principle to vary the excitation frequency and to deduce an approximate amount of material loss by noting the frequency at which an indication disappears. Using the standard depth of penetration calculation, frequency can be converted to thickness loss. This processing technique is limited. Therefore, POD analysis for this system is based on its hit-miss detection capability.

The output of the MOI system is a video image that can be recorded with a standard videocassette recorder. The MOI unit is a hand-held devise that is freely pushed across an inspection surface. There is no scanner or encoded axes to record imager position, thus, the ACDP tests required some improvisation to devise a mechanism to establish imager position relative to the specimen. This was done using a combination of rulers, video cameras, and acoustic synchronization.

Boeing/AFRL MAUS IV Eddy Current. The Mobile Automated Scanner (MAUS) IV system can perform a variety of different inspections, including eddy current and ultrasonic. On ACDP, the conventional eddy current method is being evaluated. Conventional, absolute eddy current inspections induce eddy currents in the material being inspected by applying an alternating current to a small drive coil held in proximity to the material being inspected. Defects in the material will perturb these currents, which will in turn produce changes in the magnetic fields induced by the eddy currents. Changes in these secondary induced magnetic fields are detected by monitoring either the effective impedance of the drive coil or the induced voltage in a receive coil. In either case, the output is displayed in real time on a 2-dimensional impedance plane plot. In most eddy current instruments (including the MAUS IV system), the display of the signal can be rotated in the impedance plane (phase angle rotation) to force unwanted effects (such as variations in signal due to liftoff) to appear in the horizontal component of the impedance plane. Horizontal and vertical components are digitized separately and the vertical component is employed for defect detection. The MAUS technique uses two eddy current frequencies to inspect lap joints and doublers. The first frequency is selected so that the depth of penetration is equal to the thickness of the top layer. The second frequency is selected so that the depth of penetration is an additional 0.015 inch farther into the skin structure. Phase angle is determined to make liftoff signals horizontal in the impedance plane, with the high frequency component moving to the left and the low frequency component moving to the right. Images of the vertical signal of each frequency component are created as the probe is scanned across the surface.

The approximate amount of material lost due to corrosion can be inferred from the amplitude of an indication compared to that from a calibration reference standard. The instrument gain is calibrated on an assembled collection of plates chosen to match the skin thickness to be inspected. The plates have rectangular regions of material removed from the inner surfaces to simulate hidden corrosion. Variations in the gap between layers can mask a thickness loss signal making the thickness indeterminate. In theory, it is possible to apply processing to the signal to remove the effects of gap, but the processing required to accomplish this is still in development by Boeing. At this point in the system development some operator interpretation is required and the operators at Tinker Air Force Base (TAFB) have assumed a correlation between a gap signal in the images and the presence of corrosion.

The MAUS inspection system consists of an eddy current instrument, laptop computer, and an X-Y scanner assembly. The MAUS scanner includes a track and an arm to allow large areas to be scanned in one setup. The arm is attached to a carriage that rides on a flexible track. The track can be attached to the side of an aircraft with suction cups. Several tracks can be pieced together to allow even longer scans.

NASA/Digiray RGX. This digital radiography system has a scanned electron beam x-ray source and a small aperture crystal scintillation detector. The detector output is amplified through a photomultiplier tube and other electronics. A digital image is constructed by associating the digitized signal with the current electron beam position on the face of the x-ray tube. Specimens are placed near the source to provide high resolution, low noise images. NASA Langley has worked with the RGX system to characterize it and advance its capability.

X-rays passing through the specimen are attenuated by all material in the path to the detector. This system is sensitive to thickness of the entire structure of the skin and supporting components (stringers and frames), as well as coatings, sealant, and potentially to corrosion byproduct. The detected x-ray intensity can be calibrated to thickness by using a reference standard having different thickness steps. If the expected thickness changes are small, a linear relationship can be assumed for intensity versus thickness. For the ACDP tests, NASA elected to employ an exponential fit to the calibration data.

The system tested during the ACDP formal evaluation resides in a lead-lined room at NASA Langley. Specimens are placed on the face of the x-ray tube, which is positioned approximately 45 inches below a central detector. The detector standoff can be varied, as can the lead aperture (typically 0.5 or 0.25-inch diameter) in front of the detector, to optimize signal-to-noise ratio and image resolution. Acceleration voltage, current, dwell time, and number of averages can also be adjusted to optimize the inspection. Images are collected with an extremely fine resolution pixel size of about 0.010 inch. During postprocessing (removing geometric distortion in the images and normalizing the intensity across the image), 2 by 2-inch boxes are averaged giving a processed pixel size of about 0.020 inch.

NASA Thermal Line Scan. NASA Langley has developed a scanning thermal inspection technique for corrosion detection in aircraft fuselage skin structures. This method rapidly scans a 3000-watt quartz lamp and an infrared camera across an inspection surface. The tubular lamp is 16 inches in length and is used in an upright position very close to the inspection surface. The infrared camera is located just behind the lamp housing on the scanner carriage but positioned to capture images from both sides of the heat source. In front of the lamp housing, the ambient specimen temperature is monitored while temperature increase is recorded behind the heat source.

With this technique, the increase in specimen temperature is obtained at a precise time interval after the thermal excitation by selecting a column of data from each frame of the camera output as the assembly makes its way down the specimen. The column of data selected is determined by the desired time interval and the scanning rate. The columns of data are then assembled into an image running the length of the scan. To obtain the nominal temperature increase, the data are offset by the ambient specimen temperature.

For the time intervals considered in the evaluation, the temperature increase is ideally expected to be inversely proportional to the thickness of the top layer of skin. The line-processed images can therefore be calibrated to thickness through the use of a reference standard containing different thickness steps. The calibration response curve is expected to be linear for small thickness changes. For the purposes of the ACDP evaluation, the slope of this curve was determined from the calibration data and the offset was determined from a region on the specimen of known thickness. Black paint was applied to the ACDP specimens to improved emissivity.

SRI UltraSpec. SRI has developed a swept frequency ultrasonic inspection system that uses a dual-element, broadband transducer assembly in pitch-catch mode. The transmitted waveform sweeps through a user selectable range of frequencies and the instrument identifies peaks in the frequency response of the digitized signal. These peaks are a result of resonances associated with the top layer thickness of an inspection article. Thickness is calculated from the resonance frequency and the velocity of sound in the material. The operator can adjust the response of the transducer as a function of frequency by either programming or loading a frequency amplification curve. Additional system parameters include start and end frequencies in the waveform, duration of the waveform, gate width and position, gain, peak detection threshold, and ultrasonic velocity in the material being inspected.

The UltraSpec system does not have an associated scanner. For the purposes of the ACDP evaluation, the system was interfaced with the MAUS IV instrument and scanner as an external input. Scan speeds and pixel sizes were similar to those used during data collection with the MAUS IV eddy current system. The transducer is mounted in a rubber water chamber assembly, which is fixed to a MAUS probe holder, and rides on the surface of the specimen. This assembly maintains a small gap between the transducer face and the specimen for water coupling. In its present configuration, water is fed into the chamber using a handheld water bottle through an opening at the top of the chamber.

SAIC Ultra Image IV with ACES™ Ultrasound. The ultrasonic method employed in the ACDP program is a conventional pulse-echo immersion technique which uses a high frequency (HF), broadband, focused probe. For application on-aircraft, the Ultra Image IV scanning system, outfitted with the ACES™ scanning head, is used. The Ultra Image IV scanning system consists of a ruggedized, automated X-Y scanner, integrated with an ultrasonic data acquisition/analysis instrument. The ACES™ unit is a water couplant recirculation system that makes the use of standard immersion ultrasonic techniques possible in the field.

The front surface signal is used to synchronize the gate, which is set up to look at the back surface. Data at each location of an inspection is digitized at 100 MHz with 8-bits of amplitude and time-of-flight resolution and is used to generate C-scan images of the inspection. Calibration allows time-of-flight measurements of the back surface signal to be converted to thickness of the skin layer.

SAIC Ultra Image IV with Eddy Current. The eddy current method employed in the ACDP program is a conventional fixed frequency technique using a commercially available eddy current instrument and probe. For application on-aircraft, the Ultra Image IV scanning system is used. The eddy current probe is mounted in a gimbaled holder and attached to the scanner. The coil is maintained at a fixed liftoff distance and the contact surface is protected.

To perform single frequency eddy current inspections, the output of the Nortec 2000 eddy current instrument is fed directly into the external input of the Ultra Image IV system. The frequency is set to give one 'standard depth of penetration' at 80 percent of the thickness of the top layer and the phase angle adjusted to make the liftoff horizontal. The vertical and horizontal outputs of the impedance plane display are digitized at 10 kHz with 8-bits of amplitude. Data at each scan point location is used to generate C-scan images of the inspection.

All Technologies. It was observed during the course of the optimization and test preparation that all of the participating technologies were not mature with respect to the application and were (or are) still evolving to some extent. There was a wide range in the state of the technologies; some of the technologies are currently used in the field or depot while others are laboratory setups or prototypes. Even in the case of the most advanced technologies, preparation for the evaluation raised development issues. Such issues included calibration procedures for thickness quantification, operation procedures for inspection, and registration of the images to the specimens. Several of the technologies did not have a formalized calibration procedure. In some cases, the existing calibration procedures had to be adapted to the application. In several cases the technology had no written operation procedures and would change depending on the operator. Developers were continually changing system components or software prior to the evaluation. Note that the system and the process were held fixed during the formal data collection and so the evaluation is considered a snapshot in time of the capability of each system.

It was also learned that NDE technology developers are in need of access to real aircraft components with moderate levels of corrosion (5-15 percent thickness loss) for future development. Apparently, access to appropriate specimens is limited and so more simply designed specimens that are easily acquired and interpreted are used for development. Furthermore, data from other evaluations conducted have not always been made available for feedback to the developers to advance their technology. Lack of specimen and evaluation feedback is judged to be a serious deficiency in the continued development and optimization of inspection techniques designed to detect hidden corrosion in aging aircraft.

In addition, it was learned that standardization of inspection interpretation is lacking. Standardization of system output, which involves standardization of image registration and calibration philosophies, is necessary for data fusion and for advancements towards automation. Each of the NDE systems tested in the evaluation had very different scan operations, output meanings, and computer-data formats. Some of the systems utilized manual scanners and some had semiautomated scanning systems. For example, the MOI II system was manually operated – the operator pushed the MOI head around randomly while adjusting the bias in order to find defect indications by eye. The PULSE system, as it was being used at AS&M at the time of the evaluation, was also a manually scanned system where the operator scanned the probe across the specimen. In this system, the probe was moved in a regular scan pattern within a X-Y encoded axis. The MAUS, including the UltraSpec system which used the MAUS scanner, and the Ultra Image IV systems were automatically scanned within a small area defined by an X-Y scanning axis. When necessary, the X-Y axis was physically moved to accommodate the scan areas. The x-ray systems were area scan techniques in which the specimen had to be moved to accommodate entire areas. The Line Scan Thermography system could be automatically scanned down any long lengths, but has a scan area height associated with the heat source height and the IR camera view.

The way the scanning system collected data especially effected the image registration requirements. For the evaluation, UDRI had to work with each NDE developer to create image-to-specimen registration procedures. In general, the procedures involved recording the system coordinates and the position on the specimen for the starting and ending points of each inspection. The importance of image registration and the procedures developed for each system are discussed in another section of this report.

The corresponding output meanings and output formats from each of the systems were very different as well. Specialized data analysis procedures and interpretations were required for each NDE system. Examples of actual inspection output values were thickness, voltage, time-of-flight, and scattering intensity. Calibration of the data were unique to the system as well.

Some systems required thickness calibration blocks while others used relative measures. Computer-file formats included bitmap, floating-point, video, and others. The different data-file formats had to be analyzed using different pieces of software and/or different routines. More details surrounding each systems output interpretation and file format is given in Section 3.5.1 of this report.

3.1.2.3 Data Collection

The tests and specimens used for the evaluation were specially selected and designed around the analysis. Data were collected using specific procedures, written prior to the formal test on each system. The test matrix developed, the specimens used, and the procedures followed on the formal evaluation are summarized in this section. Also presented are observations made about each NDE system during the data collection phase of the program. These observations include their potential for future automated corrosion detection application.

Test Matrix. The evaluation is ultimately designed to test the POD for different NDE systems using corroded lap joints and doublers from KC-135 or similar aircraft structures. However, along with this test is a whole matrix designed to provide the information necessary to determine POD using the analysis approach. A fundamental aspect of the analysis is that there is the relationship between the output of NDE systems and the actual thickness loss. Tests were implemented to verify thickness calibration and to verify that the correlation exists. The size of the cell on the inspection article surface that is associated with an inspection image point is based on the spatial resolution of the NDE system. A measurement of the spatial resolution of each system was made to determine the cell size. Although this aspect is not inherent to the analysis, inspection output are potentially influenced by features of a lap joint or doubler. A test of both the edge and fastener effects was implemented to determine the size of the area or zones effected so that they could be eliminated from the analysis. The POD determination requires inspection information on both corroded structures and on noncorroded structures. Tests were established on four-layer lap joints, two-layer lap joints, and two-layer doublers in both corroded and noncorroded aircraft specimens. There also were tests designed for POD using corroded and noncorroded structures with different top skin layer thicknesses.

The test matrix developed is made up of several core tests and secondary tests for repeatability and sensitivity response. For each NDE technique, the test matrix had to be altered slightly to account for differences in calibration procedures and setup parameters. The core tests include: the Setup Verification Test, the Correlation Test, the Resolution Test, the Trial Capability (POD) Test on a Engineered Specimen, the Fastener/Edge Test, and the Capability (POD) Test on a Four-Layer Lap Joint. The core tests were performed by each participating NDE developer. The secondary tests were performed as time permitted and include those tests described in Table 2. The table lists the different tests, the purpose for each test, and the specimens used. A description of the test specimens is given after the table.

Table 2. Test Matrix

Test Name	Purpose	Specimen Used
Setup Verification Test	The purpose of this test was to provide a uniform reference for all inspection systems to verify thickness calibration. The data are potentially useful for providing threshold in the POD analysis. The base material thickness of the top layer was either 0.063 inch or 0.040 inch depending on the test.	ACDP-RS Reference Specimen
Correlation Test	This test was intended to measure the response of the system/process to uniform thickness loss regions ranging from 0 to 50 percent. The purpose of the test is to establish whether a correlation exists between output and thickness loss. The base material thickness of the top layer was 0.040 inch.	ACDP-E1 Correlation Specimen
Resolution Test	The purpose of this test was to estimate the size of independent cells to use in POD analysis and false calls. This series of tests is intended to measure the spatial resolution of the system being tested. The base material thickness of the top layer was 0.040 inch.	ACDP-E2 Resolution Specimen
Capability (POD) on Corrosion Profile Specimen - Trial Test	This test was a trial to evaluate the concept of using corrosion profile engineered specimens to determine POD. It is designed to measure POD under controlled circumstances with known damage. The base material thickness of the top layer was 0.040 inch.	ACDP-E4 Trial POD Specimen
Fastener/Edge Test	This test was designed to determine the dead-response region around each fastener and next to each edge which was then excluded from the POD analysis tests. The base material thickness of the top layer was 0.040 inch.	ACDP-E3 Fastener/Edge Specimen
Capability (POD) on Four-Layer Lap Joint	This test was to measure the response of the system to naturally corroded fuselage skins in a four-layer lap joint configuration. The top skin layer thickness was 0.063 inch.	ACDP-A2 Region 2 ACDP-A4 Region 2
Capability (POD) on Doublers	This test was to measure the response of the system to naturally corroded fuselage skins in a two-layer doubler configuration. For each doubler the top layer thickness was 0.063 inch.	ACDP-A3 Region 1 ACDP-A4 Region 1
Capability (POD) on Doublers	This test was to measure the response of the system to naturally corroded fuselage skins in a two-layer doubler configuration. For each doubler the top layer thickness was 0.040 inch.	ACDP-A2 Region 3 ACDP-A4 Region 3
Capability (POD) on Two-layer Lap Joint	This test was to measure the response of the system to naturally corroded fuselage skins in a two-layer lap joint configuration. The top skin layer thickness was 0.063 inch.	ACDP-A2 Region 1
Repeatability Tests	These tests were designed to verify the repeatability capability of the various NDE systems. The repeatability tests, if performed, were on the correlation specimen or the four-layer lap joint POD specimens.	Testing was not performed on most NDE systems due to time constraints.
Response Tests	These tests were designed to determine the sensitivity of the different NDE technologies to various parameters and variables and to detect any interdependencies between the different parameters. The response tests, if performed, were done on the resolution specimen and the four-layer lap joint POD specimens.	These tests were dropped from the matrix when time was needed to finish core tests.

Description of Specimens. The development and selection of the evaluation test specimens relied on the working theory and operation of the various NDE technologies being tested. A combination of real aircraft lap joints and doublers believed to have areas with and without corrosion and specially designed engineered specimens were chosen for the evaluation. Real aircraft structures were selected since they present the inspection issues faced in the depot. Such issues include multilayered skins in the lap joints and doublers, varying skin thickness within a single structure, the presence of backing structures and back surface coatings, the presence of corrosion byproducts, and the presence of varying types of fasteners. Engineered specimens were included in the evaluation since measurements including the correlation between the NDE output and the actual thickness loss and the spatial resolution of the NDE system are necessary for the POD analysis. The design of the engineered specimens are similar to real aircraft structures with modifications to resolve issues regarding the inspection techniques of the different systems. For instance, the engineered specimens were fabricated to have the same number of skin layers and thicknesses as the aircraft specimens and had a simulated corrosion byproduct where thickness losses were machined (to accommodate the systems sensitive to the presence of the corrosion byproduct). More information regarding the specimen design and selection can be found in *The Evaluation of Hidden Corrosion Detection Technologies on the Automated Corrosion Detection Program*, a paper presented at the Fourth Joint DoD/FAA/NASA Conference on Aging Aircraft, 2000.

The specimens used during the testing are described below as either an engineered or a real aircraft specimen with a brief description and diagram of each.

<u>*Engineered Specimens*</u>. The following were each engineered to represent the same number of skin layers and thicknesses as the aircraft specimens and had a simulated corrosion byproduct where thickness losses were machined. The corrosion byproduct is necessary to accommodate the systems sensitive to the presence of the corrosion byproduct. These specimens were later dismantled during specimen characterization discussed in a later section.

- ACDP-RS Reference Standard Design.
  Two reference standards provide a mechanism to reference the inspection sensitivity to some known level. The first reference standard consists of a 1.6-mm 2024-T3 aluminum alloy plate 30.5 cm-square with four 5 cm-square regions of material removed at approximately 5, 10, 15, and 20 percent thickness loss, respectively. Simulated corrosion byproduct has been introduced, and the plate has been assembled with a second aluminum sheet with no thickness removed to create a two-layer skin configuration. Additional plates can be added to the back to simulate multilayer skin structures. The second reference standard is similar to the first, except that domes of approximately 5, 10, 20, and 30 percent thickness loss, respectively, have been machined into it. The domes remove the sharp edges of the squares and the uniform thickness across the bottom of the artifact. The correlation test specimen is also used as a reference standard for 1-mm top layer skin configurations.

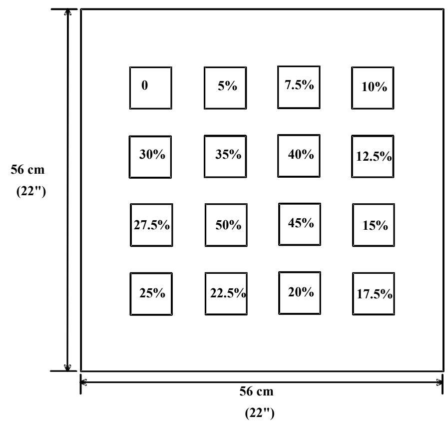

Figure 3. Correlation Specimen Design

- ACDP-E1/RS4 Correlation Specimen.
  This specimen has an array of 5 cm-square regions with depths of material removed ranging from 5 percent to 50 percent. Each square is filled with a simulated corrosion byproduct using sol-gel technology. It is approximately 56 cm-square, made from 1-mm-thick 2024-T3 aluminum alloy, and is assembled in a two-layer skin configuration with a second sheet of as-rolled aluminum.

- ACDP-E2 Resolution Specimen.
  This specimen has been designed with material removed in uniform line sets. Each set consists of three lines of a given width and separated by the same width. The width of the lines within the set is uniform and varies from 2.54 cm wide down to 0.2-mm wide. All lines are machined to a depth of 20 percent of the 1-mm thickness 2024-T3 aluminum alloy sheet. Half of the length of each line is filled with simulated corrosion byproduct while the other half remains empty. The 56 cm-square sheet with the machined line pairs is assembled with a second 56 cm-square to make a two-layer skin configuration.

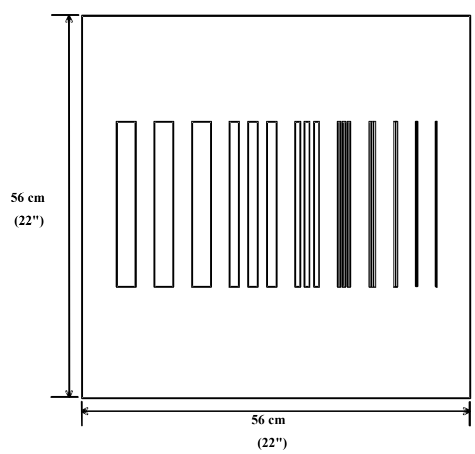

Figure 4. Resolution Specimen Design

- ACDP-E3 Fastener/Edge Specimen.
  This specimen is a 56 cm-square, made from 1-mm 2024-T3 aluminum alloy. There are two

regions where 20 percent of the thickness of the top layer has been removed and filled with simulated corrosion byproduct. The specimen is assembled into a two-layer structure. Two rows of fasteners are installed, one row where there is no material removed, and another in the middle of a rectangular area of material removal. There are several types of fasteners represented including aluminum of different sizes, steel, titanium, flush mounted (countersunk), and protruding. The structure is designed with an edge, the top layer only extending across a portion of the bottom layer. This simulates the edge of a lap joint. Part of this edge contains a region of material removal.

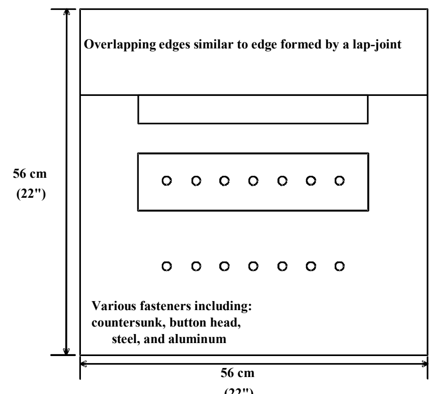

Figure 5. Fastener/Edge Specimen Design

- ACDP-E4 Trial Random Profile Specimen.
  This specimen has been made of 1-mm 2024-T3 aluminum alloy, 30.5 cm-square. Thickness loss ranges from 0 to 18 percent. Simulated corrosion byproduct was introduced and, with a second aluminum sheet, assembled into a two-layer configuration. The same POD analysis was performed on this specimen as was done to the aircraft specimen.

Figure 6. Trial Random Profile Specimen

<u>*Real Aircraft Specimens*</u>. To provide real aircraft specimens for NDE technology assessment experiments, UDRI obtained several sections from a KC-135 and a 707 aircraft fuselage having varied size and condition. From these sections, appropriate specimens were selected according to a number of criteria developed on the program to allow for a well designed experiment to be carried out with confidence.

The selection of specimens was important to provide the inspection technique with proper levels of corrosion and structural configurations that are not too complex. Specimens were desired that contained a variety of corrosion, ranging from minimal thickness loss, to significant corrosion on the order of 10 percent thickness loss or greater. From the many pieces of varied fuselage structure obtained by UDRI, specimens were studied based on configuration and structure, surface condition, and the presence or lack of corrosion.

Specimens having minimal or no corrosion are equally important to the evaluation of a corrosion detection technique. Specimens with no corrosion are useful for the purpose of false call rate measurement. For comparison purposes, these specimens were specifically selected to duplicate the structure found in those known to contain corrosion.

Characterization of the aircraft specimens done following data collection revealed that none of the skin layers inspected did in fact contain the desired 10 percent thickness loss. There were areas that had approximately 7 percent thickness loss. Specimen characterization requires each specimen be dismantled and is discussed in a later section.

- ACDP-A2 KC-135 fuselage POD specimen.
  This specimen was selected from a section located ahead of the wing on the right side of the aircraft. The specimen is approximately 70 cm by 60 cm and all skin materials are 2024-T3. This specimen has a section of lap joint and an area of spotwelded doubler. The lap joint has both a two-layer and a four-layer configuration. The lap joint shows evidence of pillowing and contains two failed rivets and three replaced rivets. Corrosion content was verified by destructively sampling a small section of the lap joint to confirm the presence of sufficient corrosion. This specimen also contains an area of 1-mm skin having a 0.75-mm spotwelded doubler.

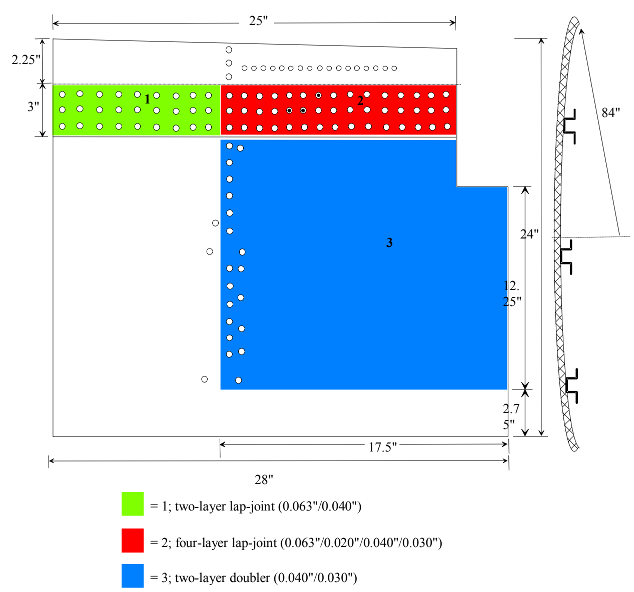

Figure 7. ACDP-A2 Specimen Design

- ACDP-A3 KC-135 fuselage POD specimen.
  This specimen is approximately 60 cm by 76 cm and contains a doubler, a lap joint, and a skin splice. The specimen was located in close proximity to specimen A2, sharing a doubler. For the purpose of this evaluation, only the 1.5-mm skin and 0.5-mm doubler

are of interest. The doubler is approximately 30 cm by 40 cm and contains spot welds as well as aluminum rivets for the stringers and support structure.

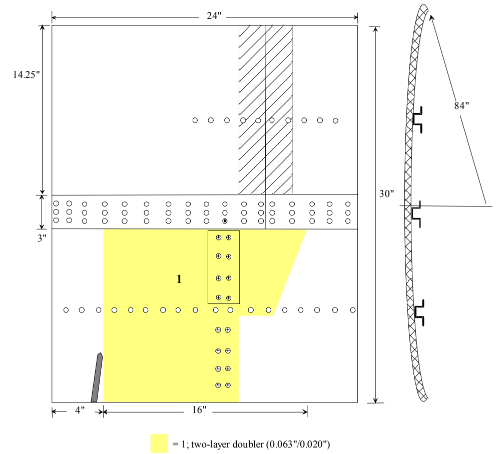

Figure 8. ACDP-A3 Specimen Design

- ACDP-A4 707 fuselage POD specimen**.**
  This specimen was selected from the 707 pieces to have similar structural features as that of the KC-135 pieces. This specimen shares essentially the same skin thickness and structural features as the KC-135 pieces. The specimen is approximately 45 cm by 76 cm and contains a four-layer lap joint, and two independent doublers. Structurally, the specimen is very similar to specimen A2, having a 30 cm lap joint comprised of four layers. The doublers also mimic that of specimen A2, having a 1.5-mm skin and 0.5-mm doubler, and a 1-mm skin and 0.75-mm doubler.

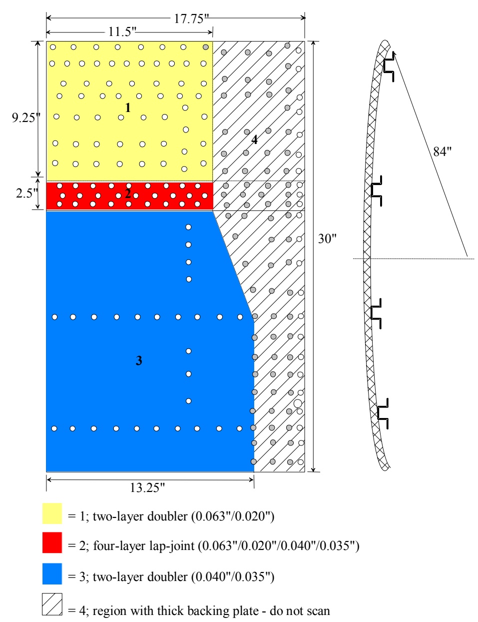

Figure 9. ACDP-A4 Specimen Design

During the testing process, several observations were made regarding the test specimens. Attributes of their design and selection had a direct impact on the results for several NDE systems. The machining process and the simulated corrosion byproduct filler used to manufacture the engineered specimens may not accurately reflect the physical attributes of real corrosion pertinent to the NDE technique. The thermal, ultrasonic, and x-ray techniques seemed to be adversely effected by either the absorbed or transmitted energy into the byproducts. It may be that the coupling between the byproduct and the aluminum is not realistic, which may account for difficulties experienced by some of the techniques. The interpretation of the POD analysis allows for the validation of these types of manufactured specimens to be used in future studies.

A few of the techniques had difficulty with the real aircraft specimens. Some of the difficulties had to do with the specimen size, complexity, and their potential for containing appropriate levels of corrosion. The aircraft specimens are relatively small section compared to the aircraft fuselage. There was a concern that the specimen were not large enough to obtain statistically significant data nor large enough to prevent significant edge effects. On the other hand, for some the breadboard systems, the specimen were difficult to accommodate because of their relatively large size. The aircraft specimens were complex in their structure as they had multiple layers within. Most of the technologies were not experienced in inspecting theses types of structures nor interpreting the data obtained from them.

Testing Procedures. Testing on the formal ACDP evaluation began in late 1998 and continued until the third quarter of 2000. Preparation for the tests on each system took several months. Procedure writing and dry run inspections were the most time consuming. The procedures used to collect the inspection data on all specimens were defined with the assistance of the NDE developers/participants prior to the evaluation in order to impart a controlled test of the ability of the system technology. Each NDE system had its own set of procedures, written specifically to incorporate a complete description of the inspection method, system setup, calibration, and inspection parameter values. The procedures also listed the steps required for specimen mounting, image registration, and data archival, which are vital to the POD analysis. Specific test procedures for each test matrix element were written in checklist form and annotated as the tests were being performed. Information regarding the test setup, system parameters, image registration, timing, and operators were recorded on the checklists. Image registration information was also kept by tracing specimen and system features on transparency film. This information along with photographs of the system and test set-ups provided needed references at later dates when the data were analyzed. A dry run of the test procedures was performed on each system prior to the official or formal data collection for the evaluation.

For all of the NDE technologies except SRI's UltraSpec and SAIC's ultrasound and eddy current systems, UDRI traveled to the developer/participant location to do a dry run of the procedures and to formally take data. Dry run and formal testing at the participants' location was an advantage for equipment and personnel resource availability. Dry run testing of the system and procedures proved to be a valuable and necessary step in the procedures as changes were typically made in system setup, system-to-image registration procedures, and in the written procedures. Before dry run testing, each experiment participant was given a briefing on the program and on the evaluation methodology. Following the formal data collection, a closing meeting was held with each participant to discuss the results.

The tests were performed with several of the NDE participant personnel and several UDRI personnel present. The NDE participant personnel acted as both the inspection operators and the facilitators of the tests. The operators were the individuals familiar with the operation of the equipment and performed the tests according to the procedures. The facilitator was a member of the NDE/I technology development team who is responsible for overseeing the equipment operation, correspondence of the system/process descriptions, and preparing the NDE equipment for the test. UDRI personnel acted as the monitor and as independent witnesses to test. The monitor was responsible for verifying that tests were performed according to protocol and procedures and had decision-making authority during the experiment preparation and execution. Witnesses were needed to complete documentation of the tests as they were performed.

Testing Observations. During the process of taking inspection data with each system, many qualitative observations were made that can be considered just as important as the qualitative results. Qualitative results noted for each system include strengths and weaknesses of the system for automated hidden corrosion detection. Strengths and weaknesses of each system are discussed in the context of the working theory and physical principles of each system and includes the future development plans of the system developers. The observations from each system are briefly discussed below:

<u>AS&M PULSE</u>: In review, the PULSE systems employs conventional pulse-echo ultrasound techniques. It uses a broadband, low frequency focused, transducer with the aid of a recirculating captured water column. Notches in the frequency domain indicate thickness resonance. The main strengths of this system is that it is a single-sided inspection technique that provides an absolute thickness measurement of the top skin layer and that it has good spatial resolution. Other merits of the PULSE system are that it gives a digital image which is easily interpreted, processed, and archived. It also could easily be modified for use in a crawler type robot. Limitations of the PULSE system include extreme sensitivity to setup parameters (such as the gate position and the FFT length) and also to temperature changes in the water. The presence of corrosion byproduct in the engineered structures, and potentially in the real aircraft structures, was also observed to be a complicating issue. It may be that returned resonance energy is damped or transmitted into the byproduct material depending on its coupling with the two aluminum layers. Another drawback to the PULSE system as it was being used for the testing on the ACDP is that it is a slow, manually scanned, system where the operator is instrumental to the process. A total number of 14 test inspections were completed in a weeks time using the PUSLE system. AS&M has worked with NASA Langely to advance the state of this technology. NASA has a similar version of this system that has an automatic scanner. However, there has been no further development underway by either AS&M or NASA.

<u>ARACOR COREX I</u>: The COREX system uses backscatter radiography. A novel aspect of this technology is that is it sensitive to the oxygen in corrosion byproducts through the entire thickness. Its greatest merit might be when it is used to look for corrosion byproducts after a potentially faster technology has found an indication of a disbond or thickness loss. Like the PULSE system, it is a single-sided inspection technique which outputs digital images that are easily handled for post processing and archival. The output of this system, however, not a direct measure of thickness loss which was the test metric. The output is the ratio of Rayleigh to Compton scattering which gives indication of oxygen, or corrosion byproducts, in the specimens. Thickness loss was inferred using an estimate of the oxygen to aluminum ratio the corrosion byproduct. Another shortcoming of this system is that the calibration is time consuming and

complex. It involves setting upper and lower bounds of single channel analyzers. The detection capability is sensitive to standoff and voxel. Radiation hazards would also be a major concern in using this system in the depot. In addition inspections using the COREX are extremely slow. Only seven test inspections were completed after 2-weeks time spent with this system. In order for this technology to become more suitable for depot use, the scan times would have to be decreased. ARACOR has proposed the use of an array of detectors to increase the speed and sensitivity of the system.

WSU Thermal Imaging: Although formal testing was not completed using this system, several observations were made during the dry run testing. This system is a pulsed thermal imaging system which can image areas and uses the premise of a 1-dimensional case where temperature change is inversely proportional to thickness. The strengths of this system are that it is a single-sided inspection technique which is fast and produces a digital image. In addition, the noncontact aspect of the inspection means it could easily be automated. However, the system, as was being used on the program, is limited by the modeling using a 1-dimensional case. The multiple layers and presence of corrosion byproducts randomly changed the expected inverse relationship between temperature and metal thickness. The inspection also requires alteration of the specimen surface by painting it black to eliminate the reflections from the flash. WSU has plans to address the issues brought out during the dry run testing and have proposed to improve upon their camera, flash techniques, and data processing.

PRI MOI Eddy Current: This manual inspection system is a novel eddy current device developed for crack detection that makes use of a magneto-optical sensor to image out-of-plane, secondary induced, magnetic fields produced by gradients in thickness. This technique is a single-sided inspection system that is conducive to rapid area scanning for significant thickness loss. It shows relatively good sensitivity in thin aluminum, especially if inspecting a single layer. The MOI II is limited in sensitivity to thickness loss when there are multiple layers and when inspecting specimens with top skin layers of 0.063 inch. The major disadvantage of this system for hidden corrosion inspection is that it is manually scanned, operated, and interpreted. It actually requires moving the scanner to see corrosion and therefore, is not readily adaptable for post processing, data archival, or automation. There are no encoded axes to record position or image registration information. The calibration has to be adjusted during inspection and interpretation of the images, which contain a nonuniform background, requires training and experience. The imaging unit is sensitive to temperature and orientation with respect to the earth's magnetic field. Due to these disadvantages only six test inspections were completed in week allocated for testing. Although the MOI system tested did not seem well suited for inspection for corrosion, it should be stated that this technology was developed for crack detection and appears well adapted for that purpose. Cracks were found during the inspections of the simpler aircraft structures with the thinner top skin layer using this system. PRI Research and Development Corporation is pursuing new developments on the system for improved corrosion detection. Those developments are aimed at reducing temperature sensitivity of the sensors, removing the appearance of magnetic domains in the image background, and in improving the sensor sensitivity to thickness changes.

Boeing/AFRL MAUS IV Eddy Current: The MAUS IV is one of the more mature corrosion inspection systems. On the evaluation, conventional eddy current methods using two frequencies were applied. The approximate amount of material lost due to corrosion is inferred from the amplitude of an indication compared to that from a calibration reference standard. This system is also a single-sided inspection technique that is sensitive to thickness loss in the top skin layer. The use of dual frequencies provides information on the gap and liftoff. The digital image output allows for data processing and archival. The data output is manually interpreted but could be adapted to work within an automated system. The technique already utilizes an automatic scan process that is relatively fast. A total of 13 test inspections were completed in a weeks time. However, the inspection times are slower than whole frame imaging techniques. Another issue with the MAUS as evaluated is that the calibration and setup used were somewhat subjective and not yet standardized. In addition, the dual frequency to eliminate gap and liftoff were not used either. Future development of this technology include an implementation program at TAFB, better dual frequency algorithms to eliminate gap signal response, and testing of various coil designs.

NASA/Digiray Reverse Geometry X-Ray ®: Digiray's RGX system was tested at NASA Langely. In this technique, the specimen is positioned near the source. It utilizes an electronically scanned x-ray source and a point detector to detect x-rays attenuated while passing through the specimen. This technique is sensitive to the entire thickness of the specimen and not just the top layer. It has very good sensitivity to material loss. The x-ray intensities are converted to thickness losses using calibration curves. The digital image output is ideal for data processing and archival. A major drawback to the use of the RGX technology is that it requires access to both sides of the specimen and may be limited by the radiation hazards. Inspections are done in areas, so they were fairly quick. A large number of inspections were accomplished over the testing period, a total of 20 tests were completed; however, image-to-specimen registration was an issue on the evaluation. Observed during the inspections is that the corrosion byproduct in aircraft specimens may hinder the thickness loss sensitivity. It may be that all of the corrosion byproduct may be retained in between skin layers and consequently all of the original aluminum is still present. NASA has proposed further developments of this technology to aid in corrosion detection. One development is to incorporate a dual energy mode in which there is discrimination between aluminum and other materials such as sealant and insulation. NASA has also investigated the use of laminography.

NASA Thermal Line Scan: This system uses a tubular lamp and IR camera scanned in tandem across the specimen. In the one dimensional case, the temperature is inversely proportional to thickness, at an intermediate time scale. An image is constructed by selecting a column of data from each frame of the camera output as the assembly scans across the specimen. This is a very fast technique in which 24 test inspections were completed. It is a single-sided inspection system which provide for front surface thickness loss measurement. The digital output allows for data processing and data archival. This system would be adaptable for use on a fully automated system. It is limited; however, by apparent issues with the interpretation of the output when there are thick or multilayers and/or corrosion byproducts. Also like the WSU thermal imaging technique, the Thermal Line Scan requires the aluminum surface be painted black to enhance transfer of energy into the specimen. Image-to-specimen registration could be problematic and the spatial resolution is also relatively poor compared to the other techniques. Future developments might include the incorporation of advanced cameras that would reduce data processing requirements and decrease processing times.

SRI UltraSpec: The UltraSpec system is a swept frequency ultrasonic inspection system that uses a dual-element, broadband transducer assembly in pitch-catch mode. The transmitted waveform sweeps through a range of frequencies and records peaks in the frequency response.

The resonance frequencies and the velocity of sound in the material are used to calculate thickness. Some of the attributes of this technique are that it can be used for multiple layers or calibrated to the top layer. It does not have an associated scanner but was easily adapted to the MAUS scanning and data acquisition system for the evaluation. Some of the disadvantages of this technique (as used on the ACDP) is that it had difficulty with thin material top layers and may have been effected by the corrosion byproducts underneath. The spatial resolution of the system was not as good as for the other ultrasonic techniques. The transducer required good perpendicular contact with the surface and relied on a manually applied water coupling. Future developments of the UltraSpec system include establishing procedures for frequency response flattening and a more robust peak search algorithm.

<u>SAIC UltraImage IV with ACES™ (ultrasound)</u>: This system uses conventional high frequency ultrasound in which the ACES water couplant recirculation device makes immersion pulse-echo techniques possible. It uses time-of-flight calibrated thickness measurement. This technique is sensitive to top layer thickness. Like the MAUS IV system, this is uses an automated scanning system that requires manual interpretation. It is a relatively quick, 11 test inspections were completed during the evaluation of this system. However, inspection times were slower that the whole frame imaging techniques. The ACES unit leaves the scan surface dry and can ride over protruding rivets unlike the other contact techniques. The output is in the form of a digital image, which allows for convenient data processing and archival. This technique could be used with a crawler type automated scanner. There were issues in using this system on the evaluation that had to do with the ACES scanner head. It was designed for angled transducers for use on an aircraft wing, but used with a vertically oriented transducer which became a natural trap for bubbles. Air entering the ACES head was also a problem near lap joint edges. The rigid scanner used for the evaluation is heavy and would require multiple people to move and operate. SAIC has proposed several further developments of this system including a redesign of the ACES head to accommodate scans on the fuselage sections and to remove trapped bubbles. They also propose to add a 360-degree rotary head for inspection around fasteners using conventional and phased array probes.

<u>SAIC UltraImage IV with Eddy Current</u>: This system uses the same rigid scanner as the ultrasound technique. It uses a conventional, single-frequency eddy current technique. The probe holder is held against the specimen pneumatically and liftoff is maintained by a felt pad on the bottom of the holder. Changes in amplitude reflect changes in top skin thickness, gap, and liftoff. Like the UltraImage IV UT technique, the eddy current method is sensitive to the top layer thickness and outputs a digital image. Thirteen scans were completed with the eddy current probe. There were less scanning issues with the eddy current probe than with the ACES head. However, the protruding rivets were a problem as well as the felt pad wearing away. As far as the data interpretation, the use of a single frequency during the evaluation did not allow for differentiation between top layer thickness changes and gap. Calibration was performed on single layers. Future developments proposed include implementing dual frequency techniques for multilayer inspection and redesigning probe holders to increase service life. The addition of a rotary scanning head to accommodate fastener hole inspection using conventional and phased array probes is also proposed.

Overall, learned from the data collection process itself is that such exercises are extremely time consuming when care is taken to assert the proper controls. Future studies on this and other test methods for evaluation should consider the following. First, the use of a screening process or the use of a prequalification test would allow for more efficient testing of only those techniques that meet basic criteria. Read more about a proposed Prequalification test aimed at screening NDE technologies and at providing inspection experience on real corroded aircraft sections in Section 3.2 of this report and in the *Automated Corrosion Detection Program Evaluation Report*. Next, perform a dry run and collect only the data necessary for the POD analysis, including repeatability data, in an impartial facility. Finally, select those techniques that show a high probability of detection to be further tested under repeat conditions and under more scrutinizing depot level inspection parameters..

3.1.2.4 Specimen Characterization

Characterization of the aircraft specimens was performed once the inspection data were taken from all the techniques on the program. Specimen characterization is key for obtaining POD information and provides the information on the actual corrosion content within the lap joints and doublers or the “a” in the “a-hat versus a” plot. The aircraft test specimen skin layers were characterized for thickness loss using a digital radiography technique. The steps taken in the specimen characterization process include aircraft specimen preparation, feature registration, specimen cut-up, and fuselage skin layer disassembly, and specimen skin layer cleaning.

The aircraft specimens were first prepared by removing all surfaces coatings. The surface coatings included sealants, primers, and top-coat paints. This step was done first to aid in the cut-up and disassembly steps later on. Chemical removers and light mechanical means were used to remove the surface coatings.

Next, an image registration method for relating the x-ray images on the individual skin layers to the original specimen structure was applied. This image registration method includes drilling small holes in the fuselage pieces before they are cut-up and making a coordinate map of the drilled holes with respect to the specimen edges and rivets. The holes were strategically placed so that two holes would appear in every 4 by 4-inch x-ray image. The coordinate map was obtained using a coordinate measuring machine (CMM).

The aircraft specimens were then sectioned into smaller pieces that were easier to handled. The specimens were cut using electrical discharge machining (EDM) to reduce the kerf (the material lost because of a cut).

Each aircraft specimen section was disassembled into individual skin layers. To take each layer apart, the rivets and spot welds were removed. Careful drilling procedures were developed in order to preserve as much material as possible. Disassembly of all cut sections from the POD specimens gave us a total of 26 specimen layers. Visual observations were made about the condition of the skin layers. Noted were the amount of corrosion byproducts present and the surface roughness due to pitting. As presumed, the most severe corrosion was found in the layers of the four-layer lap joint of specimen ACDP-A2 and little or no corrosion was observed in the four-layer lap joint of ACDP-A4. Corrosion byproducts were sampled from selected specimens for analysis. Both the bulky white (nonsoluble) corrosion products as well as the surface (soluble) byproducts were sampled. The samplings were studied using several techniques including x-ray photoelectron spectroscopy (XPS) and thermogravimetric analysis (TGA). The XPS and the TGA showed similar conclusions on the ratio of oxygen to aluminum content. The conclusion made is that the bulky products were mostly a pseudoboehmite or Al (OH)3.

After some of the corrosion byproducts were sampled, the remaining byproducts were removed. The oxide on the surface would potentially alter the x-ray inspection results. Various cleaning methods were researched and tested to assure that the cleaning process would not alter the specimen surface beyond the sensitivity level of the characterization technique. The cleaning methods used were based on part of the ASTM standard recommendation for cleaning corroded aluminum surfaces. Witness specimens of bare and clad material were placed in the nitric acid with the aircraft layers in order to monitor effects of the cleaning procedures on the base materials.

After the corroded surfaces of the specimen layers were cleaned of corrosion byproducts, they were inspected at Wright-Patterson Air Force Base (WPAFB) using a digital radiography technique. This technique uses a Fein Focus microfocus x-ray source and a Precise Optics' image intensifier detector. Along with the test pieces, the witness specimens that were exposed to the acid and step wedge calibration blocks were inspected along with each aircraft layer. The aircraft specimens themselves were inspected in a series of 4 by 4-inch areas. Data collection procedures with the x-ray system had to be optimized to reduce the effects of scattering. A lead shield in front of the detector and metal frames around specimen edges were used successfully.

Data processing was performed on each 4 by 4-inch x-ray image. First, any background variations were removed from the images by dividing out a background image taken on a piece of as-received bare aluminum alloy just before inspecting the aircraft piece. Next, the x-ray intensity values were converted to thickness values. Micrometer measurements on the step-wedge calibration blocks were modeled against the x-ray intensity values of the same blocks using a 5th order polynomial to give the conversion. Geometric distortions in the data from the x-ray detector were then removed. The correction model used was obtained from an inspection image of a square grid of machined holes with known locations. Finally, the image data were compared to micrometer readings taken on each aircraft specimen layer to determine the bias. The images were corrected for the bias in each case. After the processing is completed the 4 by 4-inch images are pieced together into a single desired image using the registration information gathered.

Characterization of all of the skin layers from aircraft specimens ACDP-A2, ACDP-A3, and ACDP-A4 showed that the maximum amount of thickness loss present came from the top layer of the four-layer lap joint in specimen ACDP-A2. The digital x-ray measured approximately 7 percent thickness loss (of a 63-mil-thick layer) which is less than the desired 10 percent thickness loss for this evaluation.

The actual thickness loss compared to the desired or expected thickness loss represents one shortcoming of the use of real specimens. Aircraft sections made available for this study were carefully selected through visual inspection as well as using a manual eddy current inspection to give reasonable assurance that a certain amount of corrosion was present in certain regions. The true condition of the aircraft structure materials, however, was not known until the disassembly and characterization procedures were completed. As a result, it is recommended that future studies of this or other evaluation methodologies should incorporate the use of multiple specimens in order to assure the presence of the desired amounts of corrosion. This also emphasizes the need to continually look for sources of specimens. Sources may include real corroded aircraft structures, manufactured corrosion profile specimens like those considered in this evaluation, and the possible use of corroded specimen structures grown in the laboratory as proposed by UDRI in the *Automated Corrosion Detection Program Evaluation Report*.

3.1.2.5 POD Data Analysis

The POD analysis is conducted using “a-hat versus a” data. The “a-hat” values are the output from the NDE system and the “a” values are from the x-ray characterization image. For each NDE technology, the inspection images are registered separately against the x-ray images of the four-layer lap joint. Image registration involves correcting the inspection images for alignment, orientation, and distortion to match the x-ray images.

Once an inspection image is registered against the x-ray, a collection of cells is defined using the appropriate cell size for each NDE system. Cell size is based on the spatial resolution and the inspection step-size and is directly measured during testing of each NDE system. The collection of cells is selected so that the specimen region of interest is covered with no overlap. The region of interest in each case excludes the fasteners and the fastener-effected zones. The routine created to carry out this process randomly selects a candidate cell location on the specimen and then tests this location for overlap and for distance from fastener-effected zones. Any candidate cells that fail these tests are rejected. Actual thickness loss values for each cell are calculated by averaging the calibrated thickness loss values from the composite x-ray image within each cell.

The actual thickness loss average (a) within each cell is paired with the corresponding system output (a-hat) which is the NDE system output value at the center of each cell. The data sets generated for each technique are then evaluated using either an “a-hat” analysis or a “pass/fail” analysis.

The “a-hat” analysis uses several assumptions. The assumptions were tested using statistical means for each NDE system’s data set. When the assumptions are not valid, the POD curves are estimated using the pass/fail analysis. The assumptions required to perform the “a-hat” analysis include the following:

- The relationship between “a-hat” plotted against a values is linear.
- The distribution of “a-hat” values about the mean trend is normal (Gaussian).
- The variance of the normal distribution is constant over the range of thickness loss values being tested.

The detection threshold for the POD analysis was selected to achieve a 90 percent probability of detecting a 6 percent thickness loss. A test for 10 percent thickness loss detection capability was originally desired but had to be redefined when the POD specimens only contained 7 percent thickness loss. For this evaluation, 6 percent thickness loss detection capability was tested. Determination of the threshold value is illustrated through the schematic representation in

Figure 10. This schematic shows a linear trend with a Guassian distribution at a_2. Assume that a_2 is 6 percent thickness loss (as required for this evaluation), the threshold is drawn so that 90 percent of the “a-hat” values lie above it. The y-intercept of the linear trend is considered the baseline. The scatter in the “a-hat versus a” data, or the amplitude about the trend, at 0 percent thickness loss is a measure of the system noise level. The discrimination capability is related to the difference between the noise level and the threshold. It should be verified that the threshold for detecting 6 percent thickness loss 90 percent of the time is above the system noise level.

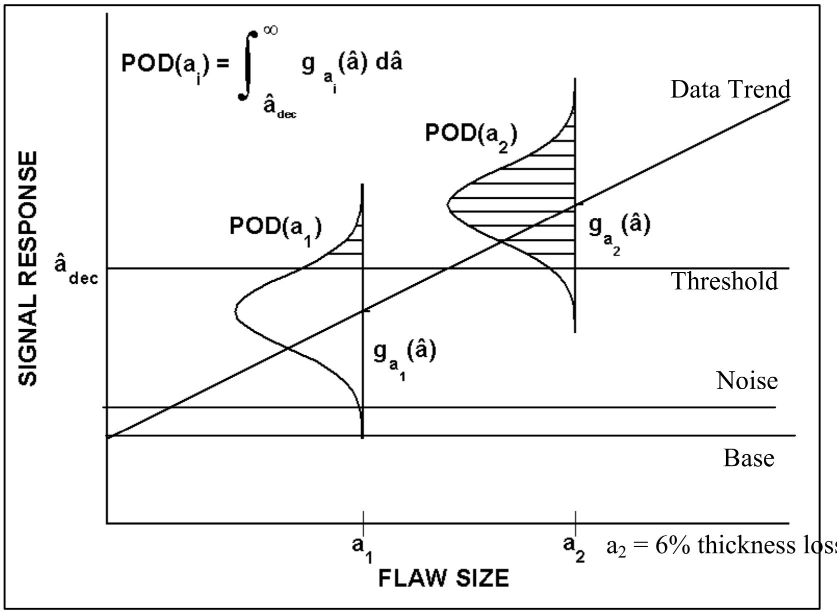

Figure 10. Conceptual Plot of the Signal Response (a-hat) as a Function of Flaw Size (a)

The POD curve is generated from the cumulative area under the normal distribution model of the residuals at each thickness loss. A schematic representation of a POD curve is shown in Figure 11. The POD curve gives information on the discrimination capability of the system. Discrimination is the ability to detect a target thickness loss with a high POD while ignoring lower levels of thickness. Discrimination capability is manifest in the steepness of the POD curve and can be quantified by the parameter sigma. The various aspects of the POD curve are described as follows:

- The thickness loss at a 90 percent probability is a convenient point to consider. In the analysis described above, the POD curves for all of the techniques should cross the point of 90 percent probability at 6 percent thickness loss, "a(90)."
- The point at 50 percent probability on the POD curve is representative of the thickness loss value that should be detected 50 percent of the time, "a(50)" which is also the point where the threshold crosses the trend in the "a-hat versus a" data.

Sigma is related to the steepness of the POD curve through the a(50) value. It is the standard deviation of the "a-hat" values (which are described by a normal distribution about the trend) divided by the slope of the linear trend which describes the a-hat data. Small values of sigma convert to a steep POD curve.

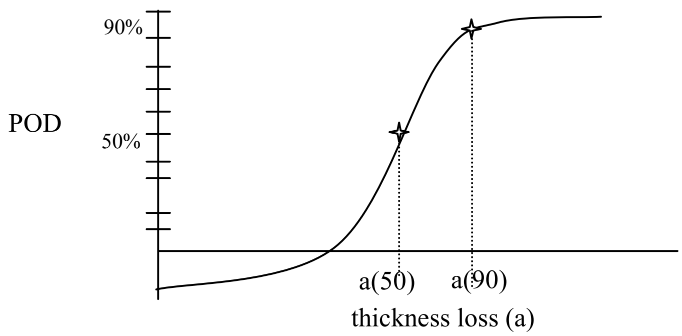

Figure 11. POD Curve

The POD analysis method as outlined above, makes use of the average thickness loss within inspection cells, which are defined according to the spatial resolution of the system. So while the metric is a measure of the extent of corrosion in an aircraft skin, different cell sizes defined for the different NDE systems will result in different characterized damage states being reported for the same region on the aircraft. This makes comparison of the probability of detection results between technologies problematic. Systems with different spatial resolutions are being evaluated against different attributes of the same corrosion condition. A quoted probability of detection is understood to apply to thickness loss over the corresponding cell size. Thus, the reader should be cautioned that the POD results from the various NDE systems should not be directly compared due to the use of cell sizes based on spatial resolution of each NDE system. Although a direct comparison between NDE systems is not the focus of this evaluation, it is the eventual goal to use POD analysis methods to make direct quantitative comparisons. Several proposed techniques for using the data collected for directly comparable POD based on a given defect defined by both thickness loss and area are given in the *Automated Corrosion Detection Program Evaluation Report***.**

3.1.3 Results

The inspection results obtained during the evaluation process are given in three sections. The first section describes the results from the tests considered critical for determining the parameters used in the POD analyses. The second section presents four-layer lap joint POD inspection results and the analyses results. The third section describes the results for one of the ancillary tests performed on the machined POD trial specimen. POD results are only given for the most promising techniques formally tested on the evaluation. Data and results for the other test types described in the evaluation procedure section of this report are not presented here as they were supplementary tests and were not critical to the POD analysis. These data are, however, available for future analysis. It should also be noted that the results presented here are relevant to the particular application of hidden corrosion detection as being addressed by this evaluation study and are representative of the system capabilities recorded at the time the data were collected.

3.1.3.1 Critical Inspection Results

A summary of the inspection results from the tests considered critical for the POD determination and thus, for the evaluation process is given in Table 3. Those critical inspection parameters are the results from the correlation, resolution, and fastener/edge tests. The data presented in the table are the parameters used in the independent POD analyses for each technology and are discussed further in the following sections.

Table 3. Summary of Inspection Results

NDI System Developer	NDI System	Technique	Correlation (Y or N)	Resolution (cell size used)	Fastener/Edge (fastener zone)
AS&M	PULSE	Ultrasonic	Y	0.23” / 0.31”	o.40”
ARACOR	COREX I	Radiography	Y	0.58”	0.60”
WSU	Thermal Imaging	Thermography	---*	---*	---*
PRI	MOI II	Eddy Current	Y**	0.25**	___**
USAF/Boeing	MAUS IV	Eddy Current	Y	0.34”	0.54”
NASA	Line Scan Thermography	Thermography	N	0.58”	0.60”
NASA	Reverse Geometry X-Ray ®	Radiography	Y	0.11”	0.40”
SRI	Ultraspec	Contact UT	Y	0.31”	0.61”
SAIC	Ultra Image IV (UT)	Ultrasonics	Y	0.11”	0.40”
SAIC	Ultra Image IV (EC)	Eddy Current	Y	0.38”	0.56”

*Thermal Imaging at WSU was not formally tested on the ACDP
**MOI is not a quantitative method, uses visual observations

Correlation Results. The correlation test was performed to confirm and demonstrate a correlation between system output and thickness. This correlation is a fundamental aspect of the POD analysis. For each NDE system the thickness output information, reduced from the inspection images, was plotted against the actual thickness of each square machined in the correlation specimen to show the relationship. Refer to Section 3.1.2.3 above for a description of the correlation specimen. An example of the data obtained from the correlation test is given in Figure 12. The figure shows the inspection image and the plot that illustrates the correlation for Boeing’s MAUS IV/eddy current system using HF. The test data from the MAUS IV/eddy current system showed a relationship between output and thickness that could be modeled.

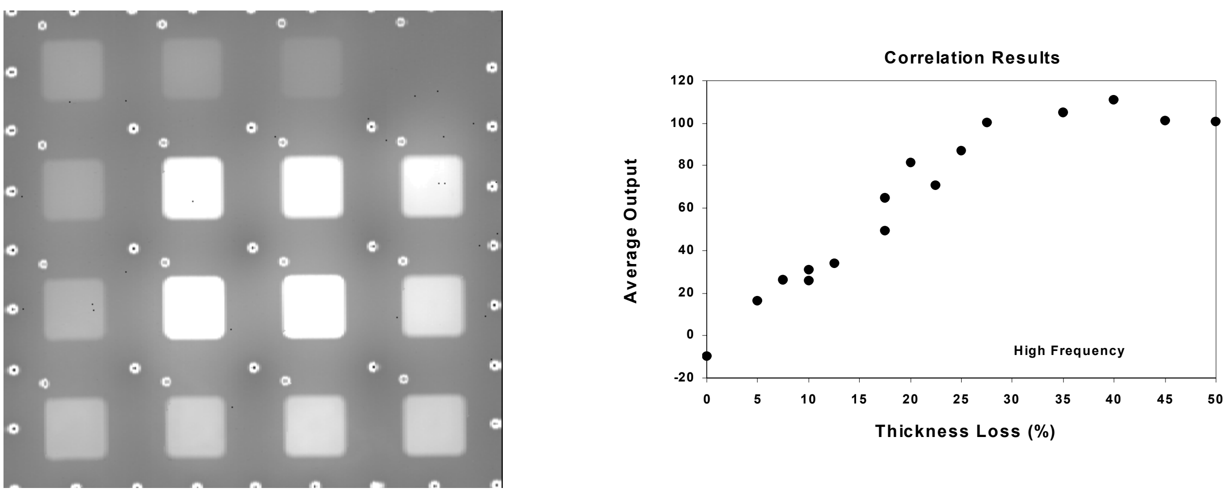

Figure 12. MAUS Correlation Inspection Image and Data

The correlation results are summarized in Table 3 as either a Y (when a correlation was determined) or a N (when no correlation was determined). The test data from all systems formally tested on the ACDP showed a correlation except for NASA’s Thermal Line Scan technique. With no apparent correlation between system output and thickness, the POD analysis was not applicable to the data from Thermal Line Scan technique. WSU's Thermal system was not formally tested and therefore no critical inspection or POD data are given for this technique. The data from PRI's MOI II system was interpreted visually using a hit-or-miss observations since the output is not quantitative. The image and thickness loss data for each of participant NDE systems are shown and discussed in more detail in the *Automated Corrosion Detection Program Evaluation Report*.

Resolution Results. The resolution test was performed to obtain a value for the 2-dimensional spatial (X-Y) resolution for each NDE system. The spatial resolution of the system is needed for determination of the cell size for the POD analysis. The cell size is based on the spatial resolution and the inspection step size. For each NDE system the thickness output, information was reduced from the inspection images and plotted over the length of the specimen to show the response profile across the machined line-pairs. Refer to the description above in Section 3.1.2.3 for the resolution specimen. A plot of the modulation between the maximum and minimum output was then used to determine where the response drops by 10 percent for each technique. This criterion, in conjunction with the flatness of the maximum and minimum response in the profile plot at the machined lines, was used to determine the spatial resolution.

An example of the data obtained from the resolution test is given in Figures 13 and 14. The figures show the inspection image and the plots that illustrate the resolution for Boeing's MAUS IV/eddy current system using HF. The MAUS IV/eddy current system shows that the smallest resolvable line-width is between the 0.5 and 0.25 inch. The maximum and minimum response is fully resolvable for the 0.5-inch line-width where they are not for the 0.25-inch line-width. The modulation plot shows that at a 10 percent drop in modulation the smallest resolvable width is approximately 0.34 inch. Further determination of the cell size used in the analysis on the MAUS IV/eddy current data took into consideration the pixel size of the inspection image.

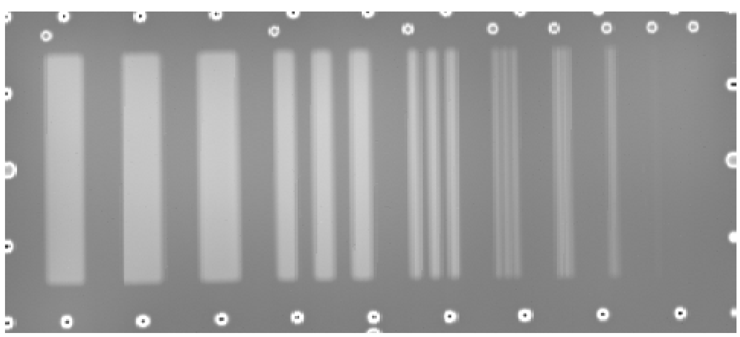

Figure 13. MAUS Resolution Inspection Image

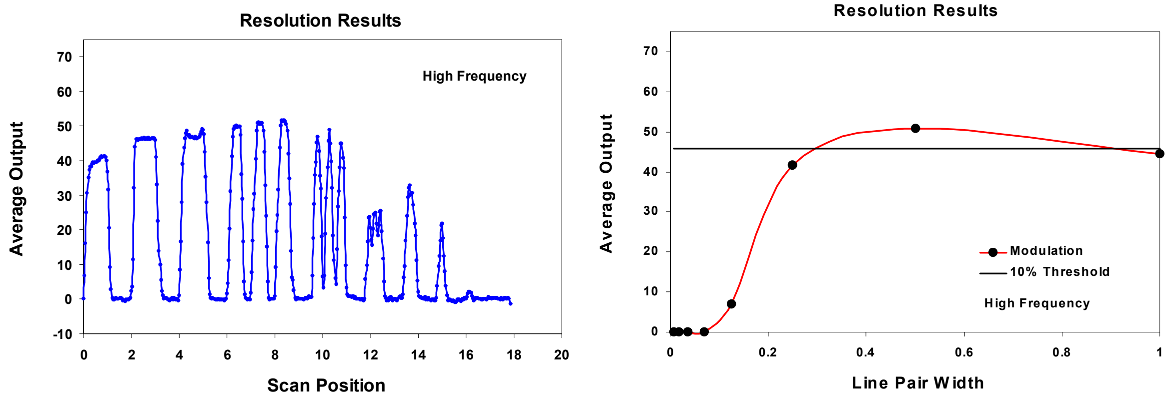

Figure 14. MAUS Resolution Data

The cell size determined for each of the techniques formally tested is shown in Table 3. The cell size for the MOI II system was estimated from visual observation of the video data output. The cell sizes shown in the table are actually the resolution size determined from the test with an adjustment for the inspection step size. The appropriate cell size for each system differs based on the physics of the technique and the operation of the system. As a result, a direct comparison of the POD calculated for each NDE system would be inappropriate since the "a" values for the different systems would not be the same. The two systems that had the best resolution and therefore had the smallest determined cell size of 0.11 inch was the Reverse Geometry X-ray system and the Ultra Image IV system using ultrasound. The image and resolution data plots for each of participant NDE system are shown and discussed in more detail in the *Automated Corrosion Detection Program Evaluation Report*.

Fastener/Edge Results. The results from the fastener/edge test are used to determine the fastener and/or edge effected zone in the system output near these types of features on the aircraft specimens. The area of the effected zone was excluded from the images before the independent cells were selected. Exclusion of the effected zones is important since the physical nature these features changes the type of inspection being conducted and presents the need for different analysis methods. The fastener/edge specimen included the opportunity to test fasteners of different types and materials and to test these fasteners in areas where thickness was removed and in areas with no thickness loss. Refer to the specimen description in Section 3.1.2.3. The zone sizes used in the POD analysis were determined from those fasteners on the fastener/edge specimen that were similar to those in the aircraft specimens inspected. When zone sizes were found to be different depending on thickness of the top skin layer, the more conservative estimate was used.

An example of the high frequency data from the MAUS IV/eddy current system on the fastener/edge specimen is shown in Figure 15. The fastener-effected zone is shown to extend out a radius of approximately 0.27 inch from the fastener center. Therefore, an effected zone with a diameter of 0.54 inch was applied to the data set over each fastener center. The diameter of the fastener-effected zone determined for each of the NDE systems is shown in Table 3. The edge-effected zone sizes were not necessary for the POD analyses and are not given. Like the cell sizes, there is a range of effected zone sizes for the different techniques. Similarly, the

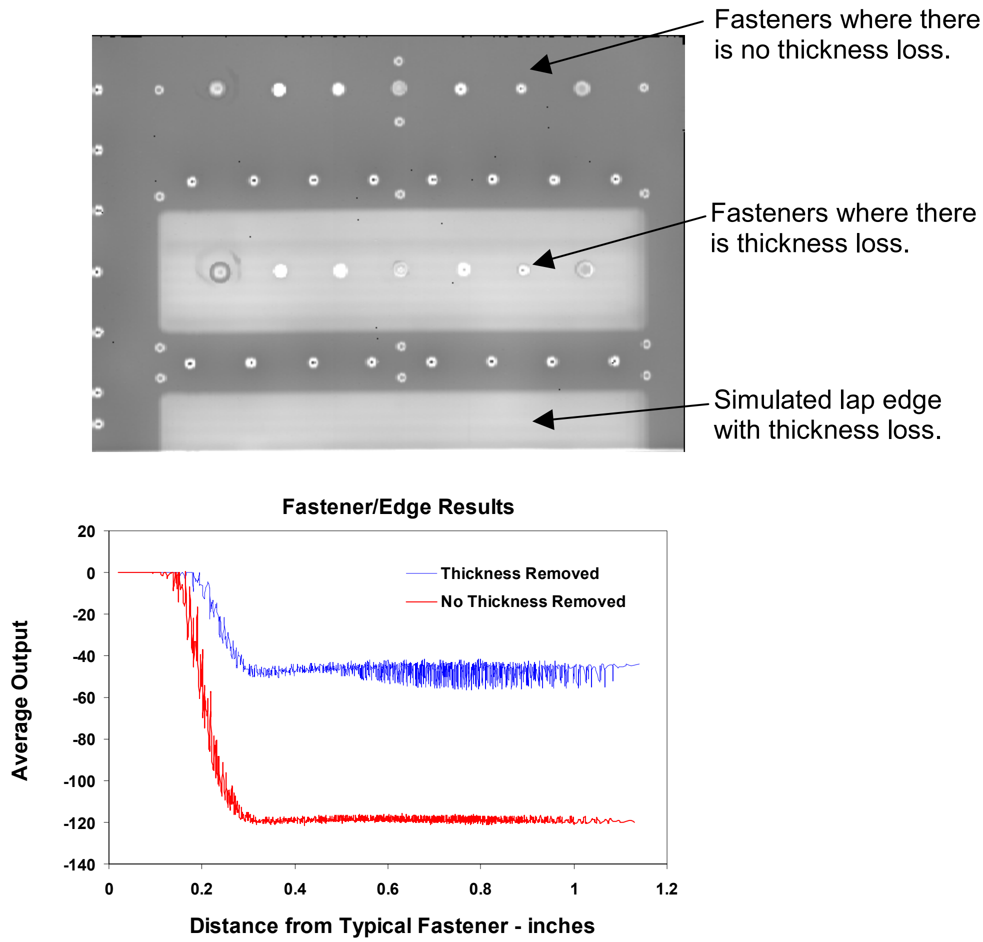

Figure 15. MAUS Fastener/Edge Inspection Image and Data

fastener-effected zone sizes are related to the physical principles of system operation. The systems that showed the least amount of adverse effects by the presence of the fasteners were the PULSE and Ultra Image IV ultrasonic systems and the Reverse Geometry x-ray system. For each of these techniques, the fastener-effected zone was 0.40 inch over each fastener location. The image and fastener-effected zone data plots for each of participant NDE system are shown and discussed in more detail in the *Automated Corrosion Detection Program Evaluation Report*.

POD Inspection and Analysis Results. Inspection results from the four-layer lap joint POD test are shown in Figures 16 and 17. The results are shown from all of the NDE systems that were formally tested except for the MOI system. The MOI inspection data are video format and cannot be shown here. Figure 16 (a) shows the enhanced composite x-ray image from the four-layer lap joint of specimen ACDP-A2 and Figure 16 (b) shows the inspection images from that lap joint. Figure 17 (a) shows the enhanced composite x-ray image from the four-layer lap joint of specimen ACDP-A4 and Figure 17 (b) shows the inspection images from that lap joint. Qualitative comparisons can be made regarding the detection capability of each NDE technology with respect to the radiography image.

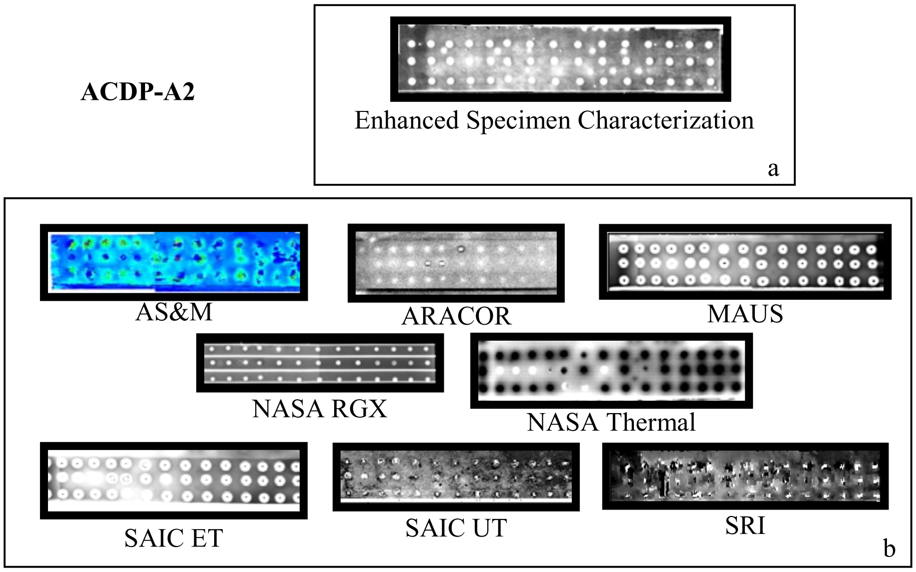

Figure 16. ACDP-A2 Inspection Images

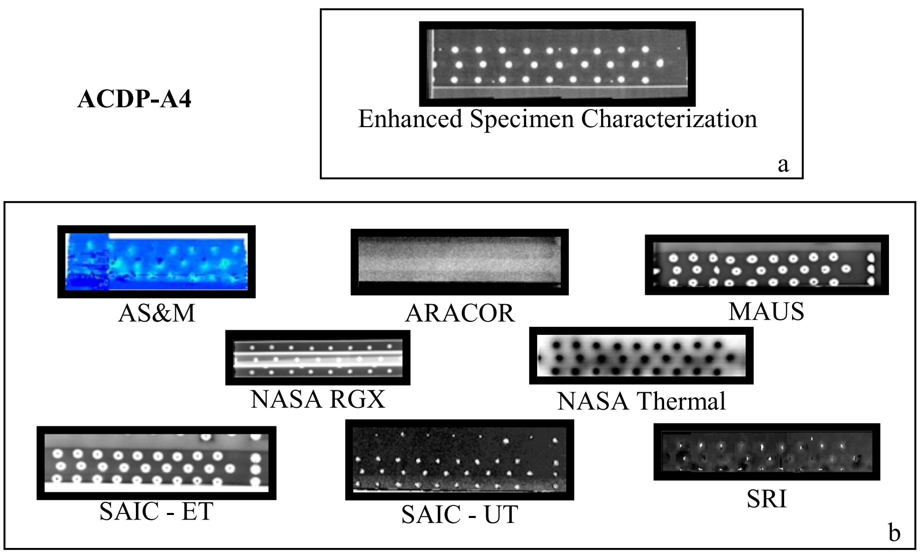

Figure 17. ACDP-A4 Inspection Images

The top layer of the four-layer lap joint from specimen ACDP-A2 was observed to have moderate to severe corrosion and was the most severely corroded specimen out of all specimen layers. Indications of corrosion are shown lighter in contrast on the x-ray image. In Figure 16 (b), indications of thickness loss can be identified in several of the inspection images. A few of the technologies do not show any indication of the corrosion present. The top layer of the four-layer lap joint from specimen ACDP-A4 had a corrosion free surface. In general, none of the NDE technologies detected thinning in this specimen. Two technologies did give what appear to be low level indications.

From the inspection images of ACDP-A2 and ACDP-A4 the “a-hat versus a” analysis was performed for each of the NDE systems, except for PRI’s MOI II system. The analysis was not preformed for the MOI system since the video-recorded data from the MOI was difficult to interpret and to apply within the scope of the evaluation. Furthermore, at the time of the testing, the operator did not identify any corrosion indications on the POD specimens with the MOI system. Although no correlation was measured between the output and the actual thickness loss for NASA’s Thermal Line Scan system, these data are discussed further. POD’s were only determined for the top layer of the four-layer lap joint of specimen ACDP-A2 for each system. The surface of the layer from ACDP-A4 was corrosion free and therefore, these data were used to determine the system noise level.

For each NDE system, the cells were defined (after excluding the fastener-effected zones from the image) using the corresponding cell size determined from the spatial resolution and the step size of the system. The actual thickness loss average (a) within each cell was paired with the corresponding system output at the center of the cells (a-hat). The data pairs for each inspection were then evaluated using the AHAT or a “pass/fail” analysis. The applicability of these analyses is briefly described in an earlier section. More detail describing the POD analyses can be found in the *Automated Corrosion Detection Program Evaluation Report*. An example of the data used in the POD analysis for the MAUS IV/eddy current system is given in Figures 18 (a) and 18 (b).

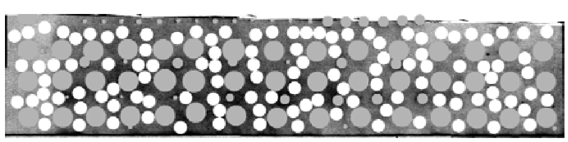

(a)

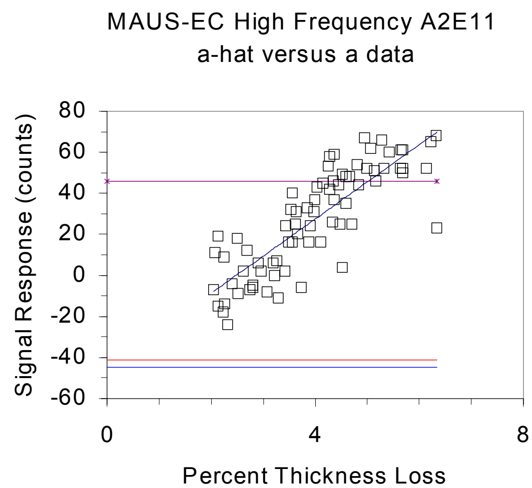

(b)

Figure 18. MAUS Analysis

Figure 18 (a) shows the cells as they were defined for the MAUS IV inspection data of ACDP-A2. The cells avoid the fastener-effected zones and do no overlap each other. The plot in Figure 18 (b) shows the “a-hat versus a” data for specimen ACDP-A2 using the high frequency tested. A linear model of the trend is used and the data about the trend is modeled as a normal distribution with a constant variance. The data trend, the signal baseline, and the noise level are shown on the plot. There is a relatively small amount of scatter in the data compared to the slope of the trend. The scatter in the data is a function of the characteristics of the corrosion profile and the system background noise. The threshold was set at an “a-hat” value of 45.9 such that 90 percent of the data is above the threshold at 6 percent thickness loss. The actual thickness loss value where the threshold crosses the trend, the "a(50)" value, is 5 percent. The plot in Figure 18 (b) shows the "a-hat versus a" data for specimen ACDP-A4 using the high frequency tested. There was no corrosion profile on this specimen and therefore, the scatter in the data represents the noise in the system response. The amplitude of the noise response is small. It was determined further that the threshold is set well above the noise level for this system.

The POD curve generated for the MAUS IV/eddy current system using the high frequency tested is shown in Figure 19. The POD curve is the cumulative area under the normal distribution model of the data at each value of thickness loss. The 95 percent confidence bound is plotted as well. The difference between the "a(90)" and "a(50)" value is a descriptor of the discrimination capability.

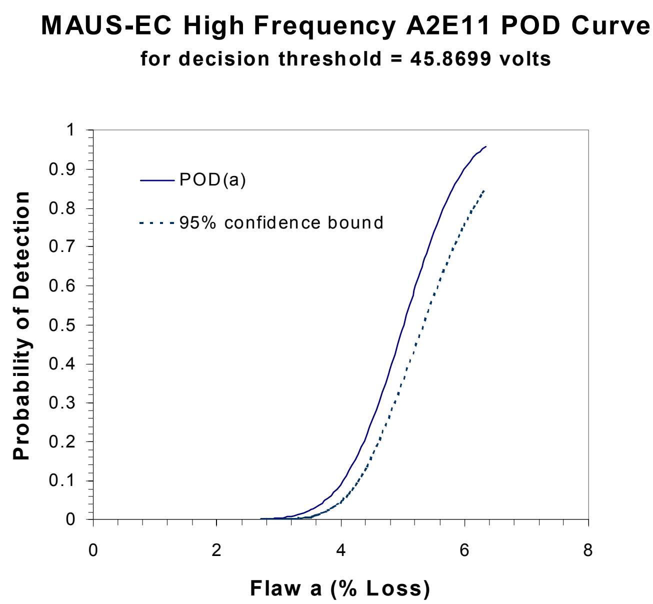

Figure 19. MAUS POD Curve

POD curves were not generated for all of the techniques. As discussed earlier, the MOI system data showed no corrosion indications for specimen A2 and the data were not applicable. Three of the other techniques:

- NASA's Thermal Line Scan
- Reverse Geometry X-ray (RGX)
- ARACOR's backscatter x-ray

have "a-hat" versus "a" data showing very large scatter in the data compared to the slope of the trend. This is an indication that there is a lack of a correlation to the thickness metric. The "a-hat" versus "a" plots for these three systems are shown in Figures 20 (a), 20 (b), and 20 (c). The sensitivity of these techniques may have been influenced by the corrosion byproducts. In the case of the Thermal Line Scan technique, the thermal properties of the corrosion byproducts may have changed the behavior of the temperature profile by thermally loading the back surface of the top skin layer. The sensitivity of the RGX technique may have also been adversely effected because the aluminum still remains within the corrosion byproducts between the layers.

Therefore, the system does not detect a loss of material. In the case of the backscatter x-ray technique, there may not have been a sufficient amount of byproducts present to achieve appropriate responses. This has to do with the principles of operation of the system and the method used to translate output to thickness loss.

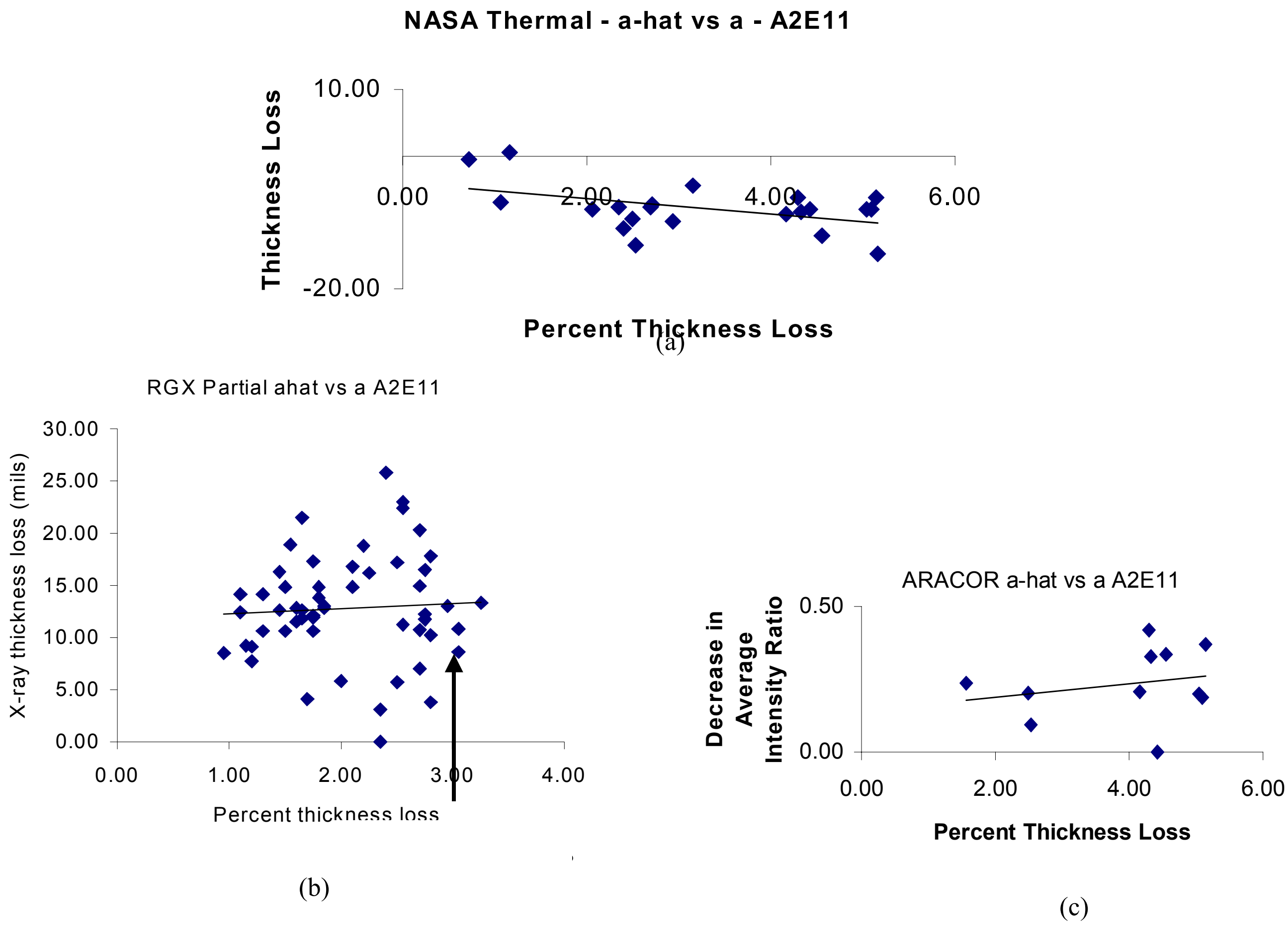

Figure 20. A-Hat vs. A Analysis

The pertinent results from the POD analysis for the techniques that are considered the most promising in terms of POD and the evaluation performed on the ACDP are given in tabular form in Table 4. Of the techniques included in this table, there are three systems that use ultrasonic methods and two systems that use eddy current methods. The output from the two EC systems and the SRI-UT system were analyzed using the "a-hat" analysis. The output from the SAIC-UT and the AS&M-UT had to be analyzed using the pass/fail analysis as it did not apply to the normal distribution model. The information in the table provides discrimination capability information. Listed are the a(90) percent thickness loss values used (approximately 6 percent thickness loss), the a(50) percent thickness loss values (for a threshold at a(90) for 6 percent thickness loss), sigma values (steepness of the POD curve through a(50)), and signal-to-noise (S/N) ratios at the threshold. Again, the values given for each technique are not directly comparable since the cell sizes used to generate the POD data are system dependent.

Table 4. POD Analysis Results

Technology	a(90)%	a(50)%	Sigma	S/N
SAIC-ET	6.0	5.2	0.62	17.0
MAUS-ET	6.0	5.0	0.77	25.0
SAIC-UT	5.6	4.1	1.19	3.7
AS&M-UT	5.6	4.0	1.11	2.2
SRI-UT	6.0	4.6	1.27	9.2

From the table, it can be observed that for two of the UT systems, SAIC-UT and AS&M-UT, the a(90) values were not exactly 6 percent thickness loss. It was not possible to threshold for 90 percent probability at 6 percent thickness loss for the output of these systems due to the discrete nature of these data. For the same reason, the a(50) values are also lower for those systems. The difference between the a(90) and a(50) values is related to the slope in the POD curve and so is sigma. A small sigma value represents a steep curve and thus, a good discrimination capability. A larger value of sigma means the scatter in the "a-hat" data about the trend is larger, and thus the discrimination capability is lowered. The two EC systems had the smallest sigma values and SRI-UT had the largest. The S/N values represent the difference between the noise level and the threshold. A larger signal-to-noise ratio means there is less interference to the thickness loss measurement due to system noise. The MAUS-EC and the SAIC-EC systems showed the largest S/N ratios over the UT systems. Of the three UT systems, SRI-UT had the largest S/N value.

The discrimination capability results as shown in Table 4 can also be represented visually through a comparison of the system images to the characterization image after being filtered for threshold. Each system's image was replotted to show only the thickness loss detected above the a(90) percent threshold. The output values that were above the threshold were plotted as white pixels and the output values that were below the threshold were plotted as black pixels. The actual corrosion profile image was replotted using two different thresholds. The first threshold was at 6 percent thickness loss for comparison to those techniques with a(90) values of 6 percent. Pixel values that were 6 percent or greater were plotted white. The image was also threshold at 5.6 percent thickness loss for comparison to the SAIC-UT and AS&M-UT systems. A visual comparison of each system's re-plotted image to the re-plotted characterization image illustrates what is observed from Table 4. The images that were threshold for 6 percent thickness loss are shown in Figure 21. The images filtered for 5.6 percent thickness loss are shown in Figure 22.

The SAIC-EC threshold image shows several localized clusters of thickness loss which appear to lie within the regions of 6 percent thickness loss identified by the x-ray characterization image. There are several areas where the inspection system did not detect 6 percent thickness loss, which is shown on the actual profile. The MAUS-EC system shows fairly good discrimination. The main cluster of white pixels shown in the MAUS-EC threshold image is very close in shape to the actual 6 percent thickness loss cluster. The two eddy current techniques had larger fastener-effected zones and at the same time relatively small pixels sizes.

A comparison between the images from the SAIC-UT system and from the x-ray shows that the SAIC-UT does not discriminate well between the different levels of thickness loss. Thickness loss indications do surround areas where there are observed clusters on the x-ray image but there are also many indications where no thickness loss is observed on the x-ray image. The resolution capability of this system is good and therefore thickness loss indications are very clearly differentiated from the fasteners. A comparison of the AS&M-UT ultrasonic

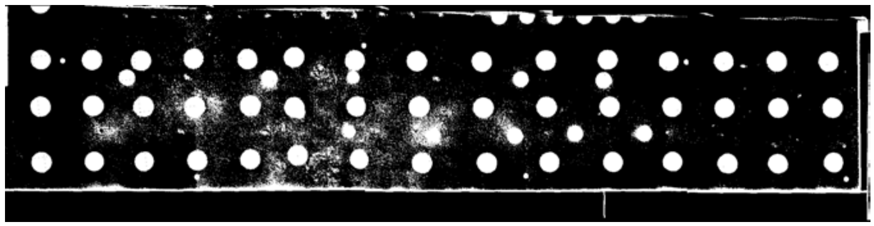

(a) Specimen Characterization

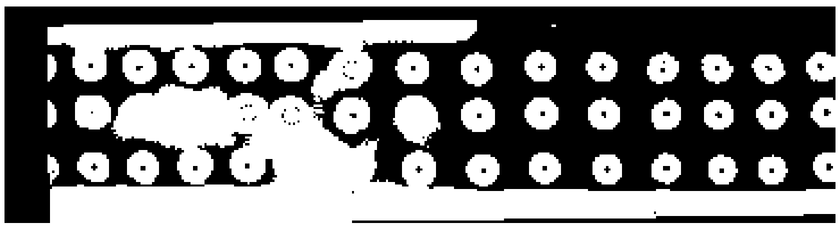

(b) SAIC-ET

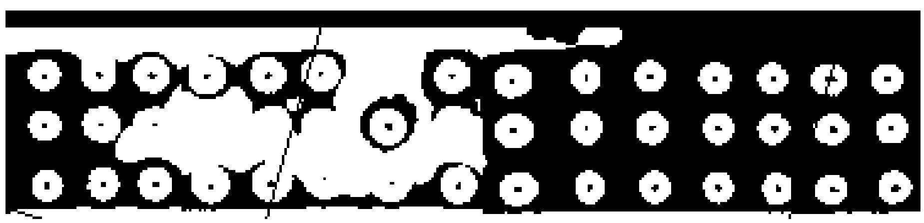

(c) MAUS-ET

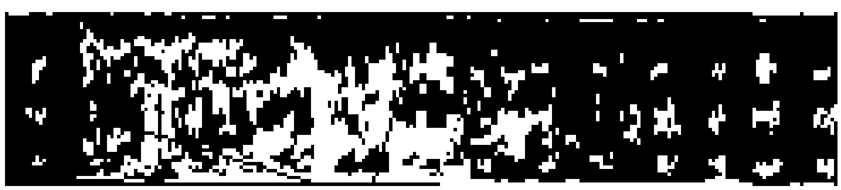

(d) SRI-UT

Figure 21. Threshold at 6 Percent Loss

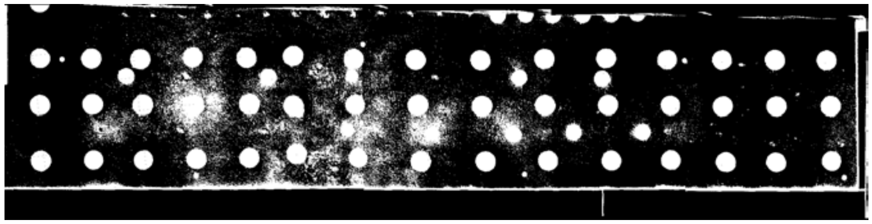

(a) Specimen Characterization

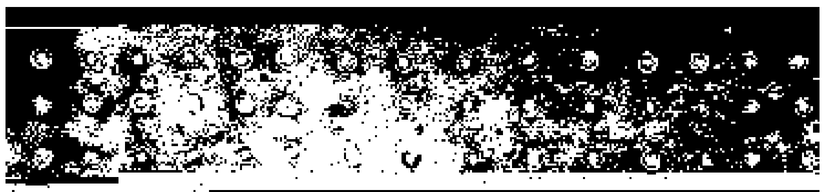

(b) SAIC-UT

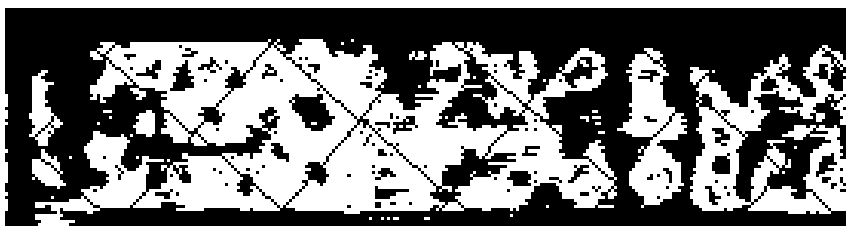

(c) AS&M-UT

Figure 22. Threshold at 5.6 Percent Loss

system to the x-ray characterization filtered image shows that system does not effectively discriminate accurately between 5.6 percent and smaller amounts of thickness loss. A majority of the inspection image has white pixels, even in areas where the actual profile shows no indications of 5.6 percent thickness loss. The filtered image from the SRI-UT system shows clusters of white pixels in similar areas as the x-ray image does. There are no large clusters of corrosion indications where there is none identified in the actual profile. The large pixel size and aspect ratio of the features in the SRI-UT image does make it difficult to discern which indications are fasteners and which represent thickness loss.

Trial POD Results. The POD concept was also tested on an engineered trial specimen. This specimen had a random surface profile machined in it to simulate a corrosion cluster. Refer to Section 3.1.2.3 above for a detailed description of the POD trial specimen. The significance of looking at a manufactured corrosion specimen is to test the possibility of using a specimen with a known corrosion profile that is easily produced and readily available. The POD for the trial specimen was only determined for the same five techniques as was determined for the aircraft specimen. The inspection image of the POD trial specimen obtained from the MAUS IV/eddy current system is shown in Figure 23. From the image the general clusters of thickness loss can be seen. The cell selection image and the plots generated from the POD analysis are given in Figures 23 (a), 23 (b), and 23 (c) below.

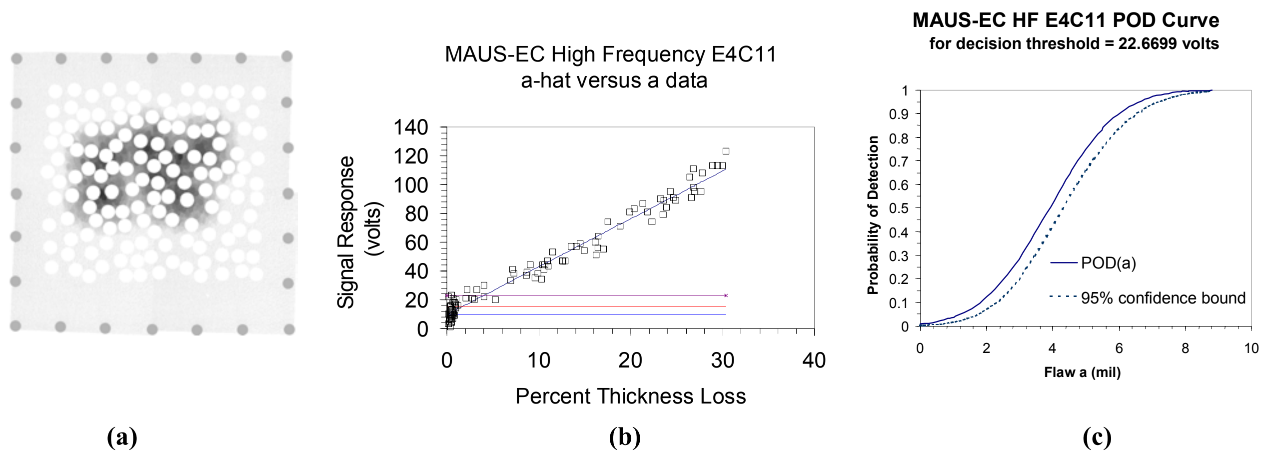

Figure 23. Trial POD Results

To determine the successfulness of using a manufactured specimen for POD assessment, a comparison would need to be made between the POD results of the engineered specimen to the POD results from the real aircraft corrosion specimen. However, this comparison would not be appropriate for the data analyzed to date. The POD for the four-layer lap joint on specimen ACDP-A2 represents that for a top layer thickness of 0.063 inch and the POD trial specimen inspected had a top layer of 0.04 inch. Inspection images for each technique were acquired on real corroded aircraft specimens with a top layer thickness of 0.04 inch and are available for future analysis.

3.1.4 Discussion

It was the goal of this evaluation to perform a POD analysis for each NDE system and to validate the evaluation methodology. There are several assumptions involved in the evaluation using a probability of detection determination. The success with which these assumptions are met ultimately determines the overall validity of this methodology. The most fundamental of the assumptions of the whole approach is that the actual corrosion profile of the corrosion in the POD test specimens can be characterized to an appropriate level. In this study, the success of the characterization results was demonstrated using a digital radiography method which could achieve greater spatial resolution and thickness sensitivity than any of the techniques tested on the individual layers of the POD specimens after being cleaned. Extensive testing of the x-ray characterization method and of the specimen preparation processes prior to application in the evaluation gave reasonable assurance of the success in using these techniques. These tests are discussed in more detail in the *Automated Corrosion Detection Program Evaluation Report*.

The basis of the POD analysis requires the NDE systems are sensitive to the corrosion metric being tested, which in this case is thickness loss. The correlation test was effective in showing this correlation for the techniques that were analyzed for POD and should be included future evaluations. The results also showed the lack of thickness loss correlation by NASA Thermal Line Scan technique as later confirmed in the “a-hat” analysis. However, in the case of the two x-ray techniques the correlation results did not properly indicate the lack of a correlation that was later determined in the "a-hat" analysis. This may be a reflection on inadequacies in the specimen design, specifically on the potential adverse effects of using the simulated corrosion byproduct. The specimen thickness may also be a factor. A 0.04-inch-thick specimen was used to verify correlation for corroded specimens that were 0.063-inch thick. The lack of correlation measured for those systems may also reflect the inadequacies of the systems themselves as they were applied in this test. Correlation determination methods for operator interpreted techniques like the MOI should be addressed more completely for future POD studies.

Another premise of the assessment method is that the output of an NDE system is a function of the thickness profile in a small region or cell. The size of the cell is based on the spatial resolution of the system. The resolution test was an attempt to ascertain the system resolution using line-pairs of different widths but uniform depth. Estimates of system resolution and therefore, the cell size were successfully determined from the test. It was, however, necessary to take into consideration the inspection step size (pixel size) to account for uncertainties in the image registration process. Therefore, the resolution determined was adjusted accordingly for each system to determine the cell size.

A typical response of many of the systems across the resolution specimen showed fluctuations in the modulation data when inspecting certain sized line widths and line-pair widths. These fluctuations may be an artifact of those flaws being nearly equal to the inspection probe size. The specimen design may have exemplified this phenomenon and may necessitate exploration into alternative specimen designs for system resolution measurement.

For the analysis, it was also assumed that a small region around each fastener and each lap joint edge would produce an output significantly different from other regions in the lap joint. For this reason, these small areas determined through the Fastener/Edge test were excluded from the inspections. In the end, only the fastener-effected zones were excluded from the inspection data, the edge-effected zones were not. An initial trial of the "a-hat" analysis on inspection data where the fastener-effected zones were not excluded showed a greatly increased amount of scatter in the data. Therefore, it was determined that such a treatment of the inspection data is necessary for POD determination. It may be that a specially designed specimens and tests may not be necessary as the same information is available from the inspection images themselves.

Application of the POD analysis to the inspection data of ACDP-A2 makes use of a linear model to describe the "a-hat" versus "a" data and a normal distribution model to describe the scatter in the data about the trend. The validity of these assumptions was tested by statistical means as described in the *Automated Corrosion Detection Program Evaluation Report*. The source of the scatter in the "a-hat" versus "a" data about the trend should be checked as well. It is assumed that the scatter is due to system noise and to large thickness profile differences within the cells compared to the average. To identify the noise level in the data, specimens similar to the corrosion specimen should be inspected and included in the analysis. Specimen ACDP-A4, used in this evaluation, was assumed to have no corrosion. For each system, the noise as determined by the zero thickness-loss specimen was less than or equal to the scatter in the data from the corroded specimen. Additional scatter is suspected to come from variations in the thickness profile within the cell.

The POD analysis, as tested, prevents a direct comparison of the different inspection techniques to each other, or a ranking of the systems, due to the cell size determination. However, the detection capability of each NDE system was assessed by a comparison of the POD inspection results to the actual corrosion profile of the POD aircraft specimen after being filtered at a 5.6 or 6 percent thickness loss threshold and by the attributes of the "a-hat versus a" data. In general, the eddy current systems that were fully analyzed seem to have good sensitivity to thickness loss and excellent discrimination capability. Noise is relative to the system, varying from marginal to excellent at this level of detection. The ultrasonic systems also have good sensitivity to thickness loss with moderate discrimination, depending on the system. Their noise level is also dependent upon the system, with two of the systems having a moderate threshold level in relation the noise and the other having a good separation between threshold and noise. The radiography systems showed poor correlation to the chosen metric. Additional testing and study needs to be done, especially with the backscatter technology. Thermal systems also showed a poor correlation to thickness loss, suggesting that the physics is different what is assumed.

Inherent in this overall approach to probability of detection assessment is that real aircraft specimens can and should be used for this purpose. However, the use of real aircraft as corrosion specimens presents a situation where the actual corrosion extent within has to be assumed through screening processes. As in the case of this test, the amount of corrosion was a lesser extent than expected and desired. A potential solution is the use of a machined corrosion standard specimen with a known thickness profile as tested in the POD trial test. The results of the POD trial tests are inconclusive. POD results need to be generated from the real aircraft specimen structures of the same baseline thickness as the POD trial specimen for comparison. Regardless, at this point in time, there are not proven alternatives available. Efforts should continue to be directed at the development of sources of real aircraft specimens and at manufactured corrosion specimens.

An interesting aspect regarding the amount of corrosion found in this evaluation may suggest that 10 percent thickness loss is significantly more than what might be considered appropriate for repair requirements or for structural integrity modeling. The POD specimen was considered moderately to heavily corroded by the amounts of byproducts present. This specimen was originally chosen on the basis of potential for being heavily corroded through a screening process which deemed it to have pillowing and failed rivet due to corrosion. Yet, the corresponding thickness loss was not as great at 7 percent. This may suggest that thresholds may need to be chosen more strictly for evaluating NDE systems to properly address the life-cycle cost problems with corrosion maintenance on the KC-135.

3.1.5 Evaluation Summary, Conclusions, and Recommendations

In summary, an evaluation methodology has been developed and validated for assessing the hidden corrosion detection capability of NDE techniques on the ACDP. The evaluation method developed during the program is based on determining POD for hidden corrosion in terms of thickness loss which lends itself to advanced approaches to inspection, automation, and corrosion management.

3.1.5.1 Evaluation Summary

The NDE techniques tested in the evaluation included methods using ultrasound, eddy current, radiography, and thermography. There was a wide range in the state of the technologies; some of the technologies are currently used in the field or depot and some are laboratory setups or prototypes. Even in the case of the most advanced technologies, preparation for the evaluation raised development issues regarding thickness sensitivity calibration and image registration, which are necessary for advanced implementation schemes. Significant improvements to the state of the technology may require continued capability assessment testing such as performed on the ACDP. In preparation for capability assessment testing, more emphasis may be needed on the NDE system development to fit automated application requirements. NDE developers need to be continually provided with realistic inspection and characterization opportunities to improve their technology. NDE developers should be required to optimize and develop calibration and image registration techniques and procedures for Air Force applications. They should also continue to work with the Air Force to standardized output results formats and data file formats for future data fusion and automation efforts.

The tests and specimens used for the evaluation were specially selected and designed around the analysis. Necessary parameters for the POD analysis such as output to thickness correlation and system resolution, as well as the POD data, were successfully generated using the test matrix developed. A combination of real aircraft structures, with and without corrosion, as well as engineered specimens of known content were necessary for this capability assessment method. Real aircraft specimens were necessary for POD determination due to the difficulties in being able to simulate the exact nature of corrosion. However, the actual amount of corrosion in real structures is unknown until they are destructively characterized. Therefore, a sufficient number of specimens should be used to assure appropriate levels of corrosion. Engineered specimens provided known defects for parameter measurement. They were manufactured with a simulated corrosion byproduct. Although carefully constructed and applied, the material may not have acted as real byproducts in between fuselage skin layers. The x-ray, thermal, and ultrasonic NDE systems tested my have been adversely affected by the engineered specimen design and manufacture.

Testing was performed over a 2-year period due to the magnitude of the scope of the evaluation. As part of the testing process, a dry run of the system operation and the procedures was performed and found to be a major contributing factor to the success of the experiments. Procedures, written specifically to incorporate a complete description of the inspection method, system setup, calibration, and inspection parameter values, were defined with the assistance of the NDE developers/participants prior to the evaluation in order to impart a controlled test. The most useful documentation kept were the procedural checklists, the specimen traces on transparencies, and the photographs.

Successful POD specimen characterization procedures were developed for the actual thickness loss determination. Techniques were developed to reasonably assure that a minimal amount of damage was done to the corrosion profile on the specimen. The digital radiography technique used had sufficient sensitivity and resolution, after being optimized, to use as a comparison of actual thickness loss. Characterization of the aircraft specimen thought to contain the most corrosion showed that it only contained a maximum of 7 percent thickness loss in some areas.

A test for 10 percent thickness loss detection capability was originally desired but had to be redefined due to the actual amount of thickness loss present. For this evaluation, 6 percent thickness loss detection capability was tested. The POD analysis conducted uses “a-hat versus a” data. The “a-hat” values came from NDE system’s output, specifically from the cell centers within the image. The “a” values are the actuals. These are the average thickness loss each cell from the x-ray characterization image. Several assumptions were made and tested regarding the data in order to determine POD using the “a-hat” analysis. When the assumptions were not valid, the POD curves are estimated using the pass/fail analysis. One aspect about the POD analysis method is that a quoted probability of detection should be understood to apply to thickness loss over the corresponding cell size. Due to the fact that cell size is determined according to the spatial resolution of the system, POD results are not directly comparable between systems. Analysis techniques to allow POD comparisons between NDE systems could be developed using a given defect defined by both thickness loss and area.

The critical inspection results from the correlation, resolution, and fastener/edge tests fed into the POD analysis. "A-hat versus a" data taken from the four-layer lap joint region by all of the NDE systems were plotted except for the MOI data, which is video format. From the "a-hat versus a" data, several of the techniques were determine to have unsuitable data for further POD analysis. A subset of the NDE systems including the MAUS-EC, SAIC-EC, AS&M-UT, SRI-UT, and SAIC-UT, were analyzed for POD capability. The two conventional eddy current and the three ultrasonic techniques all showed the ability to detect corrosion to levels of 6 percent or better. Each technique demonstrated a correlation to thickness loss with varying, but respectable, spatial resolutions and discrimination capabilities. The required threshold to achieve a 90 percent POD at 6 percent thickness loss was above the noise in each of these systems as measured on the specimens with no thickness loss.

Data from a trial manufactured POD specimen showed promise for evaluating hidden corrosion capability using this analysis. To determine the successfulness of using a manufactured specimen for POD assessment, a comparison would need to be made between the POD results of the engineered specimen to the POD results from the real aircraft corrosion specimen. However, the aircraft POD specimen analyzed and the manufactured POD specimen had different top material layer thicknesses, and therefore, the comparison would not be valid.

3.1.5.2 Conclusions

From the evaluation on the ACDP, several conclusion can be made regarding the evaluation methodology and regarding the results of the evaluation.

Pertaining to the evaluation methodology, the following are concluded:

- A quantitative assessment of corrosion detection capability for NDE techniques is successful using a probability of detection calculation based on thickness loss within independent inspection areas, or cells, on the inspection article.
- NDE system optimization is needed for hidden corrosion detection with emphasis on calibration, image-to-specimen registration, and output interpretation and format.
- A dry run of tests and concise records of procedures (checklists, transparencies, and photographs) are valuable.
- Tests for a corrosion capability assessment should include fundamental tests of capability as well as for corrosion detection using both manufactured and real corroded aircraft specimens. A number of carefully selected aircraft specimens should be included in the testing to assure appropriate corrosion content.
- Specimen characterization for actual thickness loss using the procedures in this study provides reasonable assurance that the specimen surfaces are represented accurately to the level required.

- The analysis, which uses a cell size based on the spatial resolution of the inspection technique, prohibits direct comparisons of PODs between different NDE systems. Direct comparisons are possible with further development into an approach proposed by UDRI to use a given defect defined by both thickness loss and area.
- This evaluation methodology, based on a probability of detection at a given threshold, provides the tools necessary for automation of inspections under a corrosion management maintenance philosophy. The ACDP analysis replaces the operator interpretation with a quantitative assessment that could feed into the decision making process of an automated system. The premise could extend to other corrosion metrics, other types of corrosion, or in other applications.

Pertaining to the evaluation results, the following are concluded:

- None of the techniques studied during the time frame of the ACDP evaluation were completely mature with respect to the evaluation and were in need of development
- Qualitative strengths and limitations of each system are just as important to consider as the quantitative results as far as depot level applicability.
- Quantitative results showed that the two conventional eddy current (Boeing MAUS IV and Science Applications International Corporation UltraImage IV) and the three ultrasonic techniques (AS&M PULSE, SRI UltraSpec, and SAIC UltraImage IV-ACES™) have the ability to detect corrosion to levels of 6 percent or better.
- The radiography and thermal (NASA/DIGIRAY RGX and thermal line scan technique and ARACOR backscatter x-ray) show a poor correlation between output and thickness loss using the specimens and methods in this evaluation.
- The MOI eddy current device (PRI) has poor sensitivity to thickness loss at the level found in the formal test specimens.
- WSU has difficulties interpreting data from their thermal technique on specimens with corrosion byproducts.

3.1.5.3 Recommendations

Several recommendations stem from the conclusions of this study including those for future NDE advancement and those for future evaluation studies.

For further advancement of NDE technologies for hidden corrosion detection:

- Tests such as the quantitative evaluation conducted on the ACDP should be continued in order to push developers technically to advance their technologies and to provide a mechanism for that development.
- Continual sources of real corroded aircraft structures should be provided to the NDE technology developers so that they can inspect and study the issues important to the Air Force.
- Standards for NDE system output meaning and format, calibration requirements, and image-to-specimen registration need to be developed for current and newly developed technologies to allow for transition into automated systems.

For future quantitative assessment studies, it is recommended that:

- The complete set of data generated on the ACDP (beyond the four-layer lap joint) is analyzed to further provide information of the NDE systems studied and on the analysis method used.
- The POD analysis approach developed on the ACDP is further developed so that it can be used to directly compare two different NDE technologies and rank their capability.
- The use of extensive system optimization in conjunction with prequalification testing is used to advance the current state of technology and also to ensure that NDE technologies meet certain basic requirements before extensive testing and analysis are performed.
- A military handbook detailing the hidden corrosion methodology and lessons learned on the ACDP be generated in order to streamline future efforts and to maximize the value of such exercises to the military.

3.2 Prequalification Test

As part of the ACDP an evaluation to assess the capability of different NDI systems in detecting hidden corrosion in lap joints and doublers, UDRI initiated prequalification round-robin tests. The goal of this project is to provide the government with a qualitative assessment of the corrosion detection capability of various detection technologies in a simplified format. A secondary objective, to provide feedback to vendors based on their inspection of actual corroded aircraft panels, is due to the general lack of corroded aircraft specimens available for inspection development.

The prequalification project gives NDI developers an opportunity to gain experience inspecting real corroded aircraft structures and supplements UDRI's formal evaluation of corrosion detection technologies. As part of this project, UDRI is providing qualitative information back to the participants concerning the actual corrosion condition of the aircraft specimens that have been inspected.

3.2.1 Specimens Provided

Three aircraft specimens ACDP-P1, ACDP-P2, and ACDP-P3 were provided to each participant. See Figure 24 for photographs of these specimens taken from KC-135 and 707 aircraft. Each specimen was carefully selected for their material type, structure, and potential to contain corrosion. A detailed description of each specimen was provided to the participants (listed in Table 5), which included the location from the aircraft, a drawing outlining areas of interest, and the dimensions.

(a) ACDP-P1 **(b) ACDP-P2** **(c) ACDP-P3**

Figure 24. Aircraft Specimens

3.2.2 Specimen Characterization

After the completion of the project, UDRI characterized the actual corrosion profile of each layer. First, the specimens were taken apart to expose each skin layer. Observations were made regarding the conditions of the skin layers. Corrosion by-products were removed using a 70 percent nitric acid bath and each skin layer's corrosion profile was documented using x-ray radiography.[2]

Each specimen was cut-up and numbered. These regions are shown in roman numerals in Figure 24 and are referenced in each x-ray inspection and each technology tested. The inspection regions are referenced in the x-ray images to identify the general location where corrosion was present.

In the specimen characterization results, specimen ACDP-P1 had light to moderate corrosion-affected areas covering all four regions along the stringers. A section of ACDP-P2 (Region I) was not characterized due to further investigation into a crack and pillowing observed on the surface. WPAFB is continuing evaluation on this section. Regions II and III had light to moderate corrosion affected areas with some concentrated areas of material thinning. In Specimen ACDP-P3 (Region I and Region III) had little to no corrosion. In Region II, there was light to moderate corrosion present around the lap joint areas.

In the prequalification specimen inspection results, digitized x-ray images (see Figure 25 for a representative example) were compared to the inspection data for each specimen and a qualitative assessment was performed for each technique to detect corrosion. Corresponding layers were selected for the NDE technique’s inspection capability.

[2] X-ray radiography performed by the Material Integrity Branch (AFRL/MLSA).

Table 5. Prequalification Participants, Techniques, and Detection Sensitivity

Company	Technique	Detection Sensitivity
Advanced Power Technology (APT)	Remote Acoustic Impact Doppler (RAID)	Top Layer Thickness
Boeing Corporation	Mobile Automated Scanner (MAUS) IV	Top layer Thickness
General Electric Company	Radiography	All Layer Thickness
Industrial Material Institute National Research Council Canada (IMI-NRCC)	Laser Ultrasonic (UT)	Top Layer Thickness
Physical Research, Inc. (PRI)	Magneto-Optical Imaging (MOI) Eddy Current	Top Layer Thickness
Science Applications International Corporation (SAIC)	Eddy Current (EC) C-scan	Top Layer Thickness
Science Applications International Corporation (SAIC)	Ultrasonic (UT) C-scan	Top Layer Thickness
Wayne State University (WSU)	Thermal Wave Imaging	Top Layer Thickness

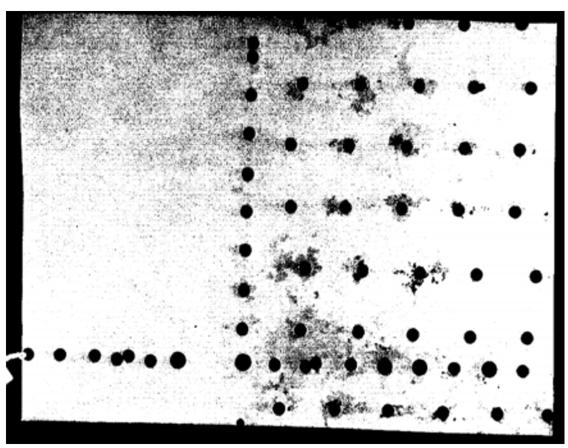

Figure 25. Digitized X-Ray Specimen Example

The following paragraphs describe the inspection results for each participant. A more detailed comparison can be found in UDRI's six individual *Prequalification Characterization Results* reports.

3.2.3 APT: *RAID*

The RAID technique detected hidden corrosion in each specimen. However, the inspection results were limited to detecting corrosion in specific areas. This technology also detected additional corrosion in areas not evident by x-ray characterization.

Inspection showed corrosion in the same general areas around the stringer of specimen ACDP-P1; however, Region I showed light to moderate areas of corrosion not evident in the characterization results. Region IV, the inspection results detected corrosion near the stringer, but showed concentrated areas not evident by x-ray characterization.

Specimen ACDP-P2 showed moderate amounts of corrosion in the same areas as the x-ray characterization (along the lap joint) and the concentrated material loss in Region III. There were some areas of concentrated corrosion detected that were not evident in characterization.

Only the stringer areas were inspected in ACDP-P3. Region I results detected corrosion, even though no corrosion was present in the x-ray results. In Region II, corrosion was detected along the side of the lap joint with one concentrated area in the lap joint. This corrosion profile was different than the x-ray profile. Region III results show corrosion along the stringer that was not evident in x-ray results. Although the RAID inspection detected the hidden corrosion in most areas, the detection of corrosion not observed in the x-ray characterization results are classified as false calls.

3.2.4 Boeing Company: *MAUS IV Eddy Current*

The MAUS IV Dual Frequency technique detected hidden corrosion in the same general areas found in UDRI's specimen characterization results. The high and low frequency images were not as clearly defined, so the gap-compensated image was used for comparison and identification. This technique supplies a percentage of corrosion detected.

Each ACDP-P1 specimen region had corrosion detected in the same areas as characterization; however, some corroded areas identified with high percentage estimates appeared to have less corrosion in the characterization profiles.

ACDP-P2 results showed moderate corrosion in the lap joint and around the fasteners and showed the same area where concentrated corrosion was present.

Specimen ACDP-P3 Region II was the only region inspected and detected corrosion in the same general areas in the lap joint.

3.2.5 General Electric: *X-Ray Imaging*

The General Electric x-ray inspection results focused primarily on the stringers and around lap joints for all the specimens. The type of corrosion detected mostly consists of pitting around the stringers and in the lap joints.

Specimen ACDP-P1, inspection results showed corrosion (pits) along the stringer, near the edge of the doubler, around the lap joint.

In specimen ACDP-P2 (data for Region III only), there were no identifiable areas of corrosion observed, even though the characterization results show significant corrosion in the lap joint.

Specimen ACDP-P3 inspection results point to an indication of corrosion on a stringer joint structure in Region I. Unfortunately, stringer structures were not evaluated in UDRI's characterization results. Regions II and III, inspection results showed slight variations (not pits) along the top portion of the lap joint and around a spot weld, respectively. The spots or pits around the spot weld in Region III were not observed in the characterization results. The detection of areas with signs of corrosion not observed in the characterizations results are classified as false calls.

As specified in the GE data report, the sections inspected were described as having many indications of corrosion. However, the images are not detailed enough for UDRI to accurately compare x-ray corrosion profiles and only a few were annotated with arrows to assist in the identification corrosion detection. The inspection technique seemed to only detect pitting rather than the general corrosion profiles seen in the x-ray characterization results.

3.2.6 IMI-NRCC: *Laser-Ultrasonic*

The IMI-NRCC Laser-UT C-Scan inspection results showed corrosion in each specimen.

In ACDP-P1, the inspection showed the corrosion-affected areas along the stringers and spot welds for all regions except Region II. The laser UT results are missing the C-scan for this stringer area. Region IV showed a wider area of detected corrosion around the stringer than is evident in the x-ray characterization.

Specimen ACDP-P2 showed corrosion-affected areas in the lap joint, and the concentrated material loss. However, Region II results show the corrosion profile concentration more to one side of the lap joint even though it was spread across the lap joint in x-ray characterization.

The results for ACDP-P3 (Region I) indicated the different thickness variations of materials, observed in the characterization results, but did not clearly identify the thickness loss in the lap joint (Region II).

3.2.7 PRI: *MOI Eddy Current Imager*

It was difficult to compare the PRI MOI eddy current results with specific areas represented by the x-ray corrosion profile. The inspection results are in a video format containing an output background of snake-like features. The operator narrated the inspection results while scanning each specimen.

ACDP-P1 regions were easier to track. General locations containing corrosion were detected in the stringer areas. The inspection of the Specimen ACDP-P2 was more difficult to determine the specific regions; however, corrosion was detected within the specimen. Specimen ACDP-P3's inspection was also subjective to the specific area, but corrosion was detected.

3.2.8 SAIC: *Eddy Current and Ultrasonic C-Scan*

The SAIC EC and UT C-scans detected hidden corrosion in the same general areas as UDRI's characterization results.

3.2.8.1 Eddy Current C-Scan

The corrosion profiles differed in the EC inspection from the x-ray characterization results. The detection of areas with suspected corrosion not observed in the x-ray results are classified as false calls.

Specimen ACDP-P1 Region I showed concentrated areas of corrosion in the same general areas, but appeared to be more extensive than the characterization corrosion profile particularly for Regions I and IV.

ACDP-P2 showed corrosion in the lap joint and in the area of concentrated material loss but did not detect corrosion near the primer location in Region II.

Only specimen ACDP-P3 Regions I and II were inspected. Region I showed the same material thickness variations observed in characterization. Region II showed corroded areas found in the lap joint.

3.2.8.2 Ultrasonic C-Scan

The UT inspection results for ACDP-P1 showed similar corrosion profiles around the stringer and details of scattered corrosion around the spot welds.

ACDP-P2 Region II results show corrosion in the lap joint and scattered corrosion around the spot welds near the primer and showed the same area of concentrated corrosion in Region III.

The UT inspection results for specimen ACDP-P3 clearly showed material thickness variations shown in the characterization and the moderate corrosion found in the lap joint. Region III showed yellow areas not clearly classified as corrosion. The characterization results shows no real corrosion present.

3.2.9 WSU: *Thermal Imaging*

WSU's thermal wave technique detected the hidden corrosion in the same areas found in UDRI's characterization results.

Specimen ACDP-P1 showed general corrosion found along the stringers.

Specimen ACDP-P2 results differed in that the corroded areas were in the brighter contrast areas. Corrosion was detected along the lap joint but some rivets were in the brighter contrast too. Areas shown in the inspection results that are not observed in the x-ray characterization results are identified as false calls. Region III results showed the concentrated area of material loss in the same area as the characterization.

Specimen ACDP-P3 results showed material thickness variations observed in Region I and the corroded area in the lap joint.

3.2.10 Summary

In general, all the techniques detected hidden corrosion in each specimen. SAIC's Ultrasonic C-scanned, Boeing's MAUS IV, and IMI-NRCC's Laser UT performed best. Overall each detected corrosion profiles similar to characterization profiles. The next best results came from SAIC's Eddy Current and Thermal Wave techniques which performed well but appeared to have false calls. The PRI MOI inspection went well, but it was difficult to follow the exact location where corrosion is present APT's RAID performed well, but seemed less sensitive to light scattered thinning. There were some areas of false calls. General Electric x-ray imaging indicated corrosion in all areas characterized; however, the detection of material thinning was not identifiable. Detection of pitting by GE was more evident.

3.3 Automation

Pursuing development of an automated inspection system for improved maintainability of aging aircraft is within the scope of the ACDP. Automation efforts include studying various automation concepts with the goal of selecting one for continuation in the program, optimizing the selected approach, and demonstrating the requisite automation capabilities on an actual aircraft structure. The following sections will address these program activities.

3.3.1 Automation Study

Preliminary automation task activities were directed at a comprehensive study of various automation concepts that might be incorporated into an integrated inspection system for hidden corrosion detection on the fuselage of aging aircraft. Feasibility, benefits, and costs were considered as they relate to a depot level corrosion implementation.

3.3.1.1 Methods, Assumptions, and Procedures

On September 20, 1996, the UDRI sent requests to 19 different organizations for ideas to integrate an automated inspection system for use on aging aircraft for the ACDP. Several tasks were identified for this effort. NDE tasks were directed at optimization, evaluation, and integration of four NDE technologies into an automated inspection system. The automation task was directed at optimization and integration of existing robotic technologies into an automated inspection system to be able to inspect for hidden corrosion on the KC-135 aircraft. The vendors were asked to bid against the tasks individually with separate prices for each task element.

In response to this request, nine vendors did not submit bids. Ten vendors submitted a total of 15 proposals, 12 of which were for NDE development. Three of the 15 proposals dealt with automation, either specifically directed towards robotics or proposing a full scale integrated solution to the inspection problem. A study was performed of the various automation concepts, focusing on the proposed technologies but also reviewing some alternatives that were not proposed. Each candidate was compared on the following basis:

- The merits of the proposed solution.
- The capabilities of the NDE technologies to be used.
- The maturity level of the NDE technologies.
- The relationship between the NDE technology and the automation concept proposed.
- The operating facility constraints (depot, field, or specialized facility).
- The level of automation.
- The potential for future applicability.
- The cost, schedule, and performance risk.

To better evaluate these various technologies, selected automation suppliers were asked to respond to a series of questions with regard to technical performance, cost, schedule and risk.

Identification of Candidate Automation Concepts. The three solutions that were proposed in response to the UDRI request were as follows:

- Aerobotics Solution – a gantry type system, which is an integrated part of a specialized facility built around the gantry.

- Berry Engineering Solution – a robot mounted on rails that moves around the perimeter of the aircraft.
- Advanced Robotic Vehicles, Inc. Solution – a skin crawler, named AutoCrawler.

There were a variety of other automation concepts investigated during this study which are as follows:

- LARPS – a ground vehicle in a specialized facility guided by wires in floor.
  - Truck-mounted localized inspection, the so called Cherry Picker approach.
  - Other Skin Crawlers:
  - ANDI (Carnegie Mellon)
  - CIMP (Carnegie Mellon)

Later in the program, UDRI investigated other technologies. The Flock of Birds technology provides 3-dimensional or more positional information that may have facilitated control of the crawler. It was deemed to be unacceptable for this application since it determines position using applied magnetic fields that are disrupted by the proximity of the aircraft being inspected. Two other track inspection systems were explored, the Catamaran Scanner by ABB-Amdata, and a vacuum track type of scanner system by Swain Distribution, Inc. While these systems are quite capable, they were not considered to advance the current state of technology in terms of automation.

UDRI also performed a search for other crawler type robots. While there are plenty of crawlers and small robots, they are mostly designed for other applications, and are not readily adaptable to crawling on an aircraft carrying an inspection payload.

Carnegie Melon has several inspection robots. Two are identified in the list above. One of their approaches is designed to inspect the crown of aircraft visually. The other approach was designed to inspect rivets using a robot that steps down a row of rivets with an alternating set of support beams attached to the aircraft with suction cups. These concepts were considered to fail to achieve a level of technology advance sought on ACDP provided by the crawler concept investigated.

Berry Engineering, Aerobotics, and Advanced Robotic Vehicles solutions were each evaluated for the above criteria using their proposal and responses to the questionnaire. The other technologies identified were not considered to be practical or cost effective or to represent a significant advance over existing semi-automated inspection systems.

Summary of Questionnaire. A questionnaire was submitted to each of the three organizations in order to best evaluate their proposed automation concept. The eight main topics and associated questions were detailed, exhaustive, and far reaching and covered the following areas:

1. Scan Speed
2. Accuracy and Repeatability
3. Remote Control and Automation
4. Price
5. Safety
6. Implementation
7. Cost, Schedule, and Performance Risk
8. Analysis of Other Solutions

Questions addressed various aspects of these topics, attempting to relate the proposed solutions to a depot implementation of an automated, integrated inspection system.

3.3.1.2 Results and Discussion

The automation study concluded with a decision for the follow-on subcontract after analyzing the proposed solutions, researching other robotic solutions, and finally selecting the best candidate.

Analysis of Responses. The solutions from the three companies were analyzed for satisfaction of the criteria from 3.3.1.1 and the survey questions above. UDRI considered technical, cost, and schedule issues for all approaches.

Berry Engineering submitted a proposal which contained many deficiencies. It did not adequately address program management. The technical requirements were not addressed nor substantiated. No specific scope of work was delineated. A subcontract with Berry Engineering was perceived to involve significant program risk to UDRI, the ACDP program, and the USAF. Berry Engineering's solution had several technical advantages and disadvantages. First of all, NASA's thermal line scan technique was proposed as the primary inspection technology for this system. If this inspection method was ready for implementation on such a robot, the system would offer the possibility of very high speed inspections. The maturity level and technical capability of the line scan thermography technique was discussed in Section 3.1 of this report, and was shown to require additional development before it could be used for this particular application.

Berry Engineering's proposed solution had many problems, too. The chief issue was that no NDE equipment had ever been attached to the proposed robot. In light of this, there were many unresolved issues. These included questions about position and alignment accuracy, consistency of scan speed, adjustment of the robot to account for the alignment of the aircraft, the effect of curvature on the inspection and the ability to integrate an NDE technology into the robotic system. This solution required a specialized facility, and/or facility modifications. It could not be assumed that it would work with contact NDE technologies. Since the thermography technique that was proposed is not ready for implementation, Berry Engineering's proposal loses most of its appeal. Both RGX and the NASA's laser ultrasonic technique, alternatively proposed inspection technologies for this system, are both extremely slow. Finally, the proposed solution was out of scope in terms of cost for the ACDP program, and represented significant cost, schedule, and performance risks.

Aerobotics proposed a fully integrated, full-scale, overhead gantry, corrosion inspection facility similar to the NDI facilities at Sacramento Air Logistic Center (SM-ALC). They proposed to demonstrate feasibility of their selected NDE technologies in Phase I. These were laser ultrasound, RGX, and neutron radiography (N-ray). Phase II would have integrated the RGX technique and a neutron generator with the robotic platforms at SM-ALC. The laser ultrasound system was already integrated with this system. Phase II would have also tested these technologies on these platforms. Phase III would have designed and built a turnkey automated corrosion detection facility and NDI system. Phase III was not priced; however, it would certainly have been a multimillion dollar undertaking. The magnitude of the proposed solution was out of scope for UDRI's program.

The Aerobotics proposal did not give adequate details of tasks to be accomplished, or how the costs were broken down by task. This solution had advantages, foremost of which was that it was based on an existing automatic robotic NDI inspection facility at SM-ALC. A fully automated, full-scale inspection facility and NDI system as propose by Aerobotics might be a desirable goal; however, their proposed solution was out of scope for the ACDP program both in cost and schedule. It required a large, full-scale, overhead gantry facility to implement. The cost for the demonstration (Phases I and II) exceeded the budget allocated for this effort on this program. The inspection facility cost would undoubtedly be several million dollars and the facility would take 2½ to 3 years to construct.

To undertake the costs of this effort the USAF would have had to be assured that the NDE technologies proposed for inclusion in this facility were adequate to the task of detecting corrosion. It could not be assumed that it would perform adequately with contact NDE technologies. The NDE technologies were assumed to be limited to those that they proposed or similar types of noncontact techniques. Their proposed solution was not the fastest, nor the most cost effective to implement. Operation costs, and potential savings were impossible to predict at that time. There were unanswered questions about the capabilities and limitations of the proposed laser ultrasound technique. There were safety concerns with regard to the proposed N-ray technique, as well as unanswered questions concerning exposure effects on various substances such as paint and fuel. Neutron radiography and Reverse Geometry x-ray require access to both sides of the surface being inspected. Aerobotics' proposed specialized facility would at least initially, and perhaps always, add flow days to the aircraft maintenance schedule. And finally, it would be difficult to operate in a semiautomated mode, and then only by skilled operators. The PDM personnel would probably not be involved in its use. Based on the collective data and analysis, the Aerobotics proposed solution was not recommended for continuation in the ACDP program.

ARVI, at the time working under the name of AutoCrawler, Inc., proposed a vehicle that could cling to the skin of an aircraft, and could move about using suction cups attached to a tractor-feed mechanism. While the robot technology existed and had been demonstrated, there was significant development to be accomplished. In particular, although the AutoCrawler could be manipulated manually and located via laser tracking mechanisms, it required additional development in order to guide the crawler using positional feedback from laser locators. Otherwise, the AutoCrawler could only be used in at most a semiautomated mode. The technology was considered to be in prototype development.

AutoCrawler's proposed solution had advantages and disadvantages. Since it could cling to the side of the aircraft, its manipulation would be much easier than the other two automation concepts studied. Based on the responses to the questionnaire, AutoCrawler is more accurate in terms of its ability to be tracked, able to adapt easily to the alignment of the aircraft, able to be integrated with both contact and noncontact NDE end-effectors, and should have provided a reasonably quick inspection of the aircraft lap joints and doublers. NDE technologies have been tested on this platform and it did not require any special facilities. The major disadvantage of the AutoCrawler was the fact that it was still considered a prototype and required additional development to achieve navigation and control of the robot in an automated inspection mode. There was also some work to be done on the suction cups. Their development costs and efforts required to implement a completely automated inspection system would be excessive given the governments direction not to emphasize robotic development on this program. In particular, navigation and control was identified as a major area of development. A semiautomated approach was adopted to reduced development efforts.

In a semiautomated mode, the AutoCrawler was the least expensive option. It was able to carry almost any NDE technology and could scan at speeds exceeding any known NDE technology requirements. It required neither an elaborate positional accuracy calibration, nor an extensive alignment algorithm; it simply mounted to the side of the aircraft. Manual or semiautomated operation was considered reasonable. Lowering the requirements to a semiautomated mode of operation and implementing appropriate management planning reduced risk. The robot could operate in the depot, facilitating and accelerating the introduction of NDE technologies into the depot. AutoCrawler's implementation would be unobtrusive, noninterfering, and would not add flow days to the depot maintenance schedule. Overall, the AutoCrawler solution represented the best alternative given the current state of the art in NDE technology, corrosion knowledge, and the realities of the PDM and depot environment.

Selection of Automation Concept for Continuation in ACDP. The three companies which submitted proposals were evaluated for the criteria listed in 3.3.1.1. The AutoCrawler was recommended for continuation on the program.

3.3.2 Optimization Phase

After selection of the AutoCrawler for continuation on ACDP, UDRI entered into discussions with ARVI on the scope of work on the proposed subcontract, considering methods to reduce risks to the program. The resulting contractual relationship with ARVI required a successful demonstration of controlled motion prior to initiating any potential follow-on efforts to integrate their technology with an inspection system. ARVI also assumed some financial risk on the project by sharing development costs in the interest in advancing the state of their technology.

3.3.2.1 Methods, Assumptions, and Procedures

Based on the results of the Automation Study and the selection of the AutoCrawler for continuation in the ACDP program, UDRI entered into a subcontract with ARVI to optimize their crawler to prepare for integration with an as-yet-to-be-determined inspection system. Automated control of the robot was the focus of this effort. Prior to initiation of the subcontract, UDRI and ARVI met to develop a conceptual design to the control function. This design is shown in Figure 26. Key components included the user interface software, Galil controller interface board, MasterCam software module (provided by Verisurf, a subcontractor of ARVI), Verisurf CAD software module, TOPCON laser tracker (supplied by another source – TOPCON), TOPCON laser to Verisurf CAD module interface software, and mechanical modifications. Note that the shaded items on the figure required development and/or modification by AutoCrawler. All other items were available off-the shelf or from other project teams.

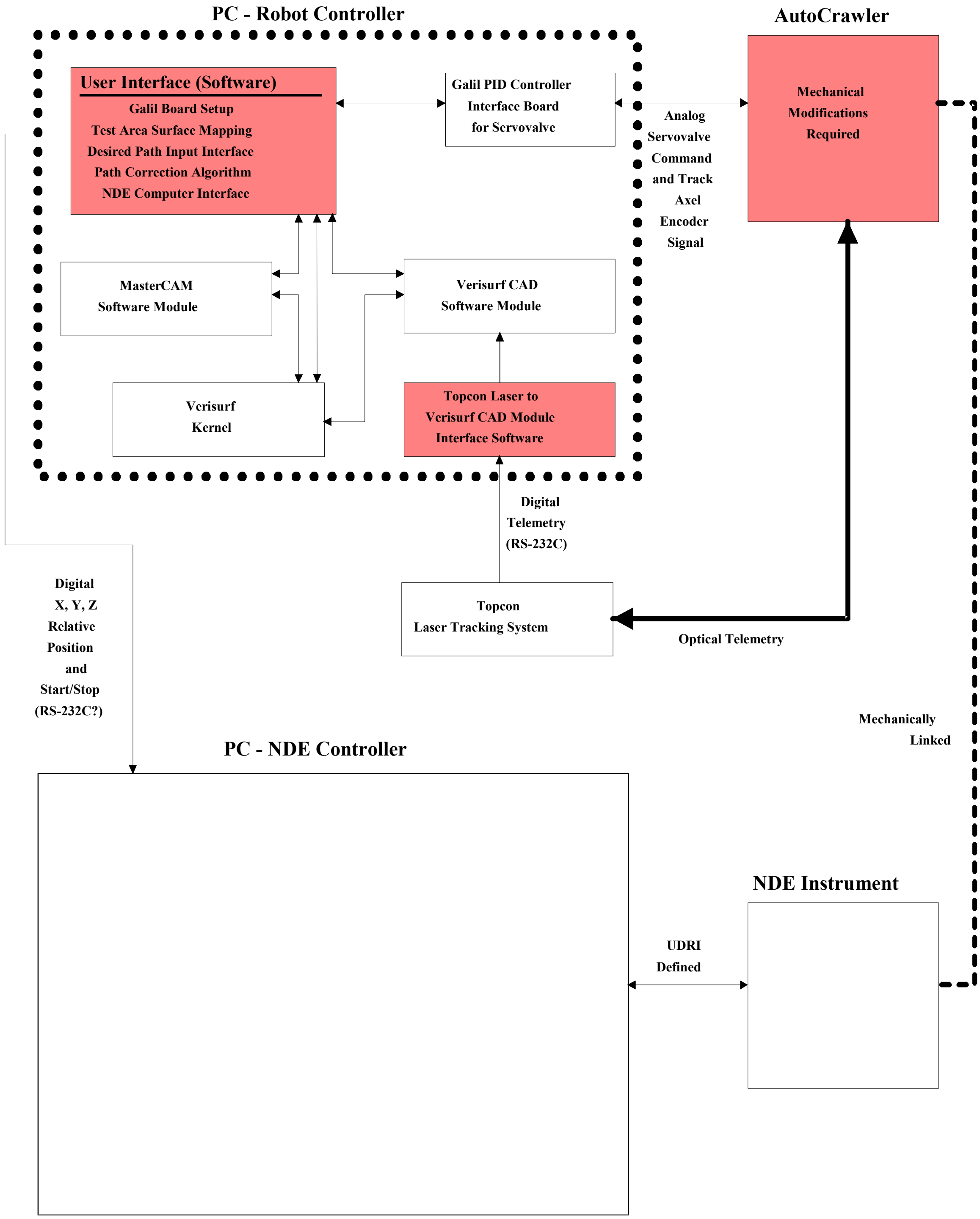

Figure 26. AutoCrawler Conceptual Design

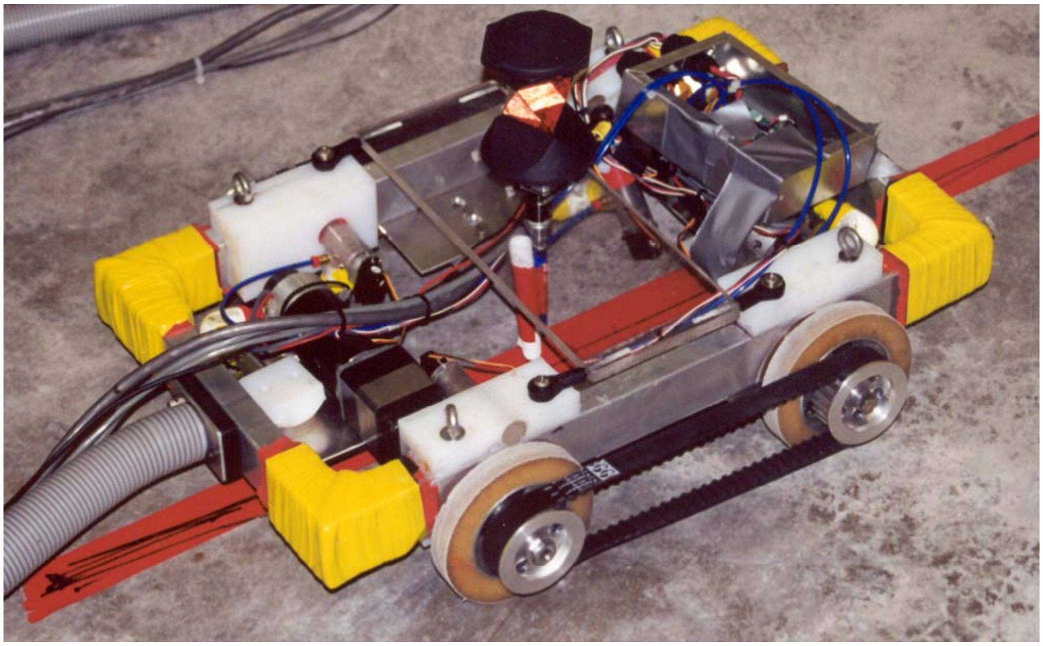

Figure 27. AutoCrawler Close-up (crawler only)

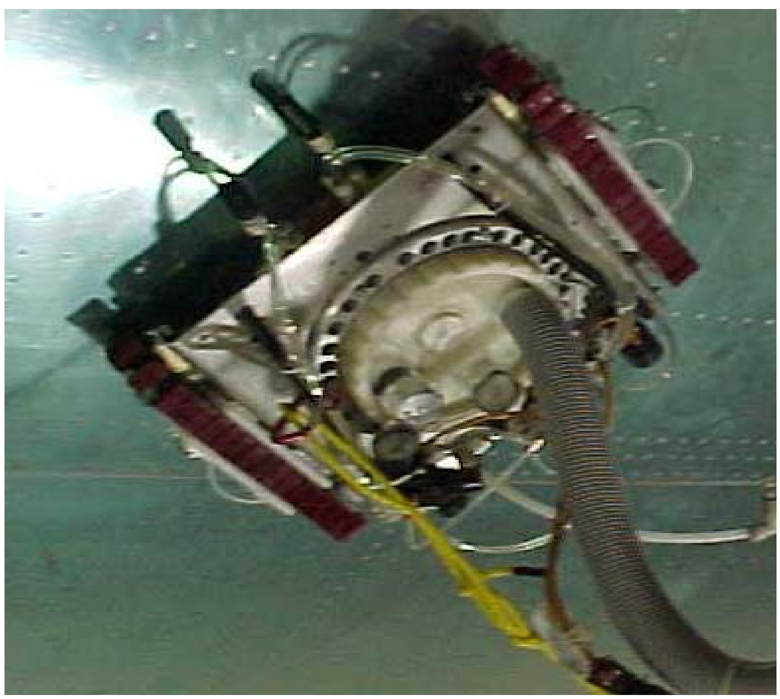

Figure 28. AutoCrawler Model M50 on Aircraft Skin

Refer to Figures 27 through 30 for details of the AutoCrawler in action.

Figure 29. AutoCrawler model AR25 on Coordinate Test

Figure 30. AutoCrawler Model AR25 Suction Cups

Subcontract Tasks. The following tasks were indicated by UDRI and the USAF as being required for continuation of the contract:

1. Laser Tracker Capability Demonstration (TOPCON). This task established the laser tracker's capability compared to requirements. Critical capabilities were specified for accuracy, repeatability, position reading update rate, and accuracy in tracking a moving target.
2. Mechanical Modifications and Computer Hardware. This task implemented the required modifications to the crawler and established the PC hardware. Critical modifications were associated with the control task as well as providing a base for interfacing inspection hardware and relevant computer capability.

3. Inner Control Loop Capability Implementation. This task developed and demonstrated if the system could run using the Galil board as its inner control mechanism.
4. Outer Control Loop Implementation and System Integration. This task added the outer control loop to the inner, integrating the laser tracker into the system for complete control.
5. Controlled Maneuver Routine Development. This task supplied the maneuver routines that would allow the crawler to locate itself at any given point (then move to any other point) and also included parking the robot (those series of moves necessary to move the crawler over a specified point).

The subcontract was to end with a demonstration of the crawler on a KC-135 tail section stationed in the UDRI DTEF in Oklahoma City, Oklahoma.

3.3.2.2 Results and Discussion

The subcontract was initiated in June of 1999 between UDRI and ARVI. Picture of the AutoCrawler are shown in Figures 27 through 30.

Summary of Subcontract. On September 2, 1999, a demonstration was conducted of the capability of the TOPCON laser tracker to meet the requirements of Task 1 of the ARVI (AutoCrawler) subcontract. The goal was to measure the accuracy, repeatability, following error, and positional update rates of the TOPCON laser tracker against the calibrated and certified Leica laser tracker. Two-thirds of the tests that were to be conducted could not be executed because the proper communication protocol for TOPCON was lacking and would not allow positions to be read from the TOPCON system. The only tests that were left concerned the position accuracy on a stationary target and repeatability. Unfortunately the system had not been calibrated recently and apparently had suffered some damage during shipping. Consequently these tests produced unacceptable results.

During the following several months TOPCON did not deliver the communications protocol to ARVI, nor did they provide ARVI with a repaired unit. There were many attempts to obtain these items, both by ARVI and UDRI. ARVI did eventually receive both the communications protocol and a repaired laser tracker unit, but only after significant delays to the program.

During the course of the subcontract for the AutoCrawler concept, several alternatives to the TOPCON laser tracker were considered. The Flock of Birds (pulsed DC magnetic fields and sensors) position measurement system was not appropriate due distortion of the magnetic fields by the metal aircraft. The Leica laser tracker was system was also considered, but was deemed to be too expensive, perhaps an order of magnitude more expensive than TOPCON. It had an exceptional accuracy, but it achieved this accuracy by averaging, making it unacceptably slow. It was concluded to be unsuitable for this purpose.

Another alternative was the Arc Second laser tracker system, which was based on a different mechanism to measure position. The system swept planes of laser light using two laser sources, each with two sheets of light. It measured the time between detection of the light by sensors mounted on a hand-held wand. It used these timing measurements to do triangulation on the wand. Arc Second visited UDRI and demonstrated their system. While it was an interesting product, there were many questions yet to be answered. Henry Seemann, from ARVI, also attended a demonstration and had some comments on the Arc Second capability. Some of the relevant points were as follows. It took Arc Second about 4 hours to setup their unit to achieve 1 mm accuracy. While UDRI was informed that the vertical working envelope is 30 degrees, Mr. Seemann said that the sheets of light were not flat (planar), and that Arc Second had to calibrate or compensate for this in their software. The errors introduced by this distortion would grow with distance from the laser sources, so that the effective working area was limited to 30 feet in range and that the system could probably only achieve the 1 mm accuracy within this range with a 15-degree vertical envelope. While these claims by Mr. Seemann had not been substantiated, it was clear that he did not believe that the Arc Second system was an acceptable alternative.

In June of 2000, ARVI performed another demonstration of the TOPCON laser tracker, in which static positional accuracy was shown to be within 0.039 inch. Positional update was 22 readings per second when no data was stored, and four readings per second otherwise. Test data for a moving target was not completed since a timestamp capability was not implemented. ARVI continued to study accuracy and tracking a moving target over the next several months.

In December of 2000, ARVI performed additional accuracy tests. Table 6 shows results of repeat measurements on a static target in various modes. These results indicate potential problems with the time-of-flight measurement that would be employed while tracking a target moving toward or away from the tracker. Table 7 shows results from tests on a moving target as a function of target velocity. These are quite unacceptable values. Table 8 gives results of a test to determine the effect of tracking mode on accuracy at a given (unspecified) target velocity. Clearly, the course tracking mode is more accurate, but errors are still unacceptably large. ARVI reported that TOPCON could give no explanation for these measurements, which were outside specified tolerances.

After these tests, ARVI informed UDRI of these problems, but indicated that they were working on methods to overcome these difficulties. Based on these results, ARVI reported that they would be able to position the robot to within one inch and by switching data collection modes they would be able to measure the actual position to within 0.039 inch.

Table 6. Repeatability Measurements on Static Target

Time of Flight Repeatability	
Mode 1 Tracking fine	0.240 inch variation
Mode 2 Tracking coarse	0.394 inch variation
Mode 3 Static fine	0.040 inch variation
Mode 4 Static course	0.060 inch variation
Angular Displacement Repeatability	
Mode 1 Tracking fine	0.022 inch variation
Mode 2 Tracking coarse	0.020 inch variation
Mode 3 Static fine	0.010 inch variation
Mode 4 Static course	0.015 inch variation

Table 7. Effect of Velocity on Measurements

0.061 inch/second	MAX	0.444”
	MIN	-0.210”
0.254 inch/second	MAX	1.237”
	MIN	-1.255”
0.417 inch/second	MAX	2.464”
	MIN	-2.121”

Table 8. Effect of Different Measurement Modes on TOPCON Data for the AR25

Coarse Tracking Mode	MAX	0.536”
	MIN	-0.534”
Fine Tracking Mode	MAX	0.844”
	MIN	-1.014”
Coarse Static Mode	MAX	1.253”
	MIN	-1.160”
Fine Static Mode	MAX	0.920”
	MIN	-1.043”

Demonstration and Discussion. The final demonstration of the AutoCrawler robot was held in March 2001. This demonstration was designed to exhibit the required capabilities of the crawler as defined in the subcontract statement of work. The primary focus was robot control. The demonstration proved to be problematic. It was well attended by interested government and industry representatives. A list of attendees is given in Table 9.

Table 9. Attendees for ARVI Demonstration of AutoCrawler Capability

Michael Waddell	AFRL/ML
Charlie Buynak	AFRL/MLLP
Robert R. Lewis	AFRL/MLS – Air Force NDI Office
Hank Tietz	ARINC
John Prati	ARINC
Henry Seemann	ARVI
Mike Jerome	ARVI
Clyde Uyehara	Boeing Co.
Al Etue	ETUE & Associates
David Campbell	OC-ALC/LAPEI
Steve West	OC-ALC/LAPEI
Don Brown	Retired General
Jackie Collier	Tinker AFB
Dick Martin	UDRI
Wally Hoppe	UDRI

A series of problems occurred that prevented a successful demonstration. The crawler could not move about on the tail due to inadequate suction cup and crawler modifications executed in the last month prior to the demonstration (to accommodate the sonic straps on the aircraft). This was complicated by the fact that ARVI designed their robot to handle the curvature of a larger aircraft than the KC-135 that was used for the demonstration. Problems with the suction cups led to onsite modifications of the robot in the days leading up to the demonstration. See Figure 30 for pictures of the suction cups on the crawler. In the process of making these modifications, ARVI strengthened the vacuum to the cups, at one point preventing the wheels from moving, which resulted in a stripped drive gear. This mechanical failure subsequently prevented the controlled motion tests from working. All in all, the demonstration was a large disappointment.

After the failed demonstration, ARVI ordered a replacement gear, which arrived the next morning. Following repairs, they performed a small demonstration to UDRI personnel of their control software on the floor of the facility. See Figure 29 for images of the crawler during these tests. ARVI placed three pieces of duct tape on the floor, and taught the system these locations by manually placing a pointer centered under the robot over each dot on each piece of tape. They then commanded the robot to move to these locations sequentially. The robot made some unexpected initial moves but eventually settled down and moved toward the correct spot. Once there it would again make some unexpected moves and head off in the correct direction for the next location.

To get an idea of how straight a path it would make and how repeatable the path was, duct tape was placed on the floor between command points in a pattern represented in Figure 31.

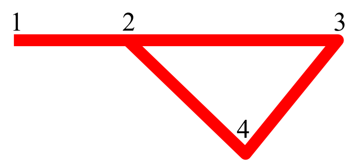

Figure 31. Repeatability Pattern

The robot was commanded to move in the following pattern: 1 – 2 – 3 – 4 – 2. It completed this task but the trail between the points was not straight. The initial unexpected moves took it off course and from there it traveled fairly straight. Deviations from a straight-line path after the initial moves were estimated to be approximately 1 inch. The initial random-looking move was on the order of several inches. The repeatability was similar. When the robot was commanded to move faster (initially it was running at 1 inch per second), the errors became progressively worse. Mr. Jerome explained this as a problem with the TOPCON laser tracker (when the robot is moving toward or away from the laser). For some reason, the measured angles were in error when moving in this direction. Speeds of 1, 2, and 4 inches per second were attempted. At 4 inches per second, the errors grew to several inches laterally.

The robot was then placed on a piece of KC-135 fuselage that was situated on the floor so that the lap joint was at a small angle from horizontal. The goal was to see what would happen if the crawler would slip while scanning. To make sure this would happen, the suction cups were not used. The resulting path errors were larger than what was seen on the floor. Since the robot was slipping when it turned to make path corrections, the errors only got worse with time. The errors were so bad, that it was necessary to install two suction cups for this test to limit the slipping. Still, the unexpected initial moves with even small slipping during turns, produced progressively larger errors making the exercise futile.

In summary, ARVI still has work to do on their control mechanism and software. They have demonstrated basic rudimentary control but the laser tracker is not accurate enough for this task, the software has at least one logic problem, and the robot has noise in its motion. That is, there is a limit to how precisely it can respond to move and turn commands. When it misses its target, the hunting routine is laborious and the errors do not allow an iterative search that is successively better. As such, they have a defined dead zone in position of ~ 0.5 inch, and in turns of ~ 1 degree. While moving from one command point to another, the robot moves to midpoints but doesn't check for accuracy in hitting the midpoints. As a result, far from the end point, it can be off quite a bit without making any corrections in position or angle. Consequently, it does not follow a path to within ~0.5 inch. The logic problem can be fixed. A new, more accurate laser tracker would help some, but the limiting problem may be the crawler design – its limitation on accurate movements coupled with the complex commands necessary to correct its position. Perhaps a new crawler design might be considered that would allow better position and orientation accuracy. AutoCrawler also has fundamental suction cup design problems, and the staff at ARVI do not seem to understand the physics of the suction cup design and the required balance between the suction cup vacuum and drive to the wheels.

In conclusion, automation of corrosion inspection systems is awaiting a breakthrough in automation and/or NDE that will overcome the automation shortcomings documented in the automation study, optimization, and demonstration.

3.4 NDE Requirements Survey

A survey of NDE requirements for depot level hidden corrosion detection was required under a contract awarded to UDRI under ACDP. The goal of this effort is to ensure a comprehensive understanding of Air Force NDE requirements and apply that understanding to the optimization of the process/system. The survey was developed and conducted to allow respondents to address other types of damage in addition to corrosion, and requested detailed information on specific structural and maintenance factors which may impact the operational characteristics of an Automated Corrosion Detection process or system.

3.4.1 Methods, Assumptions, and Procedures

UDRI was assisted in structuring the survey questions and in identifying the prospective respondents in the NDE community by the Texas Research Institute at Austin (TRI). Specifically, the TRI personnel who were operators of the Nondestructive Test Information Analysis Center (NTIAC) were under contract with UDRI.

A preliminary survey was developed which would require a relatively short time to complete (20-30 minutes) to maximize response. This preliminary draft was given to four UDRI personnel who are thoroughly familiar with NDE issues. Based on their comments and suggestions, the survey was optimized for ease of use and data collection. The final survey is shown in the Appendix.

Prospective respondents for the survey list were pulled from a variety of information resources such as:

- NDE Technology Information Analysis Center (NTIAC) mailing list
- Attendance lists from the DoD NDE Working Group meetings
- Corrosion-related lists from the other IACs
- Personal contact with the Air Force NDE community
- Telephone networking with the NDE military and commercial aircraft community

The survey was sent to 220 prospective respondents to ensure as wide a range of responses as possible. These prospective respondents included:

- Air Force customers
- other U.S. Government services (Army, Air Force, Air National Guard)

- commercial airlines
- Federal Aviation Administration (FAA)
- weapon system contractors
- rotorcraft maintainers

The final NDE Requirements Survey was delivered to this diverse group by e-mail, U. S. postal, and/or Fax transmission.

A Microsoft (MS) Excel database was constructed in preparation for the survey responses. Responses were entered into the database as they were received. The complete database is available at UDRI upon request. To increase the survey yield, numerous telephone calls were made by UDRI, requesting the respondents fill out and return the surveys.

Charts were also developed as part of the analysis process and are also available at UDRI upon request.

3.4.2 Results and Discussion

Of the 220 surveys sent, there were 64 respondents. The results are given here. Each of nine major sections of the survey is discussed separately. Response rate and diversity indicate a high level of interest in NDE problems and a broad spectrum of survey data allows for a variety of detailed analyses.

3.4.2.1 Survey Section 1

Section 1 survey questions reveal the job position, background, and experience of each respondent.

A wide variety of NDE-related positions were reported but they can be summarized in three major categories: Technician, Engineer, and Manager. The largest number of responses came from NDI Managers followed by NDI Technicians, and NDI Engineers. The various respondent organizations included the DoD (Air Force, Navy, Army, Air Force Reserve, Air National Guard), regulatory agencies (Transport Canada, Federal Aviation Administration), Weapon System Contractors, commercial airlines, and NDE technical consultants. The Air Force produced the largest number of responses (44 percent) followed by the Navy (22 percent). The remainder of the respondents were divided among the other organizations.

The specific aircraft with which each respondent was knowledgeable were categorized into Fighter, Cargo, Rotorcraft, Trainer, Attack, Commercial, Electronic Aircraft, Bomber, and other. The highest percent of the respondents were familiar with fighter aircraft (30 percent) followed by cargo aircraft (26 percent). Specific areas on the aircraft that relate to each respondent’s work fell into several categories including wings, fuselage, engine, subsystems, and other. The largest number of respondents were familiar with the fuselage and wing structures.

3.4.2.2 Survey Section 2

In Section 2, the respondents list the location(s) on the aircraft in which they are aware of damage, the types of damage prevalent, and the detrimental effect(s) on the aircraft/maintenance.

The responses indicated that locations most problematic are under fasteners, under paint, and under the outer skin. Corrosion under fasteners and second layer corrosion scored the highest in total negative effects. The types of damage discussed by the respondents include cracks and delaminations/disbonds.

The largest number of respondents indicated that their experience with cracks showed them to be located in fastener holes, structural components, and landing gear. Fastener holes, structural components, and landing gear also scored the highest in total negative effects. Responses on experience with delaminations or disbonds indicated that their detrimental locations are at control surfaces, cowlings, and skin splices. Delaminations/disbonds at control surfaces, cowlings, and skin splices also scored the highest in total negative effects.

The detrimental effects were discussed in terms of:

- Flow Time - Damage/problems increase maintenance flow time.
- Cost - Damage/problems increase aircraft maintenance cost.
- Service Life - Damage/problems decrease the service life of the aircraft.
- Safety - Damage/problems have a negative effect on aircraft safety.

The damage which has the greatest negative impact on Flow Time includes fastener hole cracks, structural component cracks, and corrosion under paint. The following locations have the most effect on maintenance Cost: fastener hole cracks, structural component cracks, and second layer corrosion. Service Life suffers the most from fastener hole cracks, structural component cracks, and structural component corrosion. The responses for damage location impact on aircraft Safety include fastener hole cracks, landing gear cracks, and structural component cracks.

3.4.2.3 Survey Section 3

In Section 3, the respondents indicate the criticality of improving existing industry techniques for various NDE applications. Damage categories are: corrosion, cracks, delaminations/disbonds, and other problems. The respondents also indicate if new/improved NDE equipment is required to satisfy each particular NDE application requirement.

Efforts to improve existing industry techniques for corrosion detection should include second layer corrosion, corrosion in multilayered structures, and corrosion under fasteners. Improving existing industry techniques for crack detection should include engine components, second layer fatigue cracks, and fastener holes. Improving existing industry techniques for the detection of delaminations and disbonds should include control surfaces, disbonds in lap joints, and corrosion damage. Existing industry techniques for the detection of other NDE problems could be improved in scanning NDE of dissimilar material stackups, alpha inclusions/particles in titanium, and in simplifying NDE calibrations.

NDE applications that are Critical include engine component cracks, lug holes at wing/fuselage cracks, and fastener hole cracks. NDE applications that are Very Important include second layer fatigue cracks, skin cracks, and corrosion in multilayered structures. NDE applications that are Important include skin splices with button head rivets, dissimilar material stack-ups, and coating thickness measurements.

New/improved NDE equipment need to scan second layer fatigue cracks, multilayered corrosion, and engine component cracks.

3.4.2.4 Survey Section 4

In Section 4, the respondents indicate the criticality of improving existing industry techniques for various NDE composite applications. The respondents also indicate if new/improved NDE equipment is required to satisfy each particular NDE application requirement for the inspection of composites.

NDE techniques for composites that are Critical include delaminations between composite laminates, adhesive bond failure, and composite skin/honeycomb core bond quality. Techniques for scanning composites that are Very Important include composite skin and honeycomb core bond quality, impact damage, and adhesive bond failure. NDE techniques for composites that are Important include porosity detection, fiber breakage, and water/chemical attack.

New/improved NDE equipment that satisfy various NDE applications for composites include composite skin and honeycomb core bond quality, adhesive bond failure, and composite repair/patches.

3.4.2.5 Survey Section 5

Section 5 ranks technologies that are useful or necessary for further industry development. The most critical needs include improving operator training/materials, reducing false calls, and improving signal-to-noise ratio of NDE signal.

NDE technology developments that are Critical include improved operator training/materials, more durable/reliable inspection equipment, and reducing false calls. Technology developments that are Very Important include reducing false calls, verification/validation of equipment capabilities, and simplified operating procedures. NDE technology developments that are Important include automated inspections, studies of human factors, and automated defect identification of NDE data.

3.4.2.6 Survey Section 6

Section 6 was filled out by 48 out of 64 respondents who reported on the reliability of NDE equipment available at their locations. Since the list of NDE systems is quite broad, many of the newer technologies were not available in the field.

The most reliable NDE systems are, regular dye penetrant, portable fluorescent penetrant inspection (FPI) equipment, and FPI booths.

NDE systems reported as Not Available by the respondents at their locations include recent technology developments that are generally unfielded. The systems most often listed as not available include air/laser coupled UT, shearography and holography, and neutron radiography.

3.4.2.7 Survey Section 7

In Section 7, respondent needs were evaluated for NDE equipment acquisitions and repairs. Equipment that is in sufficient supply as well as equipment needs were discussed.

Additional NDE equipment needed include UT transducers, eddy current probes, and training on existing equipment. NDE equipment improvements needed include training on new techniques, training on existing equipment, and portable Fluorescent Penatrant Inspection (FPI) equipment. Current NDE equipment that needed repair included training manuals, training on existing equipment and borescopes.

Some NDE equipment in current inventory was considered sufficient; these include the following:

- UT: Contact longitudinal
- UT: Surface wave
- UT: Shear wave

Some respondents reported that no additional NDE equipment was needed in the areas of neutron radiography, hammer/tap testing, and D-Sight.

3.4.2.8 Survey Section 8

Improving NDE techniques for specific types of material applications were considered. The materials reported are most important are titanium, graphite/epoxy, and high-strength steel.

3.4.2.9 Survey Section 9

In Section 9, comments are provided on NDE equipment, procedures, training and other issues. Fifteen respondents from the Air Force, Navy, Army, Airlines, and Air National Guard chose to make a total of 24 comments.

Problems Experienced included fastener holes and structural component cracks, under fastener and under paint corrosion, and control surface and cowling delaminations.

Techniques for detecting are thought to require improvements in the areas of engine component and second layer fatigue cracks, under fastener and second layer corrosion, control surface and lap joint delaminations and disbonds, and dissimilar material stack-ups and alpha inclusions in titanium.

New equipment for detecting suggested included the ability to scan for second layer fatigue cracks, second layer corrosion, and composite skin and honeycomb core bond quality. Improvements in general techniques such as reducing false calls and improved operator training and materials was also suggested.

The greatest needs for changing equipment or process included the following:

- Training on new techniques
- Eddy current probes
- Material Systems Requiring Improved NDE Techniques
- Titanium
- Graphite/epoxy

The most reliable NDE equipment was reported to be regular dye penetrants and portable FPI equipment.

3.5 Data Fusion

Data fusion uses different types of data in combination to enhance overall data for a variety of purposes. For aging aircraft inspections, data fusion involves combining inspection results from many types of sensors (multisensor fusion) and/or using results in conjunction with structural models to assess the integrity of an aircraft. The objective of multisensor fusion is to improve upon the detection capabilities of individual inspection technologies. For instance, an ultrasonic technique might measure the thickness of the top layer of skin, while an eddy current method is sensitive to the gap between layers as well as top layer thickness, and a radiographic technique is sensitive to the entire thickness and possibly the corrosion products (such as the ARACOR backscatter technique). By combining the results of more than one of these technologies, it may be possible to drastically improve the overall reliability of hidden corrosion detection.

Theoretically, the results of an inspection can also be used to make statements concerning the remaining strength and life of the aircraft or its components. To make such statements, the inspection results must be able to describe structurally relevant measurements (such as remaining thickness) and associate them with a particular structural component on the aircraft.

3.5.1 Methods, Assumptions, and Procedures

Inspection format and image registration issues, each necessary in data fusion, is considered when gathering ACDP data.

Inspection Output Standards. The inspection output was found to be quite divergent between the assortment of technologies tested in the formal ACDP evaluation. The format of each technology are discussed in the following paragraphs with due consideration given to proprietary data:

- AS&M, UT - Color bitmap images containing cells or groups of pixels representing each individual data point. A lookup table can be used to convert color to a thickness value within a range defined by the setup parameters.
- ARACOR, RT - Macintosh files that can be read as text. Each output value is the average ratio of the Rayleigh to Compton scattering intensities that were measured by their system. These values are not calibrated to thickness or thickness loss.
- PRI, MOI ET - Video stream of the inspection display, which shows the imaged out-of-plane magnetic fields visualized by the enlarged magnetic domains and the Faraday effect acting on polarized light. The magnetic domain structure is visible in the images and complicates the interpretation of the images.
- MAUS, ET - Inspection results are recorded in a proprietary format that can be displayed in system software (ImagIn). These results can also be manually selected and copied to the window clipboard for pasting into other applications. The resulting image is a bitmap in either color or gray-scale. System software can also read individual pixel values representing the eddy current amplitude. The eddy current null can be selected to be at the top middle or bottom of this scale. These values are not calibrated to thickness or thickness loss.
- NASA, RT - Raw integer data is stored in binary format. These values represent the X-ray intensity at each pixel. Each raw image can be further processed and converted to thickness with postprocessing software. The floating point output of this process is a file again stored in binary format.
- NASA, Thermal - Raw integer data from each inspection is stored in binary format, generated from the captured frames created by the infrared camera. These images are further processed and calibrated to thickness and stored as real values in binary format.
- SRI, UT - This inspection system can interface with the Boeing MAUS system to scan the specimen and create inspection images. See the MAUS format above. SRI images from the MAUS can be further postprocessed to create thickness calibrated images. Custom software accomplishes this task on copied regions from the ImagIn displayed images.
- SAIC, UT - Amplitude and time-of-flight data are captured and stored in binary image files in a proprietary format. Each value represents a number within a range of values

defined by the setup. A customized file conversion can be written to extract the time-of-flight images and convert to thickness.

- <u>SAIC, ET</u> - Horizontal and vertical components of the eddy current signal are digitized and stored in a proprietary binary format. A customized file conversion routine can be written to extract the vertical channel of data from the images to be used to calculate eddy current voltage. This technique is not calibrated to thickness or thickness loss.

These discussions clarify the need for standardization of inspection output. Image file format standardization is the first step. The industry needs to decide whether a bitmap image format is adequate, or whether a binary or text format is preferred. An 8-bit bitmap has an efficient storage capacity and the results can be easily displayed and manipulated in a number of standard software packages. On the other hand, an 8-bit bitmap has limited precision. A binary format would remedy this, but would require custom software to read and manipulate the images. Text format allows easy access to the data, but results in larger image files.

Standardization of inspection interpretation is also essential. Bitmaps allow for great flexibility in viewing the inspection results since the pallet can be easily changed to enhance contrast, for example, and many software packages exist that provide a host of image manipulation algorithms; however, bitmap files require additional steps to interpret the data in an automated or data fusion environment. Actual inspection output values (such as voltage, time-of-flight, and thickness) can only be recovered from the bitmap data by an appropriate conversion routine. As an example, one vendor's data is stored as 24-bit color bitmap images. Each color represents an integer value between 0 and 255. Each pixel value can be converted to this 8-bit integer through a reverse lookup on the color table. The resulting integer represents a thickness to be determined through interpolation from within the range defined by the inspection. For a thickness range of 0.020 to 0.40 inch, a value of 128 represents a thickness of approximately 0.030 inch. Each inspection system discussed has its own method of interpretation. A vital part of inspection interpretation is calibration. Establishing a uniform interpretation of the inspection results will enforce some form of standardization in calibration. Standardization of inspection output interpretation would address these problems.

The end result of any standardization effort will be to define the computer file format (bitmap; binary – integer, real, floating point; text), and data interpretation procedures. A common data file and interpretation format will greatly simplify access to the multiple inspection systems that will be required to advance into the realm of data fusion as a routine application.

An example of a standardized data format would specify that each image would be stored as an 8-bit grayscale bitmap. The pixel values between 0 and 255 would represent a thickness value between zero and some maximum thickness defined by the application. Another possible standardization approach would be to stipulate that each image would be stored as a binary floating point real representing thickness in inches.

Image Registration. Registration is the process by which points in the inspection image are mapped to specimen or aircraft coordinates. This was done in the ACDP formal evaluation so that the inspection results could be paired with actual thickness losses in the specimens in any given location. In a data fusion environment, it is necessary to perform registration so that data from multiple sensor types can be combined to produce a better inspection than is possible with any single inspection system or so that the inspection data can be used to define the structural condition of an aircraft component for maintenance decisions.

To understand the requirements of registration, it is helpful to define the various coordinate systems that are employed in the process. Figure 32 illustrates the three coordinate systems used in registration. First, the inspection results are typically displayed as an image made up of rows and columns of pixels. These pixels are usually indexed to the upper left-hand pixel in the image. System coordinates are defined by the inspection. In many cases, the inspection is executed using an X-Y scanner (which produces a natural set of coordinates). On other systems, images are formed by illuminating a detector of some sort (such as in an infrared camera or a digital radiography detector). Creation of images from these systems are governed by the geometry of the inspection (involving the relative spacing of the source, detector and specimen). These systems do not have an inherent coordinate system so one must be imposed using an alignment grid or some other reference. Specimen or aircraft coordinates define the relative location of features on the specimen or aircraft and provide the common reference to which various inspection systems can be anchored for multisensor fusion or to which structural condition can be tagged for structural assessment.

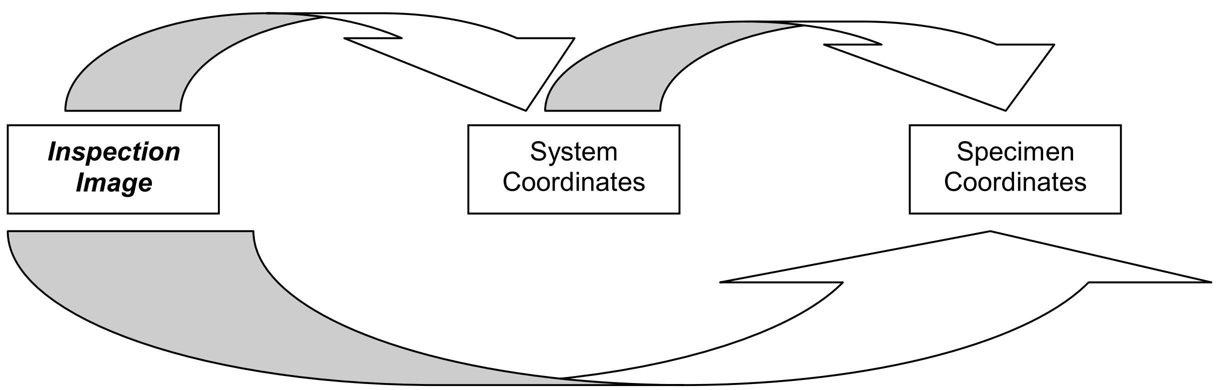

Figure 32. Three Coordinate Systems Useful in Registration

A registration map needs to be constructed between the inspection image and the specimen or aircraft coordinates. Ideally, a transformation would be created directly from the image to the specimen, shown as the bottom arrow in the figure. This is only possible if specific features are identifiable in the image for which specimen coordinates are known. This may be feasible in some instances, but experience shows that this is not always the case. Features cannot always be reliably and accurately identified in the images. Furthermore, this is a manual process that does not lend itself to automation or data fusion. More generally, it is necessary to establish the map from image to specimen coordinates by way of intermediate system coordinates shown in the figure and represented by the arrows at the top of the figure.

The map from image to system coordinates is ultimately defined by the mechanical construction of the inspection system. In systems with X-Y scanners, this mapping is usually straightforward, but not necessarily trivial. Each system is different. The transformation depends on the pixel size, scan and index step size, orientation of the image relative to the scan system, and the coordinates of the upper left-hand pixel. Pixel size is usually related to the scan and index step size. Image orientation can be proper (the same orientation in the image as is found on the specimen), flipped horizontally, flipped vertically, rotated, and/or transposed (interchange of rows and columns). Some developers have maintained a proper orientation in their images, while others have mapped the scan direction to each row in the image, regardless of which axis is used for scanning, thus producing the other possible orientations. Finally, since points in the image are indexed to the upper left-hand pixel, once the system coordinates are known for this pixel, it is possible to discern the system coordinates of all other pixels.

For systems in which inspection images are projections onto a detector, there is no natural set of system coordinates. For these systems, coordinates must be superimposed onto the system using a reference or alignment fixture. Inspection images of this fixture must be used to establish the transformation of points in the image to the points on the alignment fixture. For instance, a grid might be imaged by the inspection system; the grid forms convenient coordinate reference lines. Pixels in the image are then assigned system coordinates relative to this grid. This might involve a translation, rotation and scale, the three principle components of a linear (distortion free) transformation. The image might also be flipped, rotated, or transposed.

In general, any linear transformation involves translation, rotation and scale functions. These functions can be implemented through the use of homogeneous matrix transforms, which allow the multiple operations to be combined into one matrix. As a minimum, the coordinates of two points or features in the source and destination domains are required to define these matrix transformations. One of these features can serve as an origin for translation. The angle between the two features defines a reference for rotation. The distance between the two features determines the scale.

To perform the map from system to specimen coordinates requires constructing appropriate homogeneous transformation matrices using the coordinates on two selected features in both coordinate systems. For instance, if two fasteners are chosen as reference features, then these fasteners must be located in system coordinates and also have specimen coordinates assigned. These are complicated steps.

In an X-Y scanning system, the feature coordinates might be able to be determined by positioning the sensor over each feature and recording their coordinates in turn. If this cannot be done accurately, then some sort of pointer or reference must be aligned with the features. Such a reference pointer is not standard in these inspection systems, requiring creation of additional hardware to mount to the system. Reference points can also be marked at alternative locations on the specimen that can later be located relative to the selected features. This may require other intermediate tools. During the ACDP formal evaluation, reference marks were located relative to specimen features by tracing the marks and features onto transparency slides, digitizing the transparencies, and effectively creating a transparency coordinate system using these digitized images.

In cases for which a coordinate system is superimposed using a reference grid or alignment fixture, definition of feature coordinates must be done using the grid or fixture. Alternatively reference marks can be made on the specimen at known grid locations and these marks later located relative to the specimen features. Again, on the ACDP formal evaluation this was done by tracing the reference marks and specimen features onto transparencies for later analysis.

The selected reference specimen features must also be located in specimen coordinates. On the formal ACDP evaluation, this was done with a coordinate measuring machine (CMM), which is not practical in the depot on an aircraft. Some other mechanism must be developed to accomplish this step in the depot.

Once the location of two features is determined in each to the two coordinate frames, it is possible to map from inspection system to specimen coordinates. The map will produce a registered image in which the specimen coordinates of each pixel are known, an image that can be used in a data fusion environment.

Registration is a detailed process and several factors can further complicate the task. First, some systems do not have the same pixel spacing in the two image directions. For example, the NASA thermal line scan system has a horizontal (scan) pixel size determined by the scan speed and frame rate on the infrared camera. The vertical pixel size is determined by the specimen-to-camera distance and the lens used in the camera. There are also systems in which the image is produced by projection in such a way that the image is distorted. The NASA x-ray system produces inspection images through conical projection and features that are spaced at different distances from the source will be mapped to different radii in the image. Other forms of image distortion include scanned systems in which the sensor does not trace a straight line. The MAUS IV eddy current system uses a swivel mechanism to maintain contact with the specimen. As the probe scans over a curved specimen it is translated perpendicular to the scan direction, producing a curved inspection path. This design also has the affect of stretching the pixels out in the scan direction.

3.5.2 Results and Discussion

Many of the registration techniques employed on the ACDP formal evaluation would not be practical on an aircraft in an automated or data fusion setting. This discussion illustrates the issues that need to be addressed in such an application. In particular, further standardization of image format is needed. A uniform and standard arrangement for pixels is needed. Stipulating that the image will appear in the same orientation as the specimen or aircraft as viewed from the scanner would make pixel arrangement more consistent. Specifying that pixels should be square would probably be beneficial. Each scanning system or sensor should incorporate a mechanism to locate aircraft features relative to the scanner coordinates. Registration is a complicated task, and is dependent upon the delivery apparatus. A robotic system with a reliable guidance and location would be helpful in meeting this requirement.

In summary, data format and registration are important preliminary steps in a data fusion effort. The current state of technology in the industry reflects some of the challenges in these areas. Standardization of data format, including file format, interpretation, orientation, row and column definitions, and pixel requirements will go a long way in advancing the readiness of the industry in this arena. Guidelines for system design and automation in the area of registration will also help move the industry forward. The government should consider a workshop on data output formats and registration standards including representatives of the industry (NDE developers), data fusion experts, and end users.

3.6 Reproducibility

A critical objective of any evaluation is to measure the variability of the system being assessed. Variability for ACDP directly affects the detection capability as measured by a probability of detection assessment. Repeatability is the minimum level of variability produced in the system response due to inherent noise in the system. It is measured with tests in which all parameters and factors are held constant, typically involving a repeat of calibration. Defect-to-defect variability is a measure of variability in system response to different defects of the same size (thickness loss or crack dimension). Other factors (such as sensor and operator) will also contribute to the overall system variability and are the subject of reproducibility tests. It is hoped that these factors, which depend on the system being evaluated, are insignificant when compared to repeatability and defect-to-defect variability.

3.6.1 Methods, Assumptions, and Procedures

Certain factors might affect the variability of a system. It is helpful to classify them into different categories. There are parameters that define the system, and as such, are fixed by the processes established for an inspection. These factors are not tested except as part of system optimization. Once optimized they must remain fixed, otherwise the results of the evaluation might be invalidated. An extensive (but not exhaustive) list of such variables is given in Table 10. These system/process definition elements were compiled from ACDP evaluation procedures.

Other factors are controlled by design. Variations are inevitable in manufacture and execution of that design. These factors are limited through the implementation of proper process control procedures. This class of factor is of primary importance in a reproducibility test as each variable is tested to those limits allowed by process control. Sensors (e.g., probe, transducer) and instrumentation (driver, receiver, source, detector, filters) are important components of reproducibility tests. Calibration can be a source of variation distinct from repeatability if the repeatability test excludes calibration. The operator is an important variable for manual or semi-automated inspections.

Another class of factor includes those items that are uncontrolled, but are assumed to be random. This class includes elements of the inspection environment that may have an influence on the system response but can only be constrained to within certain limits. For example, temperature of the inspection facility might be an influencing factor. The effect of this factor is assumed to be randomized over the course of an evaluation.

Table 10. System/Process Definition Elements

Technology	System/Process	Elements
Ultrasonic		
	System Definition	
		Pulser/Receiver Filters Digitizer Gates Software Scanner Transducer frequency Transducer diameter Transducer focal length Couplant Mode of operation (longitudinal, transverse, shear, surface wave)
	Pulser/Receiver Settings	
		Repetition Rate Damping Gain Blanking Configuration (pulse/echo) Trigger Setting Rectification Setting Voltage Filters (high pass, low pass, band pass) Time Compensated Gain Setting Signal Conditioning Coefficients (frequency domain spectrum normalization)
	Gate Settings	
		Post Trigger Delay Number of Sample Points (gate range) Surface Following Mode Gate Threshold
	Digitizer Parameters	
		Data Acquisition Rate Data Acquisition Precision (number of digitization levels) Voltage Range RF/Video Mode Coupling (AC or DC) Offset
	Data Acquisition Parameters	
		Step Size Scan Speed Index Speed
	Special Mode of Operation	
		FFT Parameters (e.g., number of points in FFT window) Time-of-Flight Amplitude
	Material Parameters	
		Ultrasonic Velocity in Specimen
	Calibration	
		Calibration Method Calibration Reference Standards

Technology	System/Process	Elements
	Setup Files: Data Interpretation	
		Data Format Interpretation of Inspection Results
Eddy Current		
	System Definition	
		Instrument Digitizer Scanner Filters Software
	Probe/Coil	
		Diameter Type (absolute/differential)
	Drive Parameters	
		Drive Frequency or Frequencies (and frequency selection mode) Drive Voltage
	Receive Parameters	
		Filters (high pass, low pass, and/or band pass filter settings) Null Point
	Calibration	
		Method of Gain Calibration Method of Phase Calibration Calibration Reference Standards
	Digitizer Settings	
		Data Acquisition Rate Data Acquisition Resolution (number of digitization levels) Voltage Range Coupling (AC or DC) Offset
	Data Acquisition Parameters	
		Step Size/Speed Index Speed
	Special Modes of Operation	
		Multi-frequency Algorithms Magneto-Optical Imaging
	Setup Files: Data Interpretation	
		Data Format Interpretation of Inspection Results
Radiography		
	System Definition	
		Radiography Source Detectors Filters Amplifiers and Additional Circuitry (multichannel and single-channel analyzers) Software
	Source	
		Energy Current Source Dimensions (aperture or focal spot size) Source-to-Specimen Distance

Technology	System/Process	Elements
	Detector	
		Detector-to-Specimen Distance Mode Dimensions (aperture diameter) Settings (e.g., photomultiplier voltage)
	Digitizer	
		Zero (offset) Range (lower and upper energy limits) Dwell Time or Number of Averages Digitization Levels
	Amplifiers	
		Gain Offset
	Calibration	
		Method of Calibration Calibration Reference Standards
	Data Acquisition Parameters	
		Step Size or Image Resolution
	Setup Files: Data Interpretation	
		Data Format Interpretation of Inspection Results
Thermography		
	System Definition	
		Heat Source Infrared Camera Image Capture System Scanner (if applicable) Software
	Source	
		Source Dimensions Power Source Discharge Time Recharge Time Power Output Source-to-Specimen Distance
	Infrared Camera	
		Camera Specifications Image Size Lens Specifications (e.g., focal length) Frame Rate Temperature Sensitivity Cooling Mode and Temperature Integration Time Specimen-to-Camera Distance
	Reference Mode	
		Means of Removing Ambient Temperature of Specimen
	Calibration	
		Method of Calibration Calibration Reference Standard
	Specimen Preparation	
		Application of Paint Type of Paint
	Special Modes of Operation	
		Flash or Line Scan

Technology	System/Process	Elements
	Setup Files: Data Interpretation	
		Data Format
		Interpretation of Inspection Results

Due to the maturity level of most techniques evaluated by the ACDP (many were laboratory setups) and the limited quantity of system components (no duplicate subcomponents such as second probes or sensors), reproducibility tests, per se, were not performed. However, in the process of preparation and execution of the ACDP evaluation, several significant factors were identified that might influence the response of the corresponding system. Table 11 identifies several of these important factors. Any formal hidden corrosion detection evaluation of a production version of one of these systems should consider these factors in addition to sensor, instrumentation, and calibration factors.

Table 11. Factors Influencing Response to Corresponding System

Technology	Company	Factor	Factor Result
Thermography			
	NASA (Thermal)	Applied paint parameters	Acceptable heating levels within the specimen are reached by painting the surface of the specimen with black paint. The condition of this paint (thickness, smoothness, type of paint) should be considered during test planning.
	WSU (Thermal)	Applied paint parameters	See NASA (Thermal).
Ultrasonic			
	AS&M	Recirculation system water temperature	This system uses a fixed time delay of the gated signal used in a Fourier transform. As the water temperature changes, the timing of the ultrasonic signal within the gate changes. The Fourier transform gate is narrow and the signal rings past the end of the gate. As the signal changes location in the gate, the frequency domain response changes shape, impacting inspection results.
		Transducer standoff	This system uses a focused transducer that is a set distance from the specimen through construction of the fixture. Changes in standoff are controlled well, but as the transducer housing feet wear the standoff will change.
		FFT gate delay and length	These are system/process optimization parameters must be determined for each individual transducer. These parameters could be considered part of transducer-to-transducer variability, or their effect could be tested directly by having different engineers define these parameters for a given transducer and then measuring the effect that the difference has on the resulting detection capability.
	SAIC	Transducer standoff	This system uses a focused ultrasonic transducer mounted in a captured water circulation system that allows conventional immersion techniques to be employed. The construction of the transducer housing is designed to allow adjustment of the standoff. Standoff of the transducer effects the focal point of the ultrasound within the specimen, which might influence the results of the inspection. The brushes that maintain the water circulation system also bend as the system scans, changing standoff.

Technology	Company	Factor	Factor Result
	SRI	Transducer alignment	This system uses a contact split element transducer. If the transducer is rotated in the housing it might cause a change in the system response. If the transducer tilts it might also produce changes in the system response.
		Frequency conditioning	The detection scheme used in this system relies on the ability of the software algorithm to identify resonance peaks. The reliability with which this is carried out is enhanced by modifying the amplitude of the transmitted signal as a function of frequency. The frequency-gain function is currently defined by an engineer, and is therefore engineer dependent. Furthermore, each new transducer will require a different frequency-gain function. This adds to the transducer-to-transducer variability; however, could be studied for a given transducer to determine the impact of this particular variable.
Eddy Current			
	MAUS	Liftoff	Any eddy current technology is sensitive to liftoff changes. This factor should be considered in any test. Liftoff could be considered as part of the probe-to-probe variability, but could be tested individually by adjusting the liftoff (e.g., with Teflon tape) as a test in a reliability assessment.
	SAIC	Liftoff	This technique uses Teflon tape and a probe holder to maintain proper standoff. Changes in liftoff directly affect eddy current response, and is a typical problem in eddy current inspections. This technique is particularly susceptible to changes in liftoff due to the nature of the probe holder. There is a felt pad on the bottom of the probe housing that becomes compressed and worn after use changing the liftoff. The Teflon tape also wears reducing the minimum liftoff encountered during a scan.
	PRI (MOI)	Bias	Due to the nature of the mechanism involved in a magneto-optical scan and its sensitivity to externally applied magnetic fields (e.g., the earth's magnetic field), the developer advises adjusting the bias while scanning. This allows improved image contrast; however, effectively changes the inspection threshold during the inspection. The effects should be considered in any evaluation.
		Temperature	This system was shown to be temperature sensitive. PRI has attempted to remedy this problem, but temperature should be considered in future evaluation programs.
		Orientation	As the unit is moved about on the surface of an aircraft, its orientation relative to the earth's magnetic field changes. This affects the image contrast. Orientation of the imager should be considered as a test variable.
Radiography			
	ARACOR	Standoff	The backscatter technique relies on the relative placement of the x-ray source and the detector above the specimen. As the standoff changes the inspection volume changes.
		Detector	While system changes have already been discussed above, this system has shown definite detector-to-detector variability. It employs two detectors that are averaged together. The data collected during the ACDP formal evaluation show significant differences between the response of the two detectors. Any future implementation of this technology and corresponding capability assessments should address this variable.

Technology	Company	Factor	Factor Result
	NASA (RGX)	Detector-to-source distance	The position of the detector relative to the source produces variations in the recorded intensity. The system/process compensates for these variations through a process of background removal. This is accomplished by a calibration process that involves recording the intensity at different source-to-detector distances. Variations in the results of this process might produce variations in the detection capability.
		Offset drift	There is a drift in the offset during an inspection. Image processing steps attempt to remove image variation and image distortions, which are a function of this offset.

3.6.2 Results and Discussion

In summary, the ACDP program has defined several factors which should be reviewed when planning a comprehensive reproducibility test for any of these systems. Similar factors should be considered for other technologies that use these nondestructive inspection methods.

3.7 Advanced Transducer Design

An effort has been made to improve upon current ultrasonic corrosion detection techniques and equipment through the integration of existing novel sensor design and material use approaches. The goal is to demonstrate ultrasonic techniques, sensors, and inspections methods that will achieve current corrosion detection goals of one percent metal thickness loss resolution and high spatial resolution (1 mm or less) of localized corrosion features such as pits and cracks. The primary problem hampering current ultrasonic inspection methods is insufficient thickness resolution resulting from the use of traditional ultrasonic contact transducers.

3.7.1 Traditional Methods and Assumptions

Current ultrasonic equipment for corrosion detection uses contact transducers with frequencies in the 5-10 MHz range. Higher frequency transducers are not used because of the low power generated by traditional high frequency piezoelectric materials and because high frequency piezoelectric elements are thin and fragile. Conventional high frequency transducers use a delay line in order to protect the fragile piezoelectric element. The delay line creates numerous echoes that can interfere with detection of corrosion.

3.7.2 Advanced Transducer Development

The ideal ultrasonic inspection to detect corrosion would use high frequencies and focused transducers that do not have a delay line. This requires that the piezoelectric element be very rugged. UDRI has demonstrated the feasibility of using Aluminum Nitride (AlN) as a piezoelectric material capable of producing ultrasonic energy in the range of 30–100 MHz. AlN film is deposited on a substrate and is piezoelectric due to its structure-not because of electric poling. Its structural ruggedness results from the unique properties of the film and the substrate the film is deposited on. A high frequency, structurally rugged transducer, with diameters of 25 mm or larger should be possible.

To achieve this new transducer design, several tasks related to production must occur:

- Improve AlN adhesion to tungsten carbide substrates.
- Develop metalized coating process for AlN.
- Demonstrate the feasibility of depositing multiple films.
- Optimize chemical vapor deposition (CVD) for specific film frequencies.

- Improve uniformity of film coverage on substrate.
- Optimize the CVD process so that film thickness, output, and uniformity are repeatable.

3.7.3 Results, Conclusions, and Recommendations

Substantial improvements to the strength of adhesion of the AlN film to tungsten carbide (WC) substrates have been made during the period of performance on this project. In fact, the adhesion of the AlN film to the WC substrate is now generally so strong that failure of the film/substrate structure occurs within the WC substrate rather than at the AlN film/substrate interface. The adhesion improvements result from a combination of processes including careful chemical and physical preparation of the WC substrate prior to the CVD process, careful selection of CVD chemicals, and appropriate control of the CVD parameters.

Additional improvements were made to the sensor development processes that are necessary for demonstrating the feasibility of commercial production. Specifically, improvements were needed in the creation of electrodes for the AlN film and creating multiple films during a CVD run. It was shown that gold and platinum films could be applied to AlN films through standard sputtering processes. This method is common in the electroding process for traditional ultrasonic sensors. The procedures for depositing the AlN film were adjusted to allow films to be created on two substrates during a single CVD run. By the end of this project two films could be produced by a single CVD run on a routine basis.

Improvements in the control of CVD parameters were needed in order to produce films of the desired frequency, uniformity, and acoustic output. Based on experience with varying the duration of the CVD process and experimenting with polishing the AlN films after deposition, it became possible to produce films that emitted ultrasonic frequencies centered in the 30–50 MHz band. Similar improvements eventually resulted in films that covered the complete substrate face with substantially reduced defects.

By the conclusion of this project, UDRI could routinely produce AlN films on WC substrates that do the following:

- Produce ultrasonic energy ranging 10–100 MHz (centered between 30 and 50 MHz)
- Produce ultrasound with efficiencies similar to quartz piezoelectric elements
- Have diameters up to 25 mm

These improvements in the deposition of AlN films represent significant steps in making high frequency, rugged, ultrasonic sensors a possibility for the NDE community.

Detection of corrosion in thin structures requires focusing capability in the AlN sensor technology. A focussed, high frequency AlN sensor would provide both the spatial and depth resolution needed to detect corrosion in thin structures. During this program, trials to create focussed sensors using substrates that were shaped to produce focused ultrasonic energy were made. However, the substrate material selected ultimately proved to be defective. Budget constraints made additional attempts unfeasible. UDRI's work did show that the possibility of creating focussed AlN sensors is reasonable and should be successful with only a modest research program.

3.8 Detection Technology Evaluation Facility

DTEF is located in Oklahoma City, Oklahoma, and is dedicated to the support of the AFRL/MLLP-sponsored ACDP activities and initiatives supporting the KC-135 aircraft. The DTEF satisfies the objectives of ACDP by allowing:

- Easy access to TAFB personnel, specifically those involved with the KC-135 for evaluation and demonstration of prototype inspection systems.
- Scientific control of specimen integrity and evaluation of NDE system results in accordance with ACDP derived methodology.
- Completion and expansion of ACDP concepts to actively promote optimization of NDE technologies through funding and evaluation opportunities.

The facility is available for use on a scheduled basis to all parties involved with developing solutions for aging aircraft problems.

Figure 33. Section of KC-135 Entering the DTEF (outside view/inside view)

The facility is dedicated to the support of the ACDP, and during the term of the ACDP, is available for use by government, commercial and academic participants for NDE research involving corrosion and other damage relative to the aging KC-135 fleet. In this way, the DTEF provides diversity to the aging systems community and has the potential of providing a basis for expansion of related academic curricula. Figure 33 shows a KL-135 tail section being moved into the facility. Figure 34 shows this tail section in a fixture within the facility.

In developing the near- and far-term operational plans for the DTEF, efforts will be made to solicit participation and cooperative activities with other government organizations such as:

- FAA AANC
- NASA
- AF ALC TI organizations
- AF NDI Program Office
- AF Corrosion Program Office

Figure 34. Working in the DTEF

3.9 Presentations, Publications, and Program Reviews

The following is a list of the reports, presentations, papers, and reviews that have been developed from the research done for the ACDP by UDRI. The list is in chronological order and italicized titles indicate a presentation with an accompanying paper.

- ACDP Final Program Review (July 2, 2001), presented by Wally Hoppe to AFRL/MLLP.
- ACDP Program Review (April 19, 2001), presented by Wally Hoppe to AFRL/MLLP.
- ACDP Data Analysis Planning (March 29, 2001), internal presentation.
- ACDP Program Review (January 11, 2001), presented by UDRI to AFRL/MLLP.
- ACDP Program Review (March 1, 2001), presented by Wally Hoppe to AFRL/MLLP.
- From Cracks to Corrosion: The Evolution of a Probability of Detection Approach that Quantified Corrosion Damage in Aging Aircraft (December 7, 2000), presented by Wally Hoppe to the 2000 USAF Aircraft Structural Integrity Program Conference. Accompanying paper of the same title authored by Wally Hoppe, Norm Schehl, Charlie Buynak, Joseph Gallagher, and Alan Berens.
- *An Evaluation Methodology for the Assessment of Corrosion Detection* (November 17, 2000), presented by Wally Hoppe at the ASNT Fall 2000 Conference. Accompanying paper of the same title authored by Wally Hoppe, Norm Schehl, and Charlie Buynak.
- Status of the Automated Corrosion Detection Program – An Evaluation of Hidden Corrosion Detection Technologies (October 30, 2000), presented by Charles Buynak to the 49th Defense Working Group Meeting on NDT. Written by Wally Hoppe and Jennifer Pierce.
- ACDP Program Review (October 27, 2000), presented by Wally Hoppe to AFRL/MLLP.
- *The Evaluation of Hidden Corrosion Technologies on the Automated Corrosion Detection Program* (May 17, 2000), presented and authored by Wally Hoppe co-authored by Jennifer Pierce for the Fourth Joint DoD/FAA/NASA Conference on Aging Aircraft. Accompanying paper of the same title authored by Wally Hoppe.

- POD Specimen Characterization Plan (April 25, 2000), presented and authored by Wally Hoppe and co-authored by Jennifer Pierce for the AFRL Characterization Plan Meeting.
- NDE Technology Prequalification for Corrosion Detection Assessment (March 30, 2000), presented and authored by Philip Gloekler and co-authored by Jennifer Pierce for the AIAA Dayton-Cincinnati Aerospace Science Symposium 2000.
- Implementation of a Hidden Corrosion Detection Assessment Methodology (January 31 through February 3, 2000), presented by Wally Hoppe to the AFOSR Corrosion Review.
- Progress and Lessons Learned on the Automated Corrosion Detection Program (June 23, 1999), authored by Wally Hoppe, Norm Schehl, Jennifer Finch, and Dave Petricola for the 10th Annual Advanced Aerospace Materials and Processes – AEROMAT 1999.
- Specimen Development and Selection for Hidden Corrosion Detection Technology Assessment (May 25, 1999), presented and authored by Wally Hoppe and co-authored by Norm Schehl and Jennifer Finch to the SAMPE '99 - Evolving and Revolutionary Technologies for the New Millennium.
- Automated Corrosion Detection Program Review (May 17, 1999), presented by Wally Hoppe to AFRL/MLLP.
- ACDP Program Review (March 19, 1999), presented by Wally Hoppe to AFRL/MLLP.
- NDE Requirements Survey (February 1999), presented by George Stierlin to AFRL/MLLP.
- Status of the Automated Corrosion Detection Program (January 27, 1999), presented by Wally Hoppe to AFRL/MLLP.
- Corrosion Detection Technology Assessment Experiment Plan (October 20, 1998), presented by UDRI to AFRL/MLLP.
- Automated Corrosion Detection Program Review of Status (October 9, 1998), presented by Wally Hoppe to AFRL/MLLP.
- *Hidden Corrosion Detection Technology Assessment* (September 3, 1998), presented by Wally Hoppe to the Second Joint DoD/FAA/NASA Conference Aging Aircraft. Accompanying paper of the same tittle authored by Wally Hoppe.
- Automated Corrosion Detection Program – Status Report (June 17, 1998), presented by Wally Hoppe to the AFRL/MLLP.
- Automated Corrosion Detection Program Status Report (May 15, 1998), presented by Wally Hoppe to the AFRL/MLLP.
- Automated Corrosion Detection Program Technology Assessment (May 15, 1998), presented by Wally Hoppe to the AFRL/MLLP.
- Automated Corrosion Detection Program (January 20, 1998), presented by Wally Hoppe to the AFRL/MLLP.

- Automated Corrosion Detection Program Technical Review (October 28, 1997), presented by Wally Hoppe to the AFRL/MLLP.
- WL/MLLP Automated Corrosion Detection Program (May 1997), presented by Susan Reilly to the AFRL/MLLP.

Section 4
Conclusions

The ACDP was established to address the potential life-limiting issues surrounding the corrosion inspection and repair costs of maintaining the C/KC-135 aircraft and to advance the technologies necessary to address several aging aircraft needs as recognized by AFRL/MLLP. These needs were later identified in the National Material Advisory Board report[3] concerning improved inspections for hidden corrosion, automation and proven NDE reliability assessment in terms of POD and other metrics.

4.1 Formal Evaluation

The main emphasis on ACDP has been the formal evaluation of various NDI technologies for detection of hidden corrosion in aging aircraft. Of particular interest is crevice corrosion in lap joints and doublers on the fuselage of the KC-135 aircraft. Since no corrosion detection assessment methodology had been clearly established as a standard, the UDRI defined an acceptable, scientifically based, evaluation approach. A total of 10 technologies representing four NDE methods participated in the evaluation. Nine of these technologies inspected a combination of engineered and real aircraft panels in an orchestrated series of tests designed to measure correlation to the metric, spatial resolution, fastener and edge effected zones, and the probability of detecting thickness loss in lap joints and doublers.

In summary, the two conventional eddy current (Boeing MAUS IV and Science Applications International Corporation; SAIC UltraImage) and the three ultrasonic techniques (SAIC UltraImage, Southern Research Institute, SRI; and Analytical Services and Materials, AS&M) all showed the ability to detect corrosion to levels of 6 percent or better. Each technique demonstrated a correlation to thickness loss with varying, but respectable, spatial resolutions and discrimination capabilities. The required threshold to achieve a 90 percent POD at 6 percent thickness loss was above the noise in each of these systems as measured on specimens with no thickness loss. The radiography and thermal systems (NASA Reverse Geometry X-ray®; RGX and thermal line scan techniques, and the Advanced Research and Applications Corporation; ARACOR backscatter x-ray technique) showed a poor correlation with thickness loss. The MOI eddy current device (PRI) had poor sensitivity to thickness loss at the level found in the formal test specimens. WSU withdrew from the formal evaluation just prior to the test anticipating difficulties associated with the trapped corrosion products thermally loading the back surface of the front layer of skin, thereby changing the physics of their inspection. In general, the program successfully assessed the capability of these technologies to detect corrosion to the levels found in the test specimens for this particular application.

Each system was evaluated for other criteria that affect the ability to be incorporated into an automated inspection system. Details of these findings were discussed in the report, but certain trends were observed in the industry, primarily with regard to the maturity level of the inspection technologies. Many systems tested were laboratory setups; a few were production systems being used in the depot. In all cases preparation for the evaluation revealed development issues relative to this inspection application. Noteworthy was the need for additional development of calibration methods for thickness loss detection. Most systems were in evolution as the

[3] *Aging of U.S. Air Force Aircraft – Final Report*. National Material Advisory Board, 1997.

technology developers sought to improve their devices. Most participants were confident in their inspection approach, but when presented with specimens requiring inspection, were confronted with the fact that their system required additional development or optimization. For instance, some needed new sensors, or modified sensor designs; most required different setup parameters; many needed new calibration standards. The main reason for this situation was found to be due to the general lack of realistic specimens containing real corrosion with which to develop and optimize methods for hidden corrosion detection.

During the formal evaluation, inspection speeds were found to vary by NDE method. The thermal techniques have the potential for the greatest scan speeds. The eddy current and ultrasonic techniques, both of which are scanned methods, have moderate inspection rates. Both radiography technologies were found to be extremely slow, probably only suited for use as secondary inspection methods to be employed after a faster technology has identified a suspect region on the aircraft.

Data output formats and registration issues call attention to the general lack of standardization in inspection system computer file output formats, and a need for direction in the area of planning for advanced implementation schemes required for automation, data fusion, and corrosion management philosophies.

4.2 Prequalification

Round-robin prequalification inspections were designed to supplement the formal ACDP evaluation. In general, ultrasonic and eddy current methods performed well (Boeing, SAIC, PRI, and IMI-NRCC). The radiographic technique may have been sensitive to pits that were difficult to identify in the film radiographs used for specimen characterization but its ability to detect thinning was not conclusively shown. Conventional eddy current and ultrasonic technologies tested in the formal evaluation performed well there also. Several of these techniques should be considered candidates for further test and possible development. APT RAID technique showed promising results. The laser ultrasound system shows promise, but required application of a thin latex film to enhance ultrasonic generation. The MOI eddy current system seemed to perform well on this application; however, quantitative formal ACDP tests on 0.063-inch skins showed poor performance to the level of corrosion present in the test specimen. The MOI technology may prove to be a viable candidate for other test conditions and applications. It will probably be limited to manually interpreted applications unless or until a data presentation breakthrough occurs in this technology.

4.3 Automation Study

Automation concepts studied as part of ACDP included a large overhead gantry, a robot that traveled the circumference of the aircraft on rails, and a surface mounted crawler robot, as well as several less feasible alternative approaches. Each type was discovered to have strengths, limitations, risks, and associated developmental costs to full implementation. Among other limitations, the large gantry and the robot on rails systems are better suited to noncontact large area inspection modalities such as radiography, thermography, and laser ultrasound. In retrospect, these limitations proved paramount. Radiographic and thermographic technologies performed poorly on the ACDP formal evaluation to the levels of corrosion in the test specimens. Prequalification inspections with the laser-based ultrasound system required application of a latex film to enhance ultrasonic generation, an impractical approach in the depot. The AutoCrawler surface-crawling robot was selected for optimization and demonstration on ACDP.

It was anticipated to be the most accurate robot and to be able to scan at speeds exceeding known NDE technology requirements. This technology was expected to be able to carry most NDE systems that were being considered, both contact and noncontact. It should be able to operate in the depot with minimal interruption of depot maintenance, which would accelerate its introduction into service. Overall, the AutoCrawler solution represented the best alternative given the state NDE technology, corrosion knowledge, and the realities of depot maintenance environment.

The demonstration of the optimized AutoCrawler on the tail section housed in the DTEF in Oklahoma City was disappointing. The AutoCrawler could not be moved about on the tail section due to design problems with the suction cups and wheels. Onsite modifications led to mechanical failure of a drive gear. Controlled motion tests failed due to these mechanical problems. Subsequent tests performed on the repaired robot demonstrated rudimentary control of the robot motion. This limited demonstration revealed several remaining concerns with this technology. Fundamental design of suction cups, wheel drive, and appropriate balance of the corresponding forces has not been established for this robot. Laser tracker limitations restrict the implementation of control strategies. Accuracy and position update rates of the laser tracker are inadequate. Motion control schemes and robot movement constraints make path correction difficult, unwieldy, and impractical. Continuous feedback of positions will be required to overcome the necessary awkward movements and to maintain acceptable path following capabilities. Still, the fact that the crawler can only move forward, backward, and turn severely hampers any potential that this technology might have in this industry.

In summary, complete automation of inspections for hidden corrosion detection in aging aircraft is awaiting a breakthrough in robotics and/or inspection technology that will overcome current automation shortcomings.

4.4 NDE Requirements Survey

Sixty-four individuals responded to the ACDP NDE requirement survey. A wealth of information is available in the survey responses with regard to types of damage and location within the aircraft, required improvements to existing industry techniques, usefulness of existing technologies, reliability of existing equipment, acquisition and repair needs, and requirements for improved NDE technologies. Also included are written comments on NDE equipment, procedures, training, and other issues. A report was submitted to the government including a summary of findings. The results of the NDE requirement survey are contained in a database that is available to the government. As a database, it can be queried in many ways to search for a variety of trends.

4.5 Data Fusion

ACDP considered design constraints of a data fusion inspection system implementation. Data format and image registration are key components addressed. Each technology investigated as part of the ACDP formal evaluation used different computer file formats. Inspection step sizes were different and in some cases were not square. Output value meanings depend on the particular system. For instance, the output is a calibrated thickness loss for some systems. In other systems, the output represents a digitized voltage. Some technologies require post-processing to convert to thickness or voltage. Data format standardization is lacking in the industry.

Similarly, tools for image registration (the mechanism of defining location in the output with a spot on the aircraft) are not readily available in these technologies, which are currently designed for manual interpretation of the inspection images. An automated or data fusion implementation will require detailed and accurate registration that will require some built in method for determining system or scan coordinates for aircraft or specimen features. Standardization and guidance in the area of data output formats and image registration should be addressed in the near future to prepare the industry for advanced system implementation.

4.6 Reproducibility

Reproducibility efforts on the program identified critical inspection parameters that must be considered in future depot implementation qualification test plans. In addition to sensor and instrumentation variables, factors include technique unique parameters, some of which are given here. Testing on thermal systems should include applied paint conditions. Ultrasonic systems should be tested for variations due to transducer standoff and/or alignment. Probe liftoff is an important reproducibility variable for eddy current systems. Radiographic systems should be tested for physical spacing between source, detector and specimen. Additional factors not listed here are unique to each technology.

4.7 Advanced Ultrasonic Transducer Design

A novel ultra-high temperature ultrasonic sensor was further enhanced on this program. This program task was very successful in advancing manufacturing processes and proving the feasibility of this technology for high frequency focused transducer applications.

4.8 Detection Technology Evaluation Facility

Finally, the DTEF was established in the Oklahoma City area to facilitate test and evaluation efforts related to aging aircraft. Several pieces of a KC-135 aircraft were housed there, including an intact portion of the tail mounted in the configuration found on an aircraft. This tail section was used in the automation demonstration.

4.9 Program Summary

While the entire program addressed corrosion detection on aging aircraft, significant accomplishments of this program are primarily related to the formal evaluation. A baseline capability was measured for each system tested, which also showed general trends for each NDE method represented. Furthermore, the methodology that was proposed on the program to assess the capability of hidden corrosion detection technologies was unequivocally successful. This methodology was based on several critical assumptions that were demonstrated to be valid, confirming the methodology in its general approach and in the bulk of its particulars. The value of this approach is found as an enabling tool for inspection system implementation, automation, data fusion, and corrosion management maintenance philosophies.

Section 5
Recommendations

Recommendations for the ACDP cover formal evaluation, prequalification, automation, data fusion, reproducibility, and the DTEF.

5.1 Formal Evaluation

Results from the formal evaluation on the ACDP reveal that several of the inspection techniques tested have considerable promise. These systems (ultrasonic and conventional eddy current) should be further developed and moved towards depot level inspections. The other technologies did not show as much potential; however, the data in some cases is limiting, and additional data sets may indicate better detection capability in other applications. Therefore, the rest of the ACDP data should be analyzed. This includes tests on the other lap joint region and both doubler regions. Repeat tests and parameter variation tests should also be fully processed.

Research should be conducted into the proper statistical interpretation of the POD results from this evaluation considering that each system had a different cell size, and therefore an effectively different corrosion metric. The proposed corrosion cluster interpretation scheme should be investigated. In addition, the effect of cell size on the probability of detection results should be further studied. Calibration issues should also be addressed, in which thresholds determined from the ACDP analysis are tied to reference standard output values.

Advanced corrosion management maintenance philosophies will require corrosion characterization in which the corrosion profile is determined from the inspection results. These characterization schemes should be studied in light of the statistical POD approach presented in this program. Furthermore, the evaluation methodology should be extended to other corrosion metrics and other applications.

Finally, the evaluation methodology presented here should be standardized in a military handbook to make it available to the industry. Improvements and lessons learned should be added to reduce required costs and efforts, such as improved specimen design and condensed documentation.

5.2 Prequalification

Several technologies showed promise and should be further investigated. APT RAID technique should be considered for further test and development. The laser ultrasound system employed by IMI-NRCC required the application of a latex film to enhance ultrasonic generation. This system should be studied to determine whether or not the latex film is essential. The MOI eddy current system may yet prove to be a viable inspection system for larger levels of corrosion and other applications. This should be considered in future tests and evaluations. Conventional eddy current and ultrasonic technologies were also promising and should be considered for further test, and evaluation. The radiography technique tested was more difficult to evaluate, since it may have been sensitive to a different sort of corrosion damage. This technology may have its advantages in the area of pit detection. Further evaluation for this form of corrosion damage is warranted.

A prequalification inspection has value in that it can eliminate from consideration technologies that are immature or are otherwise unsuitable for formal evaluation of their detection capability. In the future, a phased approach to the development, test, and evaluation should be employed to inspection technique implementation.

5.3 Automation

Results of the automation study concluded that automation of corrosion inspection systems is awaiting a breakthrough in automation and/or NDE that will overcome automation shortcomings, primarily in the area of command and control to provide the necessary location parameters for data registration. Until that time, efforts at automation should be directed at incremental improvements to existing semiautomated inspection systems.

5.4 Data Fusion

Standardization and guidance in the area of data fusion output formats and image registration are essential and should be addressed in the near future to prepare the industry for advanced system implementation.

5.5 Reproducibility

Several reproducibility test variables have been identified for future evaluation programs that should be considered during planning. Without this information, reliability of inspection for the variety of NDE systems cannot be known.

5.6 Detection Technology Evaluation Facility

The DTEF was established in the Oklahoma City area to facilitate test and evaluation efforts related to aging aircraft. Recommendations for this facility include creation of a detailed map of the specimen structure and places of interest on the various components, mounting of all pieces in their respective aircraft orientations, and supplementing these sections with other specimens. A database could be setup containing results from every inspection on the specimens housed in the facility. Eventually, pieces in this facility should be destructively characterized. UDRI has transferred support of this facility to internal funds until such time as an appropriate Air Force contract is available. This continued support is desired to ensure the future availability of the valuable specimens housed there.

Section 6
References

The following documents produced outside of the UDRI were referenced within this report as sources of relevant and knowledgeable information:

- *Aging of U.S. Air Force Aircraft – Final Report*. National Material Advisory Board, 1997.
- *U.S. Combat Air Power: Aging Refueling Aircraft are Costly to Maintain and Operate*. US General Accounting Office Chapter Report 1996, GAO/NSIAD-96-160.

Please see Section 3.9 for UDRI presentations, publications, and program reviews.

Appendix

NDE Requirement Survey

The following pages represent the NDE Requirement Survey discussed in Section 3.4 of this report.

1. GENERAL

Name ________________________________

Job responsibility ________________________________

Organization ________________________________

Geographic location ________________________________

Aircraft with which you are knowledgeable ________________________________

Specific area which relates to your work

(please circle all that apply)

wings   fuselage   engine   subsystems   other ______________________

2. TYPES OF DAMAGE/PROBLEMS

In the following list, please check the **location(s)** on the aircraft in which you are aware of damage and the detrimental **effect(s)** on aircraft/maintenance.

	Location	Negative Effect			
		Flow Time	Cost	A/C Life	Safety
Type of Damage: Cracks					
Emanating from fastener holes	☐	☐	☐	☐	☐
Lap joints	☐	☐	☐	☐	☐
Second layer fatigue cracks	☐	☐	☐	☐	☐
Engine pylon strap/spar cracks	☐	☐	☐	☐	☐
Aircraft wheels	☐	☐	☐	☐	☐
Landing gear	☐	☐	☐	☐	☐
Windscreen	☐	☐	☐	☐	☐
Structural components	☐	☐	☐	☐	☐
Gas turbine engine components	☐	☐	☐	☐	☐
Other *(please specify)* __________	☐	☐	☐	☐	☐
Type of Damage: Corrosion					
Under fasteners	☐	☐	☐	☐	☐
Outer skin	☐	☐	☐	☐	☐
Second layer	☐	☐	☐	☐	☐
Lap joints	☐	☐	☐	☐	☐
Wing skin/tee	☐	☐	☐	☐	☐
Under paint	☐	☐	☐	☐	☐
Stiffeners under skin	☐	☐	☐	☐	☐
Aircraft wheels	☐	☐	☐	☐	☐
Landing gear	☐	☐	☐	☐	☐
Structural components	☐	☐	☐	☐	☐
Other *(please specify)* __________	☐	☐	☐	☐	☐
Type of Damage: Delams/Disbonds					
Skin splices	☐	☐	☐	☐	☐
Control surfaces	☐	☐	☐	☐	☐
Wind screens	☐	☐	☐	☐	☐
Cowlings	☐	☐	☐	☐	☐

3. ***IMPORTANCE***

In the following list, please indicate the importance of improving **existing industry** NDE techniques for various NDE applications *(circle the appropriate number).* If new/improved NDE equipment is required, please place a check mark in the box.

	Critical	Very Important	Important	Somewhat Important	Not Important	**New Equipment**
Type of Damage: Cracks						
Emanating from fastener holes	5	4	3	2	1	☐
Lap joints	5	4	3	2	1	☐
Second layer fatigue cracks	5	4	3	2	1	☐
Engine pylon strap/spar	5	4	3	2	1	☐
Aircraft wheels	5	4	3	2	1	☐
Landing gear	5	4	3	2	1	☐
NDE for forward spar fuselage attachment fittings	5	4	3	2	1	☐
NDE of adhesive joints	5	4	3	2	1	☐
Fatigue crack detection in skins	5	4	3	2	1	☐
Crack detection in fuselage structures	5	4	3	2	1	☐
Detecting fatigue cracks in lug holes at wing/fuselage attachment	5	4	3	2	1	☐
Weep hole cracks	5	4	3	2	1	☐
Windscreen cracks	5	4	3	2	1	☐
NDE of tear straps	5	4	3	2	1	☐
Crown splice inspection	5	4	3	2	1	☐
Detecting damage in stiffeners under skins	5	4	3	2	1	☐
Detecting cracks in fittings with short hole - edge distances	5	4	3	2	1	☐
Detecting cracks in non-jig drilled holes	5	4	3	2	1	☐
Engine components (vanes, blades, disks, combustor)	5	4	3	2	1	☐
Type of Damage: Corrosion						
Corrosion precursors	5	4	3	2	1	☐
Under fasteners	5	4	3	2	1	☐
Outer skin	5	4	3	2	1	☐
Second layer	5	4	3	2	1	☐
Lap joints	5	4	3	2	1	☐
Wing skin/tee	5	4	3	2	1	☐
Under paint	5	4	3	2	1	☐
Aluminum (e.g., 2024-T3) pitting corrosion	5	4	3	2	1	☐
Corrosion in multilayered structure and measurement of each layer thickness	5	4	3	2	1	☐

(Continued)

	Critical	Very Important	Important	Somewhat Important	Not Important	**New Equipment**
Type of Damage: Delams/Disbonds						
Disbonds in lap joints	5	4	3	2	1	☐
Windscreen delams	5	4	3	2	1	☐
Control surfaces	5	4	3	2	1	☐
Cowlings	5	4	3	2	1	☐
Corrosion damage *(see also Question #5)*	5	4	3	2	1	☐
Other Problems						
Grain noise in UT inspections	5	4	3	2	1	☐
Simplifying NDE calibrations	5	4	3	2	1	☐
Residual stress measurement	5	4	3	2	1	☐
Hydrogen detection in titanium components	5	4	3	2	1	☐
NDE of dissimilar material stack-ups	5	4	3	2	1	☐
Inspection of skin splices with button head rivets	5	4	3	2	1	☐
Coating thickness measurements (either metallic or nonmetallic coatings)	5	4	3	2	1	☐
Alpha inclusions/particles in titanium	5	4	3	2	1	☐

4. USEFULNESS

Technology developments are ongoing in the area of NDE. Please indicate which subjects listed below are **useful/necessary** for further industry development *(circle appropriate number).*

	Critical	Very Important	Important	Somewhat Important	Not Important
Probability models for remaining life based upon NDE results	5	4	3	2	1
Verification/validation of equipment capabilities	5	4	3	2	1
Characterization of damage	5	4	3	2	1
Identifying NDE signals from nondefects (e.g., fasteners)	5	4	3	2	1
Reducing false calls	5	4	3	2	1
Improving signal-to-noise ratios in NDE signal	5	4	3	2	1
Automated defect identification/ classification of NDE data	5	4	3	2	1
Simplified operating procedures for NDE equipment	5	4	3	2	1
Automated inspections	5	4	3	2	1
Decreased inspection times	5	4	3	2	1
More durable/reliable inspection equipment	5	4	3	2	1
Multiple sensor data fusion	5	4	3	2	1
Large area inspection NDE systems	5	4	3	2	1
In-situ sensors (fiber optics or microprobes)	5	4	3	2	1
Cost-benefit analyses	5	4	3	2	1
Studies of human factors (color perception, visual acuity, attentiveness)	5	4	3	2	1
Developing probability of detection (POD) curves	5	4	3	2	1
Improved operator training and training materials	5	4	3	2	1

5. *COMPOSITE CONSIDERATIONS*

In the following list, please indicate the importance of improving **existing industry** NDE techniques for various **composite material** inspections *(circle the appropriate number)*. If new/improved NDE equipment is required, please place a check mark in that box.

	Critical	Very Important	Important	Somewhat Important	Not Important	**New Equipment**
Impact damage	5	4	3	2	1	☐
Heat damage	5	4	3	2	1	☐
Composite skin/honeycomb core bond quality	5	4	3	2	1	☐
Delaminations between composite laminates	5	4	3	2	1	☐
Adhesive bond failure	5	4	3	2	1	☐
Detecting water intrusion in honeycomb composites	5	4	3	2	1	☐
Water/chemical attack	5	4	3	2	1	☐
Low observable coatings/ materials	5	4	3	2	1	☐
Fiber breakage	5	4	3	2	1	☐
Fiber/ply misalignment	5	4	3	2	1	☐
Porosity detection	5	4	3	2	1	☐
Composite repairs/patches	5	4	3	2	1	☐

6. *NDE SYSTEMS AVAILABLE AT YOUR LOCATION*

In the following list, please circle the number that best reflects the **operating condition** of NDE equipment at your facility. If your facility has more than one piece of equipment of a given type, please circle the number that best suits the equipment in general. If the equipment varies widely, circle as many numbers as needed to convey your feelings about the equipment quality.

NDE Equipment	Always Works	Typically Operable	Sometimes Operable	Rarely Operable	Never Operable	**Don't Have**
Shearography/ holography	5	4	3	2	1	☐
Penetrant						
Regular dye penetrant	5	4	3	2	1	☐
Automated penetrant NDI system	5	4	3	2	1	☐
Portable FPI equipment	5	4	3	2	1	☐
FPI booth	5	4	3	2	1	☐
Magnetic Particle	5	4	3	2	1	☐
UT: thickness gauge	5	4	3	2	1	☐
Immersion UT:						
A-scan flaw detector	5	4	3	2	1	☐
B-scan	5	4	3	2	1	☐
C-scan	5	4	3	2	1	☐

(Continued)

NDE Equipment	Always Works	Typically Operable	Sometimes Operable	Rarely Operable	Never Operable	**Don't Have**
UT: Portable B/C-scan	5	4	3	2	1	☐
UT: Shear wave	5	4	3	2	1	☐
UT: Surface wave	5	4	3	2	1	☐
UT: Contact longitudinal shear wave	5	4	3	2	1	☐
UT: Air/laser coupled	5	4	3	2	1	☐
Eddy Current:						
Meter	5	4	3	2	1	☐
Impedance plane	5	4	3	2	1	☐
Alloy sorter	5	4	3	2	1	☐
Film x-ray	5	4	3	2	1	☐
Real time x-ray	5	4	3	2	1	☐
Computed tomography	5	4	3	2	1	☐
Neutron radiography	5	4	3	2	1	☐
Hammer/tap testing	5	4	3	2	1	☐
Infrared thermography	5	4	3	2	1	☐
Resonance (e.g., Fokker bond tester)	5	4	3	2	1	☐
Imaging Systems:						☐
Borescopes (optical, digital)	5	4	3	2	1	☐
Visual inspection light source (flashlight)	5	4	3	2	1	☐
Visual inspection tools (mirrors, cleaning)	5	4	3	2	1	☐
D-Sight	5	4	3	2	1	☐
Magneto-optic imaging	5	4	3	2	1	☐
Acoustic emission	5	4	3	2	1	☐

*7. **NDE NEEDS***

In the following list, please categorize **your** needs for NDE equipment acquisitions/repairs *(circle the appropriate number).*

NDE Equipment	Additional Equipment Needed	Improved Equipment Needed	Current Inventory Needs Repair	Current Inventory Suffices	No Add'l. Equipment Needed
Shearography/ Holography	5	4	3	2	1
Penetrant					
Regular dye penetrant	5	4	3	2	1
Automated penetrant NDI system	5	4	3	2	1
Portable FPI equipment	5	4	3	2	1
FPI booth	5	4	3	2	1
Magnetic Particle	5	4	3	2	1
UT: thickness gauge	5	4	3	2	1
Immersion UT:					
A-scan flaw detector	5	4	3	2	1
B-scan	5	4	3	2	1
C-scan	5	4	3	2	1
UT: Portable B/C-scan	5	4	3	2	1
UT: Shear wave	5	4	3	2	1
UT: Surface wave	5	4	3	2	1
UT: Contact longitudinal shear wave	5	4	3	2	1
UT: Air/laser coupled	5	4	3	2	1
Eddy Current:					
Meter	5	4	3	2	1
Impedance plane	5	4	3	2	1
Alloy sorter	5	4	3	2	1
Film x-ray	5	4	3	2	1
Real time x-ray	5	4	3	2	1
Computed tomography	5	4	3	2	1
Neutron radiography	5	4	3	2	1
Hammer/tap testing	5	4	3	2	1
Infrared thermography	5	4	3	2	1
Resonance (e.g., Fokker bond tester)	5	4	3	2	1
Imaging Systems:					
Borescopes (optical, digital)	5	4	3	2	1
Visual inspection light source (flashlight)	5	4	3	2	1
Visual inspection tools (mirrors, cleaning)	5	4	3	2	1
D-Sight	5	4	3	2	1
Magneto-optic imaging	5	4	3	2	1
Acoustic emission	5	4	3	2	1

(Continued)

NDE Equipment	Additional Equipment Needed	Improved Equipment Needed	Current Inventory Needs Repair	Current Inventory Suffices	No Add'l. Equipment Needed
Training on existing equipment	5	4	3	2	1
Training on new techniques	5	4	3	2	1
Calibration blocks	5	4	3	2	1
Calibration equipment	5	4	3	2	1
Training manuals	5	4	3	2	1
EC probes	5	4	3	2	1
UT transducers	5	4	3	2	1
Other *(please describe)* _______ ________________________	5	4	3	2	1

8. MATERIALS SYSTEMS

In the following list, please categorize the importance/need of improved NDE techniques/systems for the following materials systems *(circle the appropriate number)*.

Material System	Critical	Very Important	Important	Somewhat Important	Not Important
Aluminum	5	4	3	2	1
Titanium	5	4	3	2	1
High strength steel	5	4	3	2	1
Ni-based superalloys	5	4	3	2	1
Graphite /epoxy	5	4	3	2	1
Metal matrix composites (e.g., SiC/Al)	5	4	3	2	1
Ceramic matrix composites	5	4	3	2	1
Boron/epoxy	5	4	3	2	1
Polymers (windscreen)	5	4	3	2	1
Honeycomb core composites	5	4	3	2	1
Carbon/Carbon	5	4	3	2	1

9. <u>GENERAL COMMENTS:</u>

Please give a short comment on any of the above questions that require explanation.

Appendix

List of Symbols, Abbreviations, and Acronyms

The following are terms, abbreviations, and acronyms and their definitions as used within this report. These are provided for reference and clarification and includes products and manufacturers referenced.

ACDP	Automated Corrosion Detection Program
ACES™	SAIC UltraImage IV trademarked Ultrasound Scanner
AFRL/MLLP	Air Force Research Laboratory, Nondestruction Evaluation Branch
AlN	Aluminum Nitride
ANDI	Autonomous Nondestructive Inspector, Carnegie Mellon
APT	Advanced Power Technology
ARACOR	Advanced Research and Applications Corporation
ARVI	Advanced Robotic Vehicles, Incorporated
AS&M	Analytical Services and Materials
AutoCrawler	Automated Crawling Robot, ARVI
Catamaran Scanner	Track inspection system by ADD-Amdata
CIMP	Crown Inspection Mobile Platform, Carnegie Mellon
CMM	Coordinate Measuring Machine
CVD	Chemical Vapor Deposition
DoD	Department of Defense
DTEF	Detection Technology Evaluation Facility, Oklahoma
EC	Eddy Current
EDM	Electrical Discharge Machining
FAA	Federal Aviation Administration
FFT	Fast-Fourier Transform
FPI	Fluorescent Penatrant Inspection
HF	High Frequency
IAC	Information Analysis Center
IMI-NRCC	Industrial Material Institute of the National Research Council of Canada
IR	Infrared
kerf	Matter lost due to a cut in materials
LARPS	Large Aircraft Robotic Paint Stripping

Appendix

List of Symbols, Abbreviations, and Acronyms

MAUS	Mobile Automated Scanner, McDonnell Douglas
MOI	Magneto-Optical Imaging
MS	Microsoft
NDE	Nondestructive Evaluation
NDI	Nondestructive Inspection
N-ray	Neutron Radiography
NTIAC	NDE Technology Information Analysis Center
POD	Probability of Detection
PRI	Physical Research Incorporated
RAID	Remote Acoustic Impact Doppler
RGX	Reverse Geometry X-Ray®
SAIC	Science Applications International Corporation
SM-ALC	Sacramento Air Logistic Center
SRI	Southern Research Institute
Swain Distribution	Makers of a vacuum track type of scanner system.
TAFB	Tinker Air Force Base, Oklahoma
TGA	Thermogravimetric Analysis
TOPCON	Positioning Equipment Manufacturer, ATT Metrology Services, Inc.
TRI	Texas Research Institute, Austin
UDRI	University of Dayton Research Institute
UT	Ultrasonic
voxel	The volume within an object that corresponds to a single pixel
WC	Tungsten carbide.
WPAFB	Wright-Patterson Air Force Base
WSU	Wayne State University, Indiana
XPS	X-Ray Photoelectric Spectroscopy